INVESTIGATION OF THE GEOTECHNICAL PROPERTIES OF MUNICIPAL SOLID WASTE AS A FUNCTION OF PLACEMENT CONDITIONS

A Thesis

presented to

the Faculty of California Polytechnic State University,

San Luis Obispo

In Partial Fulfillment

of the Requirements for the Degree

Master of Science in Civil and Environmental Engineering

by

Wilson Win Yue Wong

September 2009

COMMITTEE MEMBERSHIP

TITLE:	Investigation of the Geotechnical Properties of Municipal Solid Waste as a Function of Placement Conditions
AUTHOR:	Wilson Win-Yue Wong
DATE SUBMITTED:	September 2009

COMMITTEE CHAIR:	James Hanson, Associate Professor
COMMITTEE MEMBER:	Robb Moss, Assistant Professor
COMMITTEE MEMBER:	Gregg Fiegel, Professor

ABSTRACT

Investigation of the Geotechnical Properties of Municipal Solid Waste as a Function of Placement Conditions

Wilson Win-Yue Wong

An investigation of the variability of engineering properties of municipal solid waste as a function of placement conditions was conducted. Limited data have been reported for the engineering properties of municipal solid waste (MSW) as a function of placement conditions. Wastes have high variability of engineering properties due to heterogeneity in composition and component size; influence from time based effects; and presence of compressible solids. Control of moisture content of MSW at the time of waste placement provides opportunity for increased capacity at a given landfill site due to higher compacted unit weight as well as for control of other geotechnical properties. A laboratory experimental test program was conducted on manufactured municipal solid waste (MMSW) that was representative of waste stream in the United States. Large scale test equipment was used to minimize the effects of scaling on results. The experimental program included compaction, compressibility, hydraulic conductivity, and shear strength testing over moisture contents ranging from 11% to 110%. Baseline compaction curves were developed for different compactive efforts. Similar to soils, the MMSW had bell shaped compaction curves that peaked at a maximum dry unit weight and associated optimum moisture content. The compaction curve generated at modified compactive effort had a maximum dry unit weight of 5.1 kN/m^3 and optimum moisture content of 66%. Four times modified compactive effort testing resulted in a maximum dry unit weight of 5.9 kN/m^3 and corresponding optimum moisture content of 56%. The compaction curve generated for four times modified compactive effort was used as a baseline for subsequent testing. Compression index was calculated from the strain-log stress curves for total stress conditions and is referred to as apparent compression

index. Apparent compression index decreased from 1.1 to 0.34 with increasing moisture content. Secant modulus of elasticity was calculated between 1% and 25% strain and ranged from approximately 200 kPa to 4,800 kPa over the range of tested moisture contents. Tangent modulus ranged from 400 kPa to 6,200 kPa between 1% and 25% strain. Both the secant and tangent modulus peaked between 30% and 56% moisture content. Wet of optimum, the moduli of elasticity decreased with increasing moisture content. The hydraulic conductivity was measured under constant head at a hydraulic gradient of 1 and decreased asymptotically from approximately $1.3x10^{-2}$ cm/s to $8x10^{-5}$ cm/s as the moisture content was increased to optimum. The hydraulic conductivity of the MMSW increased slightly wet of optimum. The internal angle of friction of the MMSW was measured at 15% shear strain and decreased from approximately 40° to 30° with increasing moisture content. Test results demonstrated that both the molding moisture content and dry unit weight have significant impact on the MMSW geotechnical properties, although it appears that molding moisture content ultimately controls the behavior. Based on the results of the tests it was speculated that, similar to clay soils, increases in moisture content allowed for breakdown of the fabric and physical rearrangement of waste components which in turn controlled geotechnical behavior. Overall trends were comparable for MMSW and soil and included: increased dry density and increased stiffness to optimum moisture content; decreased hydraulic conductivity with increased compaction moisture content; and decreased shear strength with increased compaction moisture content. The results of the test program have environmental and economic implications for design and operation of landfills as well as post closure use.

ACKNOWLEDGMENTS

I would like to thank the geotechnical engineering professors at Cal Poly for the opportunity to learn and grow. Namely, Dr. Hanson has given me constant feedback, encouragement, and advice throughout the process. I would also like to thank my fellow graduate students for their camaraderie and putting up with my incessant questioning about anything and everything. Lastly, I would like to thank Bear for listening; my family and friends for their support; and Matt for his proficient use of scissors and friendship.

Table of Contents

List of Tables

List of Figures

Chapter 1: Introduction

In 2006 Americans generated approximately 228 million metric tons of municipal solid waste (MSW) (EPA 2008). After diversion for recycling and re-use, approximately 170 million metric tons of MSW is sent to landfills around the country. With the increasing scarcity of land and difficulties with zoning, optimizing landfill performance is critical. Waste continues to be disposed in landfills despite efforts to minimize and divert wastes.

It is necessary to gain a better understanding of the properties of municipal solid waste to maximize the amount of waste that can be placed in existing and future landfills. Optimizing waste placement would allow for increased waste density and increased landfill operational life. Additionally, an improved understanding of waste properties would allow for safer and more environmentally sound landfills, both during operation and post closure.

Although landfill design and operation has become more consistent since the introduction of legislation that requires landfills to meet or exceed specific minimum requirements including liners and daily cover soils (Tchobanoglous et al. 1993), there are still many aspects of the landfilling process that may be improved. Several current issues at landfills are: the maximization of waste density and slope angles while maintaining stability, entrapment and disposal of leachate, and post-closure reuse of landfill sites.

Field compaction of MSW is critical for control of waste and also has important environmental and economic implications. Control of the moisture content of wastes during compaction may have potential to change both the compacted dry unit weight and subsequent engineering properties of the waste. Determination of the engineering

properties of MSW is challenging due to the heterogeneity of the test material, non-standardized test methods, and subsequent variability in the measured data.

A laboratory test program was developed to determine the influence of placement conditions on the geotechnical properties of a manufactured municipal solid waste (MMSW). MMSW was used for all tests to minimize the potential problems caused by scaling issues with test equipment and to assure the use of a reproducible, yet representative test material. Despite the use of a manufactured waste material with controlled component sizes, it was necessary to use large scale testing equipment to accommodate the varying sizes of differing waste components. Waste was prepared using representative constituents to a mixture ratio calculated from United States Environmental Protection Agency (EPA) waste production and recycling data (EPA 2008). The MMSW was then tested for various properties (compressibility, hydraulic conductivity, and shear strength) as a function of the compaction characteristics of the material.

All tests were performed in large scale test equipment on an MMSW based on accepted laboratory geotechnical test methods. Laboratory compaction testing was initially conducted to establish a baseline moisture content/dry unit weight curve. Constant rate of strain compression testing was performed to determine stress/strain characteristics of the MMSW. The vertical compressibility of waste as determined by the constant rate of strain compression testing can be used to aid in the calculation of waste settlement, long-term landfill capacity, and leachate/gas well performance. Hydraulic conductivity testing in a dual ring permeameter followed. Knowledge of the range of hydraulic conductivities of MSW may be used for determination of waste slope stability, design of leachate recirculation systems, and liner integrity. The final phase of testing consisted of testing the MMSW for shear strength properties in a direct shear device.

Shear strength values of waste may be used for the estimation of waste slope stability and bearing capacity.

In this thesis, an initial review of the state of knowledge of waste mechanics and relevant soil mechanics for compaction, settlement, hydraulic conductivity, and shear strength is presented in Chapter 2. This is followed by description of the test methods used within this test program (Chapter 3). Test results and discussion follow in Chapter 4. The engineering significance of the test results is discussed with both quantitative and qualitative analysis in Chapter 5. Finally, conclusions are drawn and suggestions for future work are made in Chapter 6.

Chapter 2: Literature Review

2.1 Introduction

A review of the mechanisms controlling soil compaction, compressibility, hydraulic conductivity, and shear strength is presented in this chapter to establish a framework for the engineering properties of waste. General topics including waste classification, moisture content, and field capacity are initially discussed. A review of the literature of waste mechanics pertaining to compressibility, hydraulic conductivity, and shear strength was performed to gain an understanding of issues specific to MSW.

Although soils are often referred to as granular or fine grained to distinguish the mechanisms underlying their behavior, much of the existing literature has been performed specifically on sands and clay. With that understanding, the remainder of this work shall refer to the mechanics of fine constituents as clay-like soils or particles and granular constituents as sand-like soils or components.

2.2 Waste Classification

Classification of MSW is necessary to describe waste constituents and correlate measured engineering properties with existing data. MSW properties vary widely based on the percentage composition of the waste mass. Difficulties encountered in waste classification appear to stem more from lack of agreement on classification methodology than lack of applicable classification technology. First, a review of the current literature regarding waste classification is conducted. Next, the classification system used by the EPA is detailed.

The majority of waste classification systems consist of a breakdown of component composition (by mass or weight) of the various constituents of waste as opposed to a classification by size or properties (Siegel et al. 1990, Manassero et al.

1996, Thomas et al. 1999). Common categories of waste components include: paper/cardboard, plastics, food waste, metals, rubber, and glass (Jessberger et al. 1995). The components may be categorized into groups including: non-organic vs. organic content (which are further subdivided into degradable/putrescible and non-degradable/non-putrescible) (Landva and Clark 1990, Dixon and Langer 2006), and component particle size distribution (Grisolia et al. 1995, Kolsch 1996, Dixon and Langer 2006).

Dixon and Langer (2006) proposed that waste classification schemes should consist of terms that are both brief and meaningful, have reasonably easy to measure parameters, and have groups that collect materials by similar engineering properties. To establish the proposed classification scheme, Dixon and Langer (2006) suggested that the following information be gathered: distinctions between groups and their percentage composition, component shape, size distribution, component compressibility, and degradability.

The United States EPA employs a simpler waste classification system for the annual waste stream as components on a weight basis. Estimation of the weight of waste produced is based on a materials flow methodology (from a mass balance approach) and not based on measurement of weights actually discarded. The EPA (2008) makes specific adjustments to the production data for each waste material and category including imports, exports, and diversions. The difference between the amount produced and the amount recycled (which is directly quantified) is determined as the amount that is landfilled on an annual basis. Categories for classification, quantities of generation, and recovery data for the US are presented in Table 1 (EPA 2008).

Table 1. Waste Classification, Generation, and Recovery Data

Material type	Weight generated (million metric tons)	Weight recovered (million metric tons)	Weight to landfill (million metric tons)	Percent of total landfilled waste
Paper and paperboard	85.3	44	41.3	24%
Glass	13.2	2.9	10.3	6%
Steel	14.2	5.1	9.1	5%
Aluminum	3.3	0.7	2.6	2%
Other metals	1.7	1.2	0.5	0.3%
Plastics	29.5	2.0	27.5	16%
Rubber and Leather	6.5	0.9	5.6	3%
Textiles	11.8	1.8	10	6%
Wood	13.9	1.3	12.6	7%
Other materials	4.6	1.1	3.5	2%
Food	31.3	0.7	30.6	18%
Yard trimmings	32.4	20.1	12.3	7%
Other wastes	3.7	0	3.7	2%
Total	251.3	81.8	169.5	100%

Adoption and use of a standardized waste classification system will help to better understand the measured engineering parameters of waste, such as those to be determined in this program. Without adequate description of the components of the waste, the measured variability in waste properties is difficult to relate back to data that has been gathered previously.

2.3 Waste Moisture Content and Field Capacity

Moisture content and field capacity are important for control of engineering properties and for efficient bioreactor landfill operation. First, moisture content of MSW is discussed. Next, literature about the field capacity of waste is reviewed.

Moisture content as defined for the purposes of this research is the quotient of weight of water and weight of dry solids, which is consistent with the common geotechnical definition. Natural or incoming moisture content in wastes varies greatly as a function of the time of year, location of origin, amount of rain, and amount of organic

matter, and has been reported to range from 20% to 72% depending on the study and origin of the waste (Zeiss and Major 1992, Beaven and Powrie 1996, Moore et al. 1997, Reddy et al. 2008a).

Beaven and Powrie (1996) defined the field capacity of waste as the sum of the natural moisture content and the absorptive capacity. Once the field capacity of a material has been reached, the continued addition of water will result in the drainage of water from the sample via gravity (Tchobanoglous et al. 1993, Jang et al. 2002). Field capacity generally decreases with increased vertical effective stress, increased density, and increased age of waste. Beaven and Powrie (1996) reported field capacities of varying types of waste as a function of dry density. For a pulverized landfill waste (with maximum particle size of 150 mm) at dry unit weights ranging between 2.5 kN/m^3 and 5.9 kN/m^3, the field capacity was reported to decrease from 141% and 60% moisture content (as calculated by the ratio of weight of water to total weight.

Subsequent moisture contents are reported as the ratio of weight of water to weight of solids unless otherwise noted). Based on a comparison of the three waste types and ranges of density reported, it appears that field capacity is directly proportional to particle size and inversely proportional to dry unit weight.

2.4 Compaction

Compaction is the densification of material by mechanical energy and may include impact, vibratory, and static compaction methods. The mechanisms controlling the behavior of soil and waste compaction are discussed. Mechanisms specific to both clay and sand soils are covered, followed by aspects related to waste compaction. An outline of waste compaction completes the section.

2.4.1 Soil Compaction

To control the behavior of soils, it is often necessary to improve the soil, whether through replacement, mechanical, or chemical modification. Compaction is one means of mechanical improvement that has been used to increase density, increase shear strength, reduce settlements, and control hydraulic conductivity. First, soil compaction testing is discussed. Next, the underlying theory for the shape of the compaction curve is detailed. Next, mechanisms specific to clay and sand soils are reviewed.

The Proctor compaction test (Proctor 1933) was developed in the 1930's to determine the compaction characteristics of soil. ASTM standards D-698 and D-1557 detail current laboratory soil compaction test standards (ASTM 2007a, ASTM 2007b). The compaction test is repeated multiple times at varying moisture contents to form the basis for the compaction curve, which illustrates the relationship between dry unit weight and moisture content. Dry unit weight is calculated as presented in Equation 1.

$$\gamma_d = \frac{\gamma_m}{1+w} \quad (1)$$

where:

γ_d = dry unit weight (weight/volume)

γ_m = moist unit weight (weight/volume)

w = moisture content (%)

The results of compaction testing are generally plotted as dry unit weight versus moisture content. By repeating the compaction procedure at varying moisture contents, it is possible to obtain a compaction curve, generalized as a smooth, bell-shaped curve. Based on this curve, the variation in dry unit weight with the related moisture content may be calculated. Figure 1 presents sample compaction plots at four compactive efforts for soil including the curve connecting individual maximum dry unit weights (line of optimums) and line of saturation (zero air voids line).

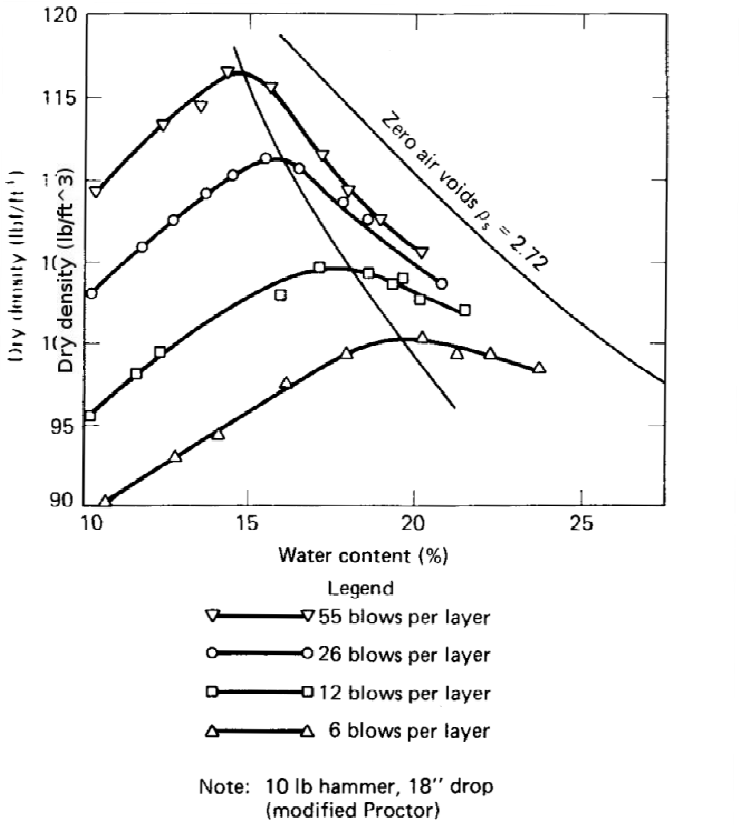

Figure 1. Compaction curves for different compactive efforts (from Holtz and Kovacs 1981 after Turnbull and Foster 1956)

The portion of the curve with a positive slope results from the decrease of friction between soil particles as water is added to reach the optimum moisture content (Proctor 1933) and is referred to as dry of optimum. The portion of the curve with negative slope is attributed to replacement of solids volume due to excess water during compaction and is referred to as wet of optimum.

The moisture content at which compaction is performed has major implications upon the strength and hydraulic conductivity of soils. If soils are compacted dry of optimum, behavior more closely matches that of brittle materials, with more strength development at low strains and a well defined point of failure. Soils compacted dry of optimum have an increased hydraulic conductivity, more capacity for swelling, and

decreased capacity for shrinkage (Holtz and Kovacs 1981). Soils compacted wet of optimum behave more similarly to plastic materials, with more gradual development of strength with increased loading and a less defined point of failure. Soils compacted wet of optimum generally have a lower hydraulic conductivity, less capacity for swelling, and more capacity for shrinkage resulting from increased structuring of soil particles and in the case of clays, development of the diffuse double layer (Holtz and Kovacs 1981).

The United States Army Corps of Engineers modified the compaction test to account for higher compactive effort. Accordingly, this modified compaction test requires that greater energy (2,700 kJ/m^3) be imparted on the soil for compaction (ASTM 2007b). The results are a similarly bell-shaped compaction curve that is shifted upwards and to the left of the standard compaction effort compaction curve, with a higher maximum dry unit weight associated with relatively lower optimum moisture content as demonstrated in Figure 1. The shift in the compaction curve is a result of the increased energy more effectively breaking down the structure of the soil despite the lower moisture content. Fine and coarse grained soils will generate different compaction curves as a result of the difference in controlling soil mechanisms, which is discussed below.

Lambe (1958a) and Olsen (1962) have proposed two differing theories of clay compaction, based on the concepts of packing structure and clods, respectively. The theory proposed by Lambe is predicated on the notion that clays are initially in a non-uniform structure that results in a decreased packing density. Increasing levels of compactive effort result in an increase in uniformity of the structure of the clay. As water is added and compactive energy increased, the plate or rod shaped clay particles become increasingly more parallel in orientation (Lambe 1958a). The increased uniformity in structure allows for a tighter packing arrangement of the particles with less void space and increased dry unit weight. When water is added to clay soil above

optimum moisture content, the clay particles are already in an optimum orientation for packing and become dispersed by the additional water, resulting in a lower dry unit weight.

The Olsen theory (1962) was based on the idea of clods, or clusters, of clay particles that may be broken down by the energy imparted during compaction. The clods at low moisture contents are held together in a flocculated arrangement via capillary action. The decreased capillary force allows for the breakdown of the flocculated structures, and reduces intra-particle friction allowing a tighter, more consistent packing arrangement (and a commensurate increase in dry density or unit weight) as optimum moisture content is approached from the dry side of optimum. Wet of optimum, the addition of water prevents clay particles from packing as tightly (Proctor 1933) due to the replacement of solids volume with water volume.

In both theories, compaction at higher energy results in breakdown of the clay structure (whether it is flocculated or in clods) at lower moisture contents and higher overall densities. Figure 1 demonstrates the continued increase in dry unit weight at lower moisture content as compactive effort is increased.

The variation of moisture content tends to have less of an effect on the dry unit weight of coarse grained soils than on fine grained soils (Holtz and Kovacs 1981). The increased ratio of volume to surface area for coarse soils results in generally larger pore spaces, greater interconnection between pores, and gravity controlled behavior. As a result, water will drain more freely through a coarse grained soil and the compaction curve will tend to be flatter with a less pronounced peak (Hilf 1991).

A phenomenon referred to as bulking has been observed in sands and other coarse grained soils. Bulking refers to the tendency of moist sands to be held in an

open structural arrangement as a result of capillarity between the sand grains (Terzaghi and Peck 1948). The result of bulking during compaction may be a compaction curve with an especially low peak (resulting in a flatter curve) or a double peak (Holtz and Kovacs 1981). Bulking is not considered for clay soils.

2.4.2 Waste Compaction

A significant amount of variability exists in the properties of MSW. To increase the density of waste during placement at modern landfills, it is compacted into place. Several researchers have documented the results of both laboratory and field compaction of MSW. Mechanisms specific to waste compaction are discussed. Next, results of previously reported data are presented herein.

The compaction curves generated from waste material generally are flatter, with a less pronounced peak than is common in soils. The change in dry unit weight is less sensitive to changes in moisture content. The optimum moisture contents for wastes are significantly higher than for most soils, ranging from 31% to 70% (Gabr and Valero 1995, Hettiarachchi et al. 2005, Itoh 2005, Reddy et al. 2008a).

Standard effort compaction (ASTM D-698) tests were performed by Gabr and Valero (1995) on 15 to 30 year old municipal solid waste recovered from drill cuttings. Due to the disturbance during auger drilling and subsequent sample reconstitution, the in-situ unit weight of the waste could not be determined. The standard effort compaction testing was conducted to estimate the probable range of dry unit weights for the waste material. A maximum dry unit weight of 9.3 kN/m^3 was achieved at a moisture content of 31%. Saturation of the sample occurred at approximately 70% moisture content and a unit weight of 8 kN/m^3. At 31% moisture content, a theoretical maximum dry unit weight of 12 kN/m^3 was estimated from the zero air voids curve.

Itoh (2005) conducted low effort (550 kJ/m^3 in comparison to 600 kJ/m^3 for standard) compaction tests on a select waste mixture and determined a maximum dry unit weight of 5.9 kN/m^3 at 20% moisture content. Higher effort tests (2,500 kJ/m^3 compared to 2,700 kJ/m^3 for modified compaction tests) resulted in a maximum dry unit of 7.8 kN/m^3 at 10% moisture content.

Hettiarachchi (2005) conducted similar experiments on a laboratory produced waste with a maximum particle size of 12.5 mm and determined a maximum dry unit weight of 5.15 kN/m^3 at 62% moisture content using standard compactive effort. The laboratory waste was generated to simulate the average composition of U.S. municipal solid waste. The composite specific gravity of the waste mixture was determined to be 1.6.

Reddy et al. (2008a) conducted standard compaction tests on waste samples obtained from the field. Samples were screened to ensure that the maximum particle size did not exceed 40 mm. Reddy et al. (2008a) reported an optimum moisture content of 70% and a maximum dry unit weight of 4.12 kN/m^3 for samples compacted using the standard compaction method. Data obtained from the tests performed by Reddy et al. was compared to the data obtained by Hettiarachchi (2005). The differences in maximum dry unit weight and moisture content were attributed to differences in maximum waste component size and well as component size distribution.

Overall, limited data has been reported for trends of waste compaction. Previous investigations have involved laboratory experiments with generally lower compactive effort than what is common in landfill applications.

2.5 Compressibility

Settlement in soil is the reaction to stress or loading leading to straining of the material. Soil settlement has been studied at length and is relatively well understood (Terzaghi and Peck 1948, Holtz and Kovacs 1981, Das 1987, Salgado 2006). In this section, soil settlement mechanisms are first briefly discussed to establish a framework for investigating waste compressibility. Next, a review of the literature regarding waste settlement is presented.

2.5.1 Soil Compressibility

The application of stress in soils is often a result of construction of a building or earthen structure at the site and is considered one-dimensionally. In this section, mechanisms of soil settlement are discussed. Next, the relationship between the application of stress and strain for soil is described and discussed.

Quantification of the compression of soils in response to loading is complicated by the non-linear and non-conservative response of soils to loading (Terzaghi and Peck 1948). Non-linearity of soil response may be described as a change in strain rate despite a constant increase in stress (Holtz and Kovacs 1981). The non-conservative nature of soils may be described as soil memory, akin to plastic deformation in other materials (Holtz and Kovacs 1981).

The total amount of compression of a soil is the sum of three mechanisms: elastic compression, consolidation, and secondary compression, or creep. Elastic compression of soil occurs as a result of the application of load to the soil, resulting in compression of the voids within the soil matrix and rearrangement of the soil particles into a tighter packing structure. Elastic compression of soil is a function of initial void ratio, applied stress, and stress history of the soil.

The application of load to soils is generally considered to result in an elastic response. Although the portion of settlement described as elastic settlement is not truly elastic, it is often approximated with the use of elastic theory. Elastic settlement occurs in an undrained state, prior to dissipation of excess pore pressures due to loading (Lambe and Whitman 1969).

Consolidation occurs as the water within the soil pore space is expelled by continued loading and is time-dependent. Continued settlement due to consolidation is generally more pronounced in fine grained soils as the hydraulic conductivity is lower and the rate of pore water drainage is orders of magnitude lower than that of coarse grained soils. Consolidation of soils is often approximated using Terzaghi's one-dimensional consolidation theory (Terzaghi and Peck 1948).

Secondary compression of soils occurs after excess pore water pressure has dissipated and at constant effective stress. The secondary compression of soils is time dependent and is particularly problematic in organic soils such as peats (Holtz and Kovacs 1981).

In addition to having different phases of settlement, the stress-strain behavior of soil is affected by compaction moisture content. Seed and Chan (1959) performed unconsolidated, undrained triaxial compression tests on two silty clay samples, one compacted dry of optimum and one compacted wet of optimum. They reported that the sample that was compacted dry of optimum had a higher initial stress-strain slope than the sample compacted wet of optimum. They attributed the measured differences to the difference in soil structure resulting from different compaction moisture contents.

Seed and Chan (1959) showed that the strength of compacted clay peaked dry of optimum. The curves reported by Seed and Chan showed a significant decrease in

strength at a specific moisture content dry of optimum. At higher levels of strain, the drop in strength, although similar in magnitude, was drawn out over a larger range of moisture content.

The stress-strain compression behavior of soil during confined compression may be described as a three part process, as detailed in Lambe and Whitman (1969). For soil, the initial portion of the stress-strain diagram shows locking (stage 1), as evidenced by an upward concavity in the plot as soil grains interlock and voids are closed. Continued stress begins to yield/crush particles, breaking off angularities and edges of soil grains, resulting in a yielding behavior, as illustrated by a downward concavity of the stress-strain plot (stage 2). Further yielding of the soil grains then begins to force the new particles to be packed into the existing voids, resulting in a tighter packing structure, more locking, and yet another change in the concavity of the stress-strain plot (stage 3).

Mechanical compression characteristics of a soil are commonly plotted on a void ratio or strain versus log stress curve. The curve is commonly approximated as a bilinear curve. The point of inflection of the curve is generally understood to represent the highest previous stress that the soil or material has been subjected to, which is known as the preconsolidation stress (Terzaghi and Peck 1948). The recompression index, c_r, represents the slope of the tangent line to the recompression curve that is located to the left of (lower stress than) the preconsolidation stress. The compression index, commonly denoted as c_c, is the tangent to the compression curve at stresses greater than the preconsolidation stress. A graphic illustrating a general void ratio versus log stress curve is presented in Figure 2.

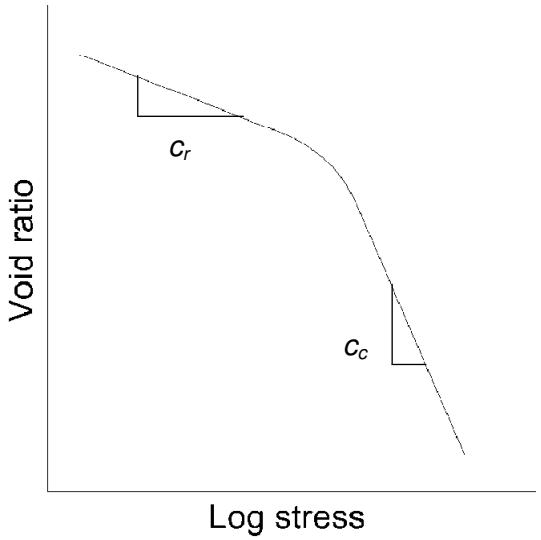

Figure 2. Void ratio versus log stress compression curve

The compression index may be used to predict the change in void ratio (and hence change in strain or settlement) for normally consolidated soils based on a change in applied stress. To account for differences in initial void ratio, it is common to calculate the compression ratio, defined in Equation 2.

$$c_{c\varepsilon} = \frac{c_c}{1+e_o} \tag{2}$$

where:

$c_{c\varepsilon}$ = compression ratio

c_c = compression index

e_o = initial void ratio

Soils with larger values of compression index will have greater settlement under loading than soils with smaller values of compression index. Values of c_c can range from 0.15 for Chicago Clay to 15 for peats (Holtz and Kovacs 1981).

Peat soils exhibit significant settlements including a large fraction of secondary compression. Peat generally has high compositional variability, high compressibility,

and large settlements (Edil and den Haan 1994, Mesri and Ajlouni 2007). Peat soils are similar to wastes in that both have significant spatial variability and exhibit significant magnitudes of secondary compression.

2.5.2 Waste Compressibility

Quantifying compressibility characteristics in MSW is more complex than doing so in soils due to its heterogeneity and the interaction of a variety of non-uniform particles. According to Jessberger et al. (1995), special attention must be paid to municipal solid waste because it has to be regarded as a mixture of soil-like and non soil-like components. Several of the mechanisms of MSW settlement coincide with the theories of soil mechanics, while others are specific to waste. Waste settlement is commonly subdivided into different phases attributed to different mechanisms. In this section, the different mechanisms of waste settlement are discussed. Next, issues specific to waste settlement are discussed. Finally, a brief discussion of MSW settlement modeling is conducted.

Historically, the settlement of municipal solid waste has been modeled after the settlement of soil (Sowers 1973). The settlement of municipal solid waste has been attributed to numerous mechanisms (Sowers 1973, Murphy and Gilbert 1985, Boutwell and Fiore 1995, Liu et al. 2006). When calculating waste settlement specifically, three general mechanisms are agreed upon: initial mechanical compression, raveling, and decomposition (Sowers 1973, Bjarngard and Edgers 1990, Edil et al. 1990, Liu et al. 2006).

Sowers (1973) includes a fourth settlement term relating settlement to physico-chemical change within the MSW. Liu et al. (2006) further separates settlement into five parts that include instant mechanical compression, secondary/continued

mechanical compression, creep effects, primary decomposition, and residual deformation and continued organic decomposition.

Interaction amongst the previously listed mechanisms may function to enhance or degrade the effects of the other mechanisms in a feedback loop (Sowers 1973, El-Fadel and Khoury 2000). For example, corrosion and break down of a hollow steel component of MSW (e.g., a cooking pot) would allow enhanced raveling within the waste mass in that area.

To quantify the total settlement of waste with the theories of soil mechanics, it is necessary to sum the effects of three interrelated components: initial mechanical compression, mechanical creep/raveling, and decomposition as presented in Equation 3. Additional terms have been included by different researchers.

$$s_t = s_i + s_c + s_d \tag{3}$$

where:

s_t = total settlement (length)

s_i = initial mechanical compression (length)

s_c = mechanical creep/raveling (length)

s_d = decomposition (length)

The first stage of MSW settlement consists of mechanical compression of waste materials. Mechanical compression, the only portion of waste settlement that is stress dependent (Sowers 1973), begins as soon as load is applied. Mechanisms that may contribute to mechanical compression include: compression of air filled voids, compression of loose, resilient materials, slippage between particles, reorientation of particles, bending of particles, and lateral expansion (Sowers 1973, Bjarngard and Edgers 1990, Bleiker et al. 1995). As defined by Sowers (1973), initial mechanical compression includes bending, crushing, mechanical distortion, and reorientation of

materials, similar in nature to the consolidation of organic soils. The amount of settlement attributed to mechanical compression of waste materials is believed to decrease with time although it is difficult to differentiate the effects of the different settlement mechanisms from each other (Dixon and Jones 2005).

The addition of load to MSW may result from overlying wastes, self-weight, daily soil covers, a landfill cap, or buildings or other infrastructure constructed on top of the landfill. It becomes necessary to quantify waste settlement to effectively design buildings and other structures that are built on or around the landfill as well as predict landfill capacity.

The second mechanism of MSW settlement consists of settlement involving raveling/creep, or movement of finer components into the voids between larger particles (Sowers 1973, Bjarngard and Edgers 1990). The voids may be a result of initial placement/orientation or may develop as a result of physico-chemical or biological changes within the waste mass (El-Fadel and Al-Rashed 1998). Raveling can result in localized, uneven settlements (Zoino 1973). Current placement procedures at landfills generally segregate out large, hollow items (Bjarngard and Edgers 1990) and as a result, the effects of raveling are considered less important in current landfill design and operation than the effects of creep.

The remaining mechanisms of settlement are solely time-based mechanisms. Although the mechanisms have been included for completeness, they were not explicitly examined within the test program.

Physico-chemical change is the contribution of corrosion, oxidation, and combustion to waste settlement (Sowers 1973). This mechanism is similar to decomposition in that it both affects and is affected by the other settlement mechanisms.

For example, increased leachate production may lead to a condition similar to that previously described for interaction between individual waste settlement mechanisms.

Decomposition or biodegradation includes fermentation and decay and plays a major role in the amount of long term settlement of a waste mass, estimated between 18% and 24% of total waste mass thickness (Coduto and Huitric 1990). Waste settlement due to decomposition is commonly divided into the two stages of aerobic and anaerobic decomposition (Tchobanoglous et al. 1993). The waste mass will begin in a state of aerobic decomposition. As the biological reactions are completed, available oxygen will be depleted and the organisms responsible for anaerobic decomposition will begin to dominate the remainder of decomposition settlement (Edgers et al. 1992). There is a significant amount of conversion of solid matter to gas and liquid within both portions of decomposition. The conversion of solids changes the void ratio and may feed back into the mechanism of raveling and creep.

It is difficult to quantify many of the parameters necessary to accurately predict the biological mechanisms responsible for waste decomposition (El-Fadel and Khoury 2000) although it is necessary for accurate prediction of waste settlement. Various settlement models (Yen and Scanlon 1975, Edil et al. 1990) are refined when decomposition effects are taken into account (Edgers et al. 1992, Lee and Park 1999, El-Fadel and Khoury 2000, Park and Lee 2002).

Other environmental factors may affect the magnitude and rate of settlement for waste. For example, temperature may play a role in the settlement characteristics of waste. Lamothe and Edgers (1994) found that waste compressibility increased nearly twofold for a synthetic waste material heated from 20°C to 35°C in laboratory tests. The

increased compression was attributed to a softening of the particle contacts of the waste as well as a change in the structural viscosity of the material.

Unlike soil solids, which are generally considered incompressible, many of the solid components comprising MSW are compressible and may therefore undergo an increase in density and specific gravity as load is applied (Hudson et al. 2004, Hettiarachchi et al. 2005). Specific gravity is defined as the ratio of unit weight of solids to unit weight of water; an increase in specific gravity of a component results in a commensurate increase in the dry unit weight of that component. Variation of moisture content and initial composite dry unit weight would have the potential effect of changing the specific gravity of the individual components. Change in specific gravity of the individual waste components will affect the measured composite, or general, properties of the waste mass.

Hudson et al. (2004) quantified the increase in specific gravity of field obtained laboratory samples and reported an increase in specific gravity of waste solids from 0.876 to 1.303 as a result of a stress increase from 34 kPa to 463 kPa. The stress increase also resulted in an increase in dry unit weight from approximately 3.8 kN/m^3 to 7.0 kN/m^3.

Sowers (1973) proposed that, to mitigate excessive landfill settlements, it might be desirable to control environmental factors to retard decomposition (known as dry tomb landfilling), thereby reducing decomposition related settlement. That stands in contrast to the current trend of bioreactor landfills where numerous techniques are employed to expedite decomposition and settlement. This has been a result of a fundamental shift in the approach to landfill settlement.

Even when a sufficient understanding of the variety of mechanisms responsible for waste settlement is achieved, further difficulty arises due to the variability of waste through time, from region to region, and even from one portion of a landfill to another (Dixon and Jones 2005). The heterogeneity of component properties within the waste mass adds additional complexity to attempts to monitor and model waste settlement.

The quantification of waste settlement has been based on the monitoring of actual waste settlement, followed by modeling to project future settlement. Numerous researchers have conducted field monitoring of waste settlement (Merz and Stone 1962, Coduto and Huitric 1990, Grisolia et al. 1995, El-Fadel and Al-Rashed 1998).

Other researchers have used large-scale laboratory testing of field obtained waste samples in an attempt to preserve the heterogeneity and structure of the waste for investigating advanced behavior of wastes. For example, Hudson et al. (2004) measured the effects of pore water pressure and gas accumulation upon the change in composite density and drainable porosity of field obtained waste samples in a large-scale testing device.

Numerous models have been proposed to estimate settlement of waste materials. Each model is based on one of four different fundamental approaches including: soil-mechanics based models (Sowers 1973, Rao et al. 1977, Oweis and Khera 1986, Morris and Woods 1990), rheological models for soil applied to waste (Gibson and Lo 1961, Zimmerman 1972), empirical models (Yen and Scanlon 1975, Edil et al. 1990, Deutsch et al. 1994, Ling et al. 1998), and biodegradation-induced settlement models (El-Fadel et al. 1989, Edgers et al. 1992, Soler et al. 1995, Park and Lee 1997). Marques et al. (2003) proposed a composite settlement model for waste that included instantaneous mechanical, time based mechanical, and decomposition

contributions to settlement. The Marques et al. model was a good fit with the field reported settlements at a local landfill based on the use of parameter values.

The aforementioned models were developed to predict the settlement based on either laboratory prepared or field samples of MSW while others mentioned above were based on field measurements. Specific waste mixtures were monitored for settlement and mathematical models were fit to their settlement curves with the aid of fitting factors that were site and composition specific. It is unknown whether use of the models on other waste compositions would yield satisfactory results. As such, the models tend to be composition/location specific and extrapolation of the trends implied by the models is difficult.

Currently available literature documents a wide variety of geotechnical studies on both field and laboratory waste samples. Sample disturbance, representative sampling, and heterogeneity limit the applicability of data obtained from field-derived samples. To date, the data gathered on laboratory synthesized MSW has been based on relatively simple waste samples. Limitations of manufactured waste include limited particle size heterogeneity and particle shape. A laboratory manufactured sample with additional particle size and compositional heterogeneity will ensure specimen heterogeneity.

Limited data has been reported related to trends in MSW behavior based upon initial placement conditions including moisture content and dry unit weight. Specific laboratory and field determined settlement values, while suitable for documentation of conditions at specific landfills with specific waste mixtures, are difficult to extrapolate to other sites of different waste streams. Gaining a better understanding of the trend based effects of different placement parameters on waste settlement will aid in calibration of

the models and provide a generalized framework in which to understand fundamental behavior of waste.

2.6 Hydraulic Conductivity

Hydraulic conductivity measures the facility with which a permeant liquid may move through a material. The hydraulic conductivity relates the velocity of a fluid through a porous medium to the hydraulic gradient. In this section; the mechanisms controlling the flow of permeant liquid through soil are discussed along with several of the factors that complicate the understanding of flow through soils. The conduction of permeant liquid through MSW is discussed. Relationships between the mechanisms responsible for control of soil hydraulic conductivity and MSW are discussed. Finally, issues specific to the hydraulic conductivity of wastes are detailed.

2.6.1 Soil Hydraulic Conductivity

Hydraulic conductivity in soils is commonly used within Darcy's Law to determine the velocity of liquid through a soil as a function of the hydraulic gradient as presented in Equation 4.

$$v = ki \tag{4}$$

where:

v = velocity (length/time)

k = hydraulic conductivity (length/time)

i = hydraulic gradient (length/length)

Darcy's Law is based on the premise that flow is laminar, steady, and through a saturated media. Once flow reaches a critical state, flow becomes turbulent and Darcy's Law is no longer valid but as long as the aforementioned premises are upheld, fluid velocity will increase linearly with increased hydraulic gradient. Multiplication of both

sides of the equation by the cross-sectional area normal to the direction of flow expands the equation to describe the flow (in volume) as the product of the hydraulic conductivity, gradient, and area.

Although Mitchell and Soga (2005) stated that as long as all system variables are held constant, Darcy's Law is valid, numerous studies have been conducted demonstrating Darcy's law to be invalid under specific conditions in soil. Factors that may account for the non-linear correlation of flow with gradient include: localized zones of consolidation or swelling, non-Newtonian water flow properties, and migration of fine particles that may result in blocking and unblocking of flow paths (Mitchell and Soga 2005). Research has disproven any significant relationship between unusual/non-Newtonian fluid properties and non-linear flow behavior and as such, the remaining factors that may invalidate Darcy's law are swelling/consolidation zones, and migration of fines.

Swelling particles may have a significant effect on the hydraulic conductivity of soils through alteration of the soil fabric. Soil fabric is defined by Holtz and Kovacs (1981) as the geometric arrangement of particles whereas soil structure includes both the fabric and interparticle forces. With swelling, flow pathways may close and the tortuosity of the flow path to any permeant liquid may increase. Research performed by Hardcastle and Mitchell (1974) indicated that the hydraulic conductivity of soil mixtures with increasing amounts of swelling clay experienced up to an 80% decrease in hydraulic conductivity.

It has been demonstrated that particle migration may cause non-linearity in the relationship between flow and hydraulic gradient (Mitchell and Soga 2005). This effect may be especially pronounced for soils in which there are particles that are not load

bearing. The low intraparticle stress on the non-load-bearing particles may allow displacement by even moderate hydraulic gradients. As with swelling particles, the migration of non-load-bearing particles may have the effect of blocking flow pathways and shifting the distribution of voids, resulting in decreased hydraulic conductivity.

For the examination of hydraulic conductivity in clays, the soil fabric is considered on three levels: the microfabric, the minifabric, and the macrofabric (Mitchell and Soga 2005). The microfabric of a soil describes the individual soil components and their assemblage (as in the flocculated clay structures and the voids formed within each). The minifabric is related to the packing of the microfabric structures. The resulting interconnection of the pores between flocculated clay structures determines hydraulic conductivity at the minifabric level. The macrofabric includes large voids within the soil structure including cracks, holes, and other large pores that may potentially dominate the flow through the soil. Modification and understanding of the soil fabric is necessary to fully comprehend and control the hydraulic conductivity of a soil because differing compaction conditions may result in variable hydraulic conductivity values. As demonstrated by experiments performed by Benson and Daniel (1990), the hydraulic conductivity values for clays were strongly dependent upon the compaction conditions which were used to modify the soil fabric.

The hydraulic conductivity of the MMSW was found to decrease with increasing moisture content. Lambe (1958b) showed that for a Jamaica sandy clay, the hydraulic conductivity decreased toward an asymptotic low value as moisture content of the soil increased. Mitchell (2005) reported similar results for a silty clay compacted under constant effort. The tests on both the sandy clay and silty clay showed a decrease in hydraulic conductivity as moisture content was increased to the optimum moisture content. Wet of optimum, the hydraulic conductivity of the soils remained in a minimum

range and was less sensitive to changes to increasing moisture content. The decrease in hydraulic conductivity in soils was attributed to a weakening of the flocculated structure by additional water that became more susceptible to changes in fabric. The weakened structure was reoriented through the application of compactive effort into a less permeable configuration.

Anisotropy is another factor affecting the hydraulic conductivity of soils. Anisotropic flow may result from the orientation of platy particles or stratification of deposits. Research performed by Mitchell (1956) has revealed ratios of horizontal to vertical hydraulic conductivity ranging from less than 1 to greater than 7 in undisturbed clays.

Hydraulic conductivity in sands and some silts is largely a function of void ratio. A direct proportionality exists between the hydraulic conductivity of uniform sands and the void ratio term (presented in Equation 5 as the right most term of the equation) of the Kozeny-Carman equation.

The Kozeny-Carman (1956) equation for calculation of the permeability through a porous media is an alternative method for calculation of the hydraulic conductivity that factors in properties of the permeant liquid, tortuosity of the flow path, and particle shape, and void ratio. The Kozeny-Carman equation has been demonstrated to work well for uniformly graded sands and silts but is not effective for clay type soils (Lambe and Whitman 1969, Mitchell and Soga 2005). The Kozeny-Carman equation (as presented in Lambe and Whitman 1969) is presented in Equation 5.

$$k = \frac{1}{k_0 S^2}\left(\frac{\gamma}{\mu}\right)\frac{e^3}{(1+e)} \quad (5)$$

where:

k = hydraulic conductivity

k_0 = Kozeny-Carman empirical factor

S = specific surface area per unit volume of particles

γ = unit weight of permeant

μ = viscosity of permeant

e = void ratio

The hydraulic conductivity of a soil is a function of the degree of saturation, effective grain size, fabric, void ratio, composition, pore geometry/tortuosity, and fluid characteristics (Lambe 1951, Lambe and Whitman 1969, Hillel 1971, Holtz and Kovacs 1981). Significant difficulty has been encountered during attempts to separate out the effects of the various factors affecting soil hydraulic conductivity. As with the mechanisms responsible for the compression/settlement of waste, the mechanisms controlling hydraulic conductivity are coupled and it is difficult to discern between the contributions of individual mechanisms although it is known that both fabric and void ratio play large parts in influencing specimen hydraulic conductivity.

Peats may be considered an intermediate between soil and waste. Both materials have high heterogeneity, large void ratios, high variation in particle size and shape, and relatively large moisture contents (compared to conventional inorganic soils). The unique structure of peats results in widely variable hydraulic conductivity that ranges from the values typically determined for sands to those typically determined for clays. Mesri and Ajlouni (2007) report hydraulic conductivities for peat varying from $1x10^{-10}$ cm/s to $1x10^{-2}$ cm/s, decreasing with decreasing void ratios and with increasing overburden stress. There is a great amount of variability in the hydraulic conductivity of soils and peats as well as MSW.

2.6.2 Waste Hydraulic Conductivity

The hydraulic conductivity of a waste mass is more difficult to accurately determine than that of an equivalent soil mass. The heterogeneity of waste introduces variables not present in the determination of the hydraulic conductivity of soils. Certain components of MSW may act similarly to granular soils, while other components may behave as clay soils with respect to hydraulic conductivity.

The majority of the models used to estimate the hydraulic conductivity of soil assume a saturated condition, which is rarely the case for wastes in landfills (Capelo and DeCastro 2007). As well, Darcy's Law, which is commonly used, assumes laminar flow throughout the microfabric of the soil mass whereas a waste mass may also have macropores (resulting from changes within the macrofabric) in which water may begin to flow turbulently, leading to a non-linear increase in fluid velocity with hydraulic gradient (Capelo and DeCastro 2007). The variability of conditions and test materials has led to a wide range of reported hydraulic conductivities. Examples of the variability of hydraulic conductivity in MSW are presented in Table 2.

Numerous researchers have reported that the hydraulic conductivity in a waste mass varies as a function of burial depth or effective stress (Landva and Clark 1990, Powrie and Beaven 1999, Jain et al. 2006, Reddy et al. 2008b) similar to the trends observed for peats. Unit weight may be related to effective stress through burial depth; as effective stress increases due to increasing burial depth, the change in void ratio and compression of waste components may lead to an increase in unit weight. A study performed by Landva and Clark (1990) was conducted to measure the hydraulic conductivity of waste as a function of unit weight. Results of testing performed by Landva and Clark showed variation in hydraulic conductivity between $1x10^{-3}$ cm/s and

$4x10^{-2}$ cm/s in waste obtained from various Canadian landfills with moist unit weights varying between approximately 10 kN/m^3 and 14.5 kN/m^3 (1990).

Table 2. Survey of Published Hydraulic Conductivity Data
(as presented in Jain et al. 2006)

	Reference	Hydraulic conductivity (cm/s)	Direction	Test
Laboratory	Fungaroli and Steiner (1979)	$10x10^{-4}$ to $10x10^{-2}$	Vertical	Constant head
	Korfiatis et al. (1984)	$8\ x10^{-3}$ to $1.3\ x10^{-2}$	Vertical	Constant head
	Noble and Arnold (1991)	$8.4x10^{-5}$ to $6.6\ x10^{-4}$	Vertical	Constant head
	Bleiker et al. (1993)	$1\ x10^{-8}$ to $3\ x10^{-7}$	Vertical	Falling head
	Chen and Chynoweth (1995)	$4.7\ x10^{-5}$ to $9.6\ x10^{-2}$	Vertical	Constant head
	Landva et al. (1998)	$2\ x10^{-6}$ to $2\ x10^{-3}$	Vertical	Constant head
	Landva et al. (1998)	$4\ x10^{-5}$ to $1\ x10^{-3}$	Horizontal	Constant head
	Powrie and Beaven (1999)	$3.7\ x10^{-6}$ to $1.5\ x10^{-2}$	Vertical	Constant head
	Jang et al. (2002)	$2.91\ x10^{-4}$ to $2.95\ x10^{-3}$	Vertical	Constant head
Field	Ettala (1987)	$5.9\ x10^{-3}$ to 0.25	Vertical	Pumping test (Jacob method)
	Oweis et al. (1990)	$1.0\ x10^{-3}$ to $2.5\ x10^{-3}$	Vertical	Pumping test (Theis method)
	Shank (1993)	$6.7\ x10^{-5}$ to $9.8\ x10^{-4}$	Vertical	Slug test
	Townsend et al. (1995)	$3\ x10^{-6}$ to $4\ x10^{-6}$	Vertical	Zaslavasky wetting front
	Landva et al. (1998)	$10\ x10^{-3}$ to $3.9\ x10^{-2}$	Vertical	Flow nets
	Wysocki et al. (2003)	$1.2\ x10^{-5}$ to $6.3\ x10^{-4}$	Vertical	Pumping test

The trend showing a decrease in hydraulic conductivity with increasing unit weight observed by Landva and Clark was later corroborated by work performed by Al-Thani et al. (2003), Durmusoglu et al. (2006), and Reddy et al. (2008b). Al-Thani et al. (2003) were able to model hydraulic conductivity at varying depths within a large scale test cell by varying the vertical load applied to the test waste material. The work performed by Al-Thani et al. (2003) demonstrated the trend of decreasing hydraulic conductivity with increased depth. The depth of burial of the waste was modeled

between 10.5 meters and 29.5 meters. Both the calculated best fit and worst case hydraulic conductivities decreased a minimum of one order of magnitude with variation of the simulated depth of burial.

Measurement of hydraulic conductivity in waste masses may be complicated by the inclusion of materials of significantly different hydraulic conductivity. The horizontal deposition and compaction processes used in landfills structures the waste in a way that tends to orient materials horizontally, creating a discontinuous, impermeable boundary to vertical water or leachate flow (Xie et al. 2006, Olivier and Gourc 2007). Flat, impermeable sheet-like components such as plastics may greatly alter the fabric of the material with respect to the predominant flow paths. As well, the use of horizontally deposited cover soils (daily and interim) of differing hydraulic conductivities and thicknesses introduces further heterogeneity to the flow regime within landfills. Due to the potentially significant difference in hydraulic conductivity of cover soils, field measured hydraulic conductivity values, while representative of landfill system behavior, may be less representative of waste material hydraulic conductivities.

The effects of placement in lifts, horizontal orientation of components, and use of cover soil will often cause waste to behave anisotropically in regards to hydraulic conductivity, with higher conductivity in the horizontal as opposed to the vertical direction (Xie et al. 2006, Dixon and Jones 2005). All the factors that may be sources of variability in the measurement of hydraulic conductivity of soil are present in waste. MSW is heterogeneous, has large variability in particle size and shape, is often deposited in a stratified manner with a predominant particle orientation (perpendicular to gravity flow), has particles susceptible to particle migration, has components that may swell, and is comprised of a mixture of compressible and non-compressible components.

Measurement of hydraulic conductivity in wastes is complicated by the transient nature of the test material. Olivier and Gourc (2007) stated that instantaneous hydraulic conductivities may be more “instructive” than values obtained by averaging the data over the length of the test. One factor supporting Olivier and Gourc’s statement may be based on the idea proposed by Chen and Chynoweth (1995) that hydraulic conductivity of waste will continue to vary with time as the test material changes.

The concept of transient hydraulic conductivity was supported in work done by Chen and Chynoweth (1995) that reported 3 distinct phases of MSW hydraulic conductivity as a function of time. The phases consisted of an initial sharp decrease followed by a sharp increase and concluded with a gradual decline of measured hydraulic conductivity. As such, ASTM standards for hydraulic conductivity testing may or may not have suitable termination criteria in regards to maximum allowable percentage variance over subsequent measurements for MSW.

As waste components swell, rearrange, and are broken down, the fabric of the waste changes with time. Consequently, long periods of time are required to reach steady state conditions. Xie et al. (2006) stated that, for a sample of similar size to that used in this test program (maximum particle size of 40 mm), the minimum time necessary to reach a steady state between inflow and outflow would be approximately 1 to 4 months.

Durmusoglu et al. (2006) determined that the hydraulic conductivity of wastes was not particularly sensitive to the applied hydraulic gradient. As such, it is likely that composition and placement conditions were partially responsible for the wide variation of measured hydraulic conductivities. No experimental programs were identified that attempted to quantify the effect of the variation of both molding moisture content and dry

unit weight on the hydraulic conductivity on waste. Similar to the laboratory testing that has been performed for measurement of compressibility, the currently available data are based on simplified waste mixtures that may or may not accurately represent actual waste. Examination and understanding of general trends within waste mechanics may be more illustrative than individual values that will inherently be tied to specific waste mixtures and test conditions.

2.7 Shear Strength

This section will detail the current state of knowledge regarding shear strength in soils and waste. A basic review of soil shear strength is performed. The factors influencing the development of MSW shear strength are discussed in the framework of soil mechanics. Lastly, mechanisms specific to shear strength in waste are documented.

2.7.1 Soil Shear Strength

In soils, strength is measured in terms of shear strength. Soils do not generally have much, if any, strength in tension due to the particulate composition of soils. Shear strength in soils is the resistance to shear deformation of the soil mass and is described by internal angle of friction and cohesion. Shear strength in soils results from particle interlocking, particle interference, and sliding resistance (Terzaghi and Peck 1948).

Internal angle of friction (ϕ) is a function of mineralogical composition, shape, gradation, void ratio, and organic content of the soil and is measured in degrees (Holtz and Kovacs 1981, Coduto 1999). The contribution of friction angle to the shear strength of a soil is a function of the vertical effective stress at a given point in the soil. A higher confining stress on the soil element will result in a higher frictional component of shear strength as presented in Equation 6.

Cohesion is interparticle attraction (Bowles 1997) or tendency of a soil to adhere to itself. Cohesion is independent of the effective stress in the soil (Holtz and Kovacs 1981) and is a function of the colloidal forces within soil. The shear strength of a soil is typically described by the Mohr-Coulomb failure criteria (Holtz and Kovacs 1981):

$$s = \sigma(\tan\varphi) + c \tag{6}$$

where:

s = shear strength (force/area)

σ = effective stress (force/area)

ϕ = effective internal angle of friction (°)

c = cohesion (force/area)

The shear strength envelope is plotted on a shear stress versus normal stress plot. Coarse grained soils generally have little to no cohesion and greater internal angles of friction whereas fine grained soils generally have a strength envelope dominated by cohesion with lower internal angles of friction. Description of the strength behavior of sand and clay soils follows.

As moisture content in clay soil is increased, the mechanisms responsible for the shear strength change. When the clay soil is dry of optimum, the soil tends to behave more like a cohesionless soil, with a relatively high angle of friction and low cohesion as potentially angular, flocculated structures dominate the shear strength behavior. As the clay soil approaches optimum moisture content the internal angle of friction decreases and the cohesion increases to maximum cohesion at optimum moisture content (Cokca et al. 2004). This response is due to the breakdown of the flocculated structures, which decreases frictional resistance to shearing and to increasing moisture content, which lubricates the movement of clay particles past each other.

The shear strength of sands is not as sensitive to changes in moisture content as in clays. Instead, shear strength of sandy soils is primarily dependent on relative density, void ratio, and gradation (Holtz and Kovacs 1981). Better grading of sandy soils also tends to increase internal angle of friction. With other factors held constant; poorly graded materials have lower friction angles than well graded materials.

Frictional shear strength is also developed in peats. High friction angles have been reported for peat by numerous researchers. Values within the 50° to 60° range are not uncommon for fibrous peats tested in triaxial compression (Mesri and Ajlouni 2007). However, large strains are required to mobilize the maximum frictional resistance in fibrous peats, on the order of 5 to 10 times that required for mobilization of friction angle in soft clay.

2.7.2 Waste Shear Strength

Multiple factors including scaling/boundary effects and representative heterogeneity have made the laboratory determination of shear strength values of MSW challenging. Kockel and Jessberger 1995 (as reported by Jessberger et al. 1995) have suggested that the fabric of waste with regard to shear strength may be modeled as an aggregate of particles smaller than 120 mm in size within a reinforcing matrix of fibrous particles greater than 120 mm in size.

Numerous studies have been conducted to evaluate MSW shear strength in the laboratory. As with the majority of MSW geotechnical data, properties are site- and composition-specific and vary greatly. Gabr and Valero (1995) have suggested that shear strength parameters may vary as a function of specimen age, composition, size, and density. Edincliler et al. (1996) also includes pre-test processing, the test method, and test conditions in the list of factors influencing the shear strength parameters.

Often, interpretations of MSW shear strength studies assumed that waste shear strength is based heavily on friction and has little to no cohesion component (Siegel et al. 1990, Howland and Landva 1992). Previously determined shear strength parameters are listed in Table 3. There is a large amount of variability in the shear strength parameters of municipal solid waste based on a variety of testing conditions.

Measured values of internal angle of friction presented in Table 3 vary from 15° to 59° with a mean value of approximately 30°. Values varied by as much as 26° within one set of results from an individual investigation (e.g., Kavazanjian 2001). The measured values of cohesion presented in Table 3 vary from 0 kPa to 64 kPa with an average value of 14 kPa.

Numerous MSW shear strength values have been gathered from field data or back-calculated from slope failures or cut slope experiments. Shear strength values determined from field samples show a wide range due to the large variety of possible compositions. The use of cover soil in current landfills adds compositional heterogeneity and strength anisotropy to field gathered waste samples (Jain et al. 2006). The horizontal compaction of waste tends to orient large, fibrous particles in the horizontal plane (Bray et al. 2009), affecting the interlocking of components that is responsible for waste shear strength at high strains.

It is advantageous to use laboratory tests to eliminate some of the uncontrollable variability that may influence the data collected from field shear strength tests. Unfortunately, problems arise with the use of laboratory tests including the necessity of disturbing and remolding MSW (if samples are obtained from operating landfills) and use of a representative waste (if laboratory generated) that still duplicates field conditions closely enough to be meaningful.

Table 3. MSW Shear Strength Parameter Summary (adapted from Dixon and Jones 2005)

Reference	Year	Cohesion (kPa)	ϕ (degrees)	Method	Notes
Landva and Clark	1986	19	42	Direct shear	Old refuse
Landva and Clark	1986	16	38	Direct shear	Old refuse
Landva and Clark	1986	16	33	Direct shear	Old refuse aged one additional year
Landva and Clark	1986	23	24	Direct shear	Fresh, shredded waste
Landva and Clark	1986	10	33.6	Direct shear	Wood waste/refuse
Siegel et al.	1990	0	39 to 53	Triaxial test	5 different compositions of waste, 16 -39% strain
Howland and Landva	1992	17	33	Direct shear	10 to 15 year old, 25% strain
Cowland et al.	1993	10	25	Direct shear	Deep trench in waste, suggested values
Del Greco and Oggeri	1993	15.7	21	Direct shear	Tests on baled waste, lower density bales
Del Greco and Oggeri	1993	23.5	22	Direct shear	Tests on baled waste, higher density bales
Golder and Associates	1993	0	41	Direct shear	Project specific testing
Jessberger	1994	7	38	Not stated	Reporting Gay and Kaiser (1981)
Jessberger	1994	10	15	Back analysis	Reporting Spillman (1980)
Jessberger	1994	10	17	Back analysis	Reporting Spillman (1980)
Jessberger	1994	0	30	Estimate	From field observations
Jessberger	1994	0	40	Estimate	From field observations
Jessberger	1994	7	42	Simple shear	Reporting Gay and Kaiser (1981). 9 month old MSW
Jessberger	1994	28	26.5	Suggested values	Reporting Gay and Kaiser (1981). Fresh MSW
Fassett et al.	1994	10	23	Suggested values	Suggested by authors
Kolsch	1995	15	15	Suggested values	Suggested by authors
Kolsch	1995	18	22	Back analysis	Suggested by authors
Gabr and Valero	1995	16.8	34	Triaxial test	Remolded drill cuttings
Gabr and Valero	1995	0 to 27.5	20.5 to 39	Direct shear	Remolded drill cuttings
Benson et al.	1996	20	35	Suggested values	Suggested by authors
Benson et al.	1996	24	42	Direct shear	For moist and soaked waste samples
Kavazanjian	2001	16 to 30	33 to 59	Simple shear	Fully degraded waste
Reddy et al.	2008	31 to 64	26 to 30	Direct shear	Fresh waste
Reddy et al.	2008	38	16	Triaxial test	Fresh waste

An envelope placing maximum and minimum expected bounds on shear strength parameters based on available data was published by Singh and Murphy (1990) and shows an inverse relationship between cohesion and friction angle in waste; an increase in frictional shear strength correlates with a decrease in apparent cohesion values. More recent shear strength data gathered by Edincliler et al. (1996) updated the Singh and Murphy shear strength envelope to be largely frictional with only a small portion of strength generated by cohesion. The updated envelope shown in Edincliler et al. (1996) is presented in Figure 3.

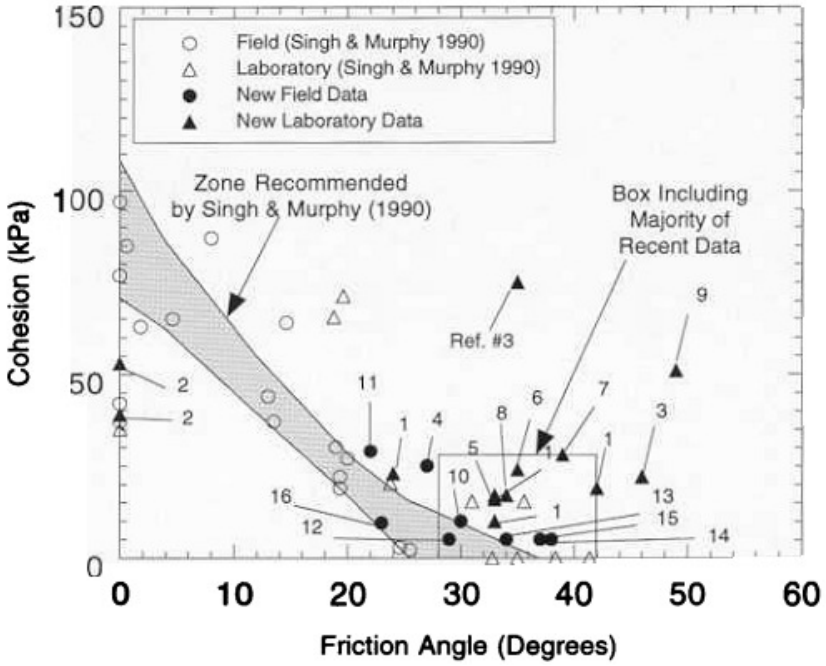

Figure 3. MSW cohesion versus friction angle as presented by Edincliler et al. (1996)

In laboratory and field data reported in Table 3, internal angles of friction in excess of 30° have been reported (Landva and Clark 1986, Jessberger 1994, Gabr and Valero 1995, Kavazanjian 2001, Bray et al. 2009). However, there appears to be reluctance to use friction angles in that range due to the large strain values that are

commonly necessary to mobilize the aforementioned friction angles (Siegel et al. 1990, Howland and Landva 1992, Gabr and Valero 1995, Kockel and Jessberger 1995).

Kavazanjian (2001) and Bray et al. (2009) related the large (greater than 20%) strain values necessary for mobilization of shear strength to the use of triaxial tests for determination of MSW shear strength. Similar to the high levels of strain required for mobilization of peak friction angles for peats, triaxial tests inherently strain the material significantly more than direct shear tests to reach the at-rest stress condition and as such, strain values to reach representative friction angles may be quite high. Kavazanjian (2001) and Bray (2009) report that the use of direct shear testing for determination of shear strength properties of MSW is appropriate.

There does not appear to be agreement from test to test regarding the strain rate and total displacement that should be used as termination criteria for the direct shear test for MSW. In laboratory testing relatively high strains are not uncommon, as waste continues to gain strength with increasing strain. Various researchers have tested for shear strength to differing levels of strain. Gabr and Valero (1995) tested a reconstituted waste sample to 10% strain in direct shear testing and to 20% in triaxial testing. Kavazanjian (1999) tested waste samples to 10% strain in direct shear. Caicedo (2002) determined shear strength values at 6.7% strain. Reddy et al. (2008a) tested fresh MSW to 15% strain.

Municipal solid waste has apparent cohesion as well as an internal angle of friction. Apparent cohesion in soils is the result of the capillary menisci between soil grains in partially saturated soils (Holtz and Kovacs 1981). In waste, the apparent cohesion is primarily a result of the fibrous components within the waste mass that interlock and act to provide reinforcement (Kockel and Jessberger 1995, Konig and

Jessberger 1997) as opposed to capillarity between particles. However, Konig and Jessberger (1997) reported that the activation of the tensile strength of the fibrous components within MSW requires large (on the order of 20%) strain. As well as the large strain required for mobilization, the effects of apparent cohesion in waste are also strongly dependent upon orientation with respect to the plane of shearing, with up to a two-fold difference in shear strength for samples tested under low normal stress in a direct shear apparatus based on sample orientation (Bray 2009).

Some analyses on the shear strength of MSW have incorporated multi-linear shear strength envelopes (Manassero et al. 1996, Landva and Clark 1990). These shear strength envelopes imply different mechanisms for the development of shear strength based on the level of overburden or confining stress similar to the bilinear failure envelope that has been proposed for some clays (Holtz and Kovacs 1981).

Limited information has been reported on the influence of placement conditions on shear strength of MSW. Although data for a variety of waste conditions exists, it has been collected through a wide variety of sampling or collection methods and tested or back calculated in different ways. As such, the data is generally not comparable. A systematic investigation is needed to evaluate shear strength parameter trends of MSW as a function of compaction conditions.

2.8 General Trends

General trends for soil geotechnical properties as a function of placement conditions were researched for comparison to waste. Figure 4 presents the general trends reported by various researchers as presented in Holtz and Kovacs (1981).

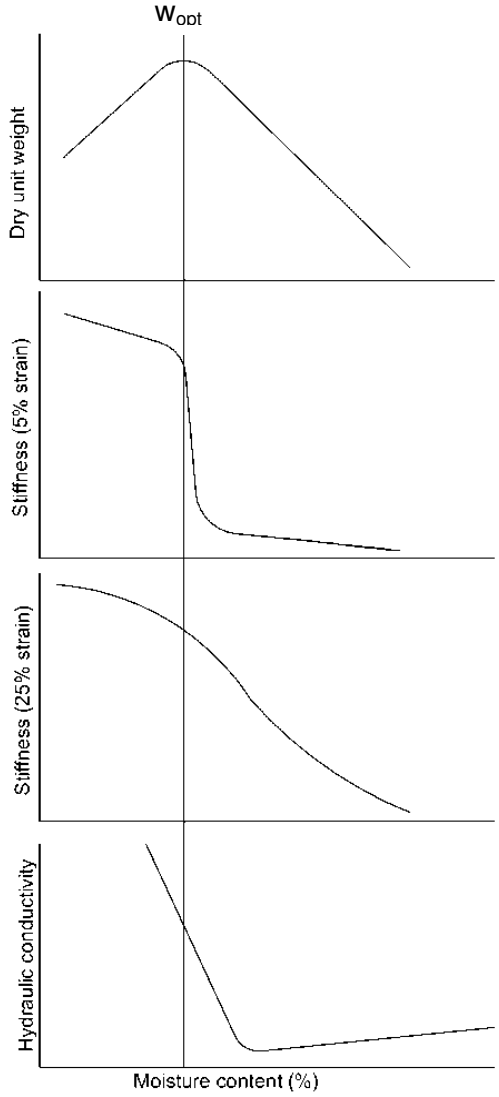

Figure 4. Engineering properties of soil as a function of compaction moisture content

Stiffness of soil at low strains decreases sharply wet of optimum. Stiffness of soil at high strains decreases more gradually. The hydraulic conductivity of the soil decreases sharply through optimum moisture content and continues to decrease to a minimum value, increasing slightly past the minimum value.

Chapter 3: Experimental Test Program

3.1 Introduction

A laboratory test program was undertaken to evaluate the engineering properties of MSW as a function of compaction conditions. The objectives of the test program were to establish the baseline compaction behavior for MSW (variation of dry unit weight with molding moisture content) and the geotechnical parameters associated with that baseline behavior. To ensure that the results were comparable, the test material was generated from the same stock of components mixed in the same ratios. Experimental procedures consisted of the determination of compression characteristics, hydraulic conductivity, and shear strength trends as a function of placement parameters such as molding moisture content and dry unit weight. By holding variables other than the placement conditions constant, it was possible to discern trends in the behavior of the MMSW and attempt to correlate the trends to established principles of soil and waste mechanics.

This chapter details the test program beginning with the description and classification of the test material. Documentation of the compaction testing follows. A brief discussion of the sample preparation methods used for the remainder of the test program is next. Development and description of test instrumentation and apparatuses along with test procedures for constant rate of strain compression, hydraulic conductivity, and shear strength testing completes the chapter.

3.2 Test Material

Manufactured municipal solid waste (MMSW) was assembled from various representative materials based on data released by the EPA (2008). Initial proportions were based upon EPA published data outlining proportions of waste as generated at the

source. The difference between the source waste stream and recovered waste streams was calculated to determine proportions of waste as sent to the landfill. EPA categories that contained two materials (eg; rubber/leather) were apportioned in an attempt to more accurately represent MSW as delivered to the landfill. In addition, broad categories (e.g., paper, plastic, rubber/leather) were subdivided by weight between different material types using classifications provided in Appendix A of Miller and Clesceri (2002). The EPA group for paper was subdivided into 18.6% paper and 5.8% cardboard. The EPA group for plastics was separated into 13.2% high density polyethylene and 3.0% low density polyethylene. The EPA group consisting of rubber and leather was divided into 2.6% rubber and 0.8% leather.

A representative, heterogeneous, reproducible waste mixture was prepared for use throughout the testing program. The MMSW consisted of representative materials from each EPA waste category and was comprised of a variety of components to maintain heterogeneity. Weight percentages of each component were maintained throughout the test program. Detailed information regarding the waste components as used in the MMSW are provided in Table 4.

A total of 15 materials were used to represent various components of MSW. Based on the size of the various testing apparatuses, waste components were prepared in the laboratory to maintain a 50 mm maximum size during compressibility, hydraulic conductivity, and shear strength testing. An apparent volume was calculated, where possible, in order to provide a sense of scale of each component. Components were approximated as box shaped, cylindrical, or spherical for apparent volume calculations.

Table 4. Waste Components and Preparation

EPA Category	Actual Material	Nominal Particle Size (mm)	Apparent Volume (mm^3)	Equivalent Diameter (mm)	Laboratory Preparation	Moisture content (%)	Specific Gravity	Reference
Paper	Shredded paper	3 x 32	10	1.3	Cross cut shredded	6.8	1.53	(Weyerhaeuser Company 2008)
	Cardboard	50 x 50	7500	12.1	Cut	9.0	1.53	(Weyerhaeuser Company 2008)
Glass	Broken glass	Variable, 50 max[1]	Varies	Varies	Broken	0	2.6	(Lide 2008)
Steel	Nails	32	230	3.8	None	0	7.86	(Lide 2008)
Aluminum	Al shavings	Variable, 20 max	Varies	Varies	None	0	2.7	(Lide 2008)
Other metals	Al shavings	Variable, 20 max	Varies	Varies	None	0	2.7	(Lide 2008)
Plastics	Plastic chips	Variable, 10 max	60	2.4	None	0	0.95	(Brandrup and Immergut 1989)
	Plastic bags	50 x 50	50	2.3	Cut	0	0.92	(Alger 1989)
Rubber/leather	Shredded tires	Variable, 20 max	3,000	9.0	None	0	1.1	(Lide 2008)
	Leather coupons	50 x 50	2,500	8.4	Cut	13.7	0.86	(Lide 2008)
Textiles	Textile coupons	50 x 50	1,250	6.7	Cut	5.0	1.27	(Cotton Inc. 2008)
Wood	Wood chips	Variable, 30 max[1]	Varies	Varies	None	10.6	1.53	(Weyerhaeuser Company 2008)
Other materials	Concrete fragments	Variable, 50 max[1]	Varies	Varies	Crush, sort	0	2.59	Jansen (2009)
Food	Dog food	13 (diameter)	930	6.1	None	7.6	1.22	Previous experiment
Yard	Grass clippings	Variable, 50 max	Varies	Varies	None	260	0.94	Previous experiment
Other	Soil	Variable, 2 max	Varies	Varies	None	4.6	2.65	Experiment

[1] Particle size was limited to 25 mm for bulky materials during preparation of MMSW to be used for compaction testing

Consideration was given to the maximum particle size in relation to the size of each testing apparatus; components had to be small enough to avoid scaling issues with test equipment but large enough to allow for size heterogeneity. Typically, the maximum particle size is limited to no greater than one-tenth of the testing apparatus dimension (ASTM 2007a, ASTM 2007b). Maintaining particle size heterogeneity was also important for the test program. The maximum component size chosen as a compromise between minimizing potential scaling issues while maximizing heterogeneity was 50 mm for the large scale tests. Due to the smaller dimensions of the compaction mold, the maximum component size was limited to 25 mm for compaction testing. The apparent volume of each component was calculated based on an approximately cylindrical, spherical, or box shape. The nominal equivalent particle diameter was calculated to aid in conceptual comparison of the differing waste components as idealized spheres.

Eight of the components were assumed to have nonzero initial moisture contents and moisture content was measured. The materials containing moisture included: shredded paper, cardboard, leather, textile, wood chips, dog food, grass clippings, and soil. Components assumed to be dry included: glass, steel, aluminum, HDPE plastic chips, LDPE plastic film, rubber, and concrete. All components were stored separately in original packaging (when available) or in sealed containers to minimize drying throughout the test program. The same relative weight of each component was used in each test sample.

3.3 Compaction Tests

Compaction testing was performed to determine the moisture content-dry unit weight relationship for the MMSW. Tests were performed in a 152.4 mm diameter Proctor mold with a mechanically raised, automatic compactor. Four sets of compactions tests were completed: two with conventional hydration at modified Proctor

compactive effort (modified) and four times modified Proctor compactive effort (4x modified) compaction energy, and two with non pre-wet hydration at modified and 4x modified compaction energy. Conventional hydration consisted of bringing the samples to target moisture contents all at once immediately after sample mixing with 16 to 24 hours of hydration prior to compaction testing, in accordance with ASTM D-698 (2007a) and D-1557 (2007b) for soils. The non pre-wet hydration samples were mixed, brought to 30% moisture content, allowed to hydrate for 16 to 24 hours, and then brought to the target moisture content immediately prior to compaction testing (within 5 minutes) to evaluate the viability of wetting field waste immediately prior to placement.

Testing was performed at both modified and 4x modified compaction efforts to determine the variability in compaction characteristics as a function of compaction effort. The tests conducted at 4x modified compactive effort were used as the basis for the remainder of the MMSW test program. The high level of compactive effort was selected to represent field waste compaction conditions.

3.3.1 Conventional Hydration Compaction Tests

It was determined that the natural moisture content of the MMSW was approximately 11%. The natural moisture content of 11% was used in all subsequent calculations for MMSW preparation.

Samples were prepared to fill a 152.4 mm diameter, 2.124×10^{-3} m^3 volume mold, based on the internal volume of the mold specified in ASTM standard D-1557 (2007b). Individual waste components were placed into a 76 L trash bin based on percentage by weight. Samples were mixed thoroughly by hand while being hydrated to target moisture contents. Compaction samples were double bagged and sealed with tape prior to testing to maintain moisture conditions.

Samples were hydrated using a hand pump garden sprayer. The sprayer was filled with water, placed on an electronic balance, and then the scale was tared. Water was sprayed onto the sample and the change in weight of the sprayer was measured periodically to monitor the weight of water sprayed onto the sample. Water was sprayed onto the samples during mixing to bring the modified samples to 30%, 50%, 70%, 90%, 110%, and 130% moisture content. The 4x modified compactive effort samples were hydrated to 11%, 30%, 50%, 70%, 90%, 110%, and 130% moisture content. The MMSW was mixed during and after hydration to ensure even distribution of moisture throughout the sample. After standing at the target moisture content for roughly 24 hours, the sample was tested using automatic soil compactors equipped with sector face hammer heads.

Prior to testing, hammer drop heights, weights, and hammer head characteristics were verified against ASTM standards. Drop heights and hammer weights were adjusted as necessary to meet ASTM standards. Two automatic soil compactors were used in the test program: a Soiltest compactor and Ploog compactor. Photographs of the automatic compactors used are presented in Figure 5. Several mechanical issues were encountered during the use of the automatic compactors. Steps were taken to assure the correct operation of the compactors to ensure data validity.

The MMSW was compacted into the mold at modified (5 lifts, 56 blows per lift, 44.5 N hammer with 457 mm drop height) and 4x modified (5 lifts, 224 blows per lift, 44.5 N hammer with 457 mm drop height) compaction efforts. A total of 17 tests were performed using the conventional hydration method.

After each compaction test was completed, the collar was removed and excess material was scraped off using an aluminum straight edge. The mass of the mold

(without the collar) and MMSW was recorded and then the MMSW was removed from the mold. The entire sample was then transferred into a metal bowl and weighed again to verify sample mass. Samples were placed in a temperature controlled, forced air convection oven set at 100°C.

(a) Soiltest compactor (b) Ploog compactor

Figure 5. Automatic hammers used for compaction testing

3.3.2 Non Pre-wet Compaction Tests

The third and fourth test sets were conducted using a non pre-wetting method. Based on the calculated natural moisture content from the conventional hydration tests, water was added to bring the waste to a moisture content of 30%. The 30% moisture content value was selected as a general value of moisture content for incoming landfill wastes (Von Stockhausen 2007). The waste was allowed to hydrate at 30% moisture

content for approximately 24 hours. Immediately prior to testing, varying amounts of water were added to bring the waste to 30%, 40%, 50%, 60%, 70%, 90%, and 110% moisture content. Samples were tested within 5 minutes of the secondary addition of water. The goal of the testing was to determine the viability of water addition immediately prior to compaction in changing the maximum achievable unit weight in a landfill environment.

Non pre-wet compaction curves were generated for both modified and four times modified compaction efforts. A total of 19 tests were performed using the non pre-wet hydration method. Tests were performed on a combination of the Soiltest and Ploog automatic compactors.

3.4 Sample Preparation

Samples were prepared in a similar manner for the remainder of the testing program (constant rate of strain compression, hydraulic conductivity, and shear strength testing). Calculations were made to determine the combined weight of sample necessary to reach target unit weights based on the calculated internal volume of the testing apparatus. Components were added to the waste mixture to reach a predetermined percentage of the combined weight and mixed thoroughly. Water was added to bring the sample to the target moisture content based on the initial moisture content of 11% using conventional hydration procedures. Samples were stored for a minimum of 24 hours in a sealed container prior to testing. Loading the entirety of the prepared sample into the various testing apparatuses assured that the target unit weights were met.

3.5 Compressibility Tests

The next phase of testing consisted of determination of the compression characteristics of the MMSW at varying moisture contents and unit weights corresponding to the 4x modified compaction test results. The test cell used for testing was built specifically for large scale testing. A hydraulic load frame was used to apply load at a constant rate of strain to the sample.

The test cell consisted of a steel wall cylindrical vessel with steel base and a removable loading cap. The test cell had an inner diameter of 300 mm and a height of 330 mm. The test cell consisted of a 10 mm thick steel tube welded to a 13 mm thick base plate. A brass ball valve was threaded into the side of the test cell approximately 13 mm from the base plate and allowed leachate in excess of the field capacity of the waste to drain freely.

The contents of the test cell are described from the base upward. Uniformly graded, angular gravel of 20 mm nominal diameter was packed to a 50 mm nominal thickness and provided bottom drainage. The gravel was overlain by sheet of Tencate Mirafi G-Series drainage geocomposite consisting of 2 sheets of non-woven geotextile bonded to both sides of a molded drainage media with a total thickness of 10 mm that served to prevent the migration of fines into the gravel bed. The waste sample occupied the next 200 mm of the test cell. A second layer of 10 mm thick drainage geocomposite was inserted between the top of the sample and the cap of the test cell to provide filtration and drainage.

The test cell cap consisted of 13 mm thick plate steel machined to tolerance to fit inside the test cell. The test cell cap included 2 lifting hooks, and one drainage port. Two holes were drilled in the cap to allow for the insertion of the two lifting hooks for cap

removal. A third hole was drilled for drainage or the introduction of water to the sample if necessary (for future tests). A spherical socket was machined into a load distribution plate to assure vertical load transfer through a steel ball bearing. A schematic diagram and photograph of the test cell are presented in Figures 6 and 7.

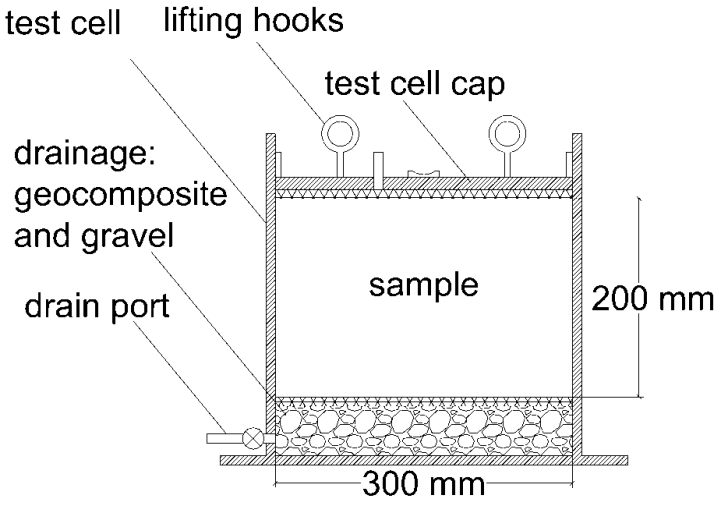

Figure 6. Schematic diagram of test cell

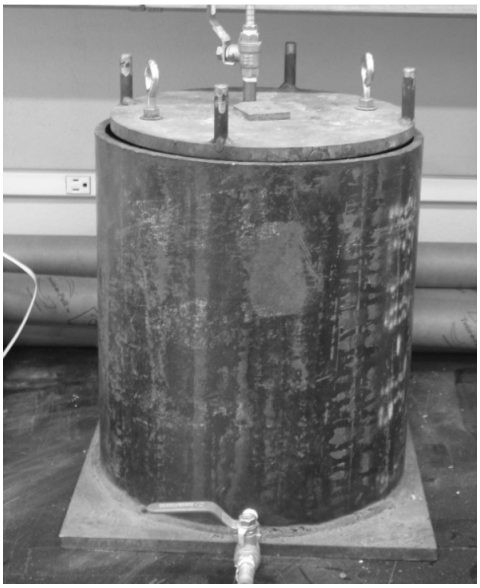

Figure 7. Photograph of test cell

The test cell had been used for testing of wet samples and had developed a layer of rust along the inside surface. A wire brush was used to clean the inside surface of the test cell and the inner wall was sprayed with silicone based lubricant to inhibit continued corrosion and reduce friction with the cap. To further reduce binding between the top cap and the sidewall of the test cell, high-vacuum grease was applied to the outer edge of the test cell cap before each test.

An MTS model 322 hydraulic T-load frame was used to load the samples during testing. The loading piston had a maximum stroke length of 150 mm. The hydraulic actuator had a maximum capacity of 500 kN. The load cell used for force measurement was an MTS brand load cell with a maximum capacity of 500 kN with a maximum error of 0.5% load at 18 kN. The load frame was fitted with a ball-end rod to apply load onto the socket plate of the test cell cap. Measurements (both displacement and force) in the compressive direction were recorded. The load frame instrumentation was used to record time, position/displacement of the piston head, force required, and strain every 30 seconds. An upper stress limit of 100 kPa was set for the tests.

Between each lift of waste, the sample was compressed both by hand and by using the cap paired with the hydraulic load frame. Loads induced on samples during sample placement varied depending on the remaining amount of sample that needed to be placed into the test cell and were maintained below approximately 5 kN. The entirety of each sample was loaded into the test cell in 7 to 15 lifts of varying thickness (decreasing in thickness from approximately 100 mm) and compressed to a specific volume prior to testing to ensure that the initial unit weights of the samples met target values.

Samples were prepared to an initial height of 200 mm. Each constant rate of strain compression test commenced immediately after the sample was loaded into the test cylinder. Tests were completed within 36 hours of initial sample preparation to minimize the effects of decomposition on measured values. The testing program consisted of a constant rate of strain intended to compress the samples 100 mm in 12 hours (strain rate of 1.16×10^{-5}/s)to achieve up to 50% strain on the sample.

3.6 Hydraulic Conductivity Tests

Tests were conducted in a specialized permeameter built for the test program to determine the short term hydraulic conductivity of the MMSW test material representing as-placed conditions. Tests were run under constant head conditions and varied in length based on equipment limitations and the hydraulic conductivity of the sample.

A large scale, rigid wall, dual-ring permeameter was constructed from a steel drum for hydraulic conductivity testing of the MMSW and other large particle size samples. A large scale Mariotte bottle was constructed to provide constant head conditions for the permeability tests.

The dual ring permeameter was built using a 30 L steel salvage drum with a removable lid, a stainless steel separation ring, and one inlet port and two outlet ports. A 50 mm width, 3mm thick stainless steel bar was rolled into a circular shape (280 mm diameter) with a metal bender and welded to create the separation ring that would be used within the permeameter. The separation ring was spot welded concentrically within the base of the drum. The gaps between the ring and the base of the drum were filled with silicone caulk along both the inner and outer contacts to prevent liquid transfer between the inner and outer zones. One inner and one outer drainage port were

constructed with various bulkheads and plumbing and electrical fittings as described below.

The inner drainage port consisted of a 25 mm internal diameter bulkhead located at the center of the base plate of the drum. The perimeter drain consisted of 19 mm plumbing and electrical fittings. Due to the nature of the connection, the perimeter drain was sealed using silicone caulk. Each drain was connected by means of a 90° elbow to a lateral pipe to convey the water out from beneath the base of the permeameter. Flow was directed upward at the termination of the lateral pipe by means of an additional 90° elbow to assure that permeant liquid exiting the permeameter would always be at the same height and to prevent loss of constant head conditions. The outlet of both the central and perimeter drain were set at the same level. The inlet consisted of a 25 mm bulkhead fitting assembled onto the removable lid of the drum with a barb connection for attachment of a 25 mm inner diameter hose. A fitting was added to the system to allow air within the supply line to be purged.

The bottom of the permeameter was lined with a 10 mm thick composite drainage layer to provide filtration and prevent the clogging of the drainage ports by the test material. Next, uniformly graded, angular gravel with 20 mm nominal diameter was placed to a nominal thickness of 50 mm. An upper layer of 10 mm geocomposite layer was placed on top of the gravel to maintain separation of the testing material and the drainage layer. Careful attention was paid to the overall height to ensure that the upper geocomposite drainage layer did not exceed the height of the stainless steel separation ring. A schematic diagram and photograph of the permeameter are presented in Figures 8 and 9.

A watertight seal for the permeameter was achieved by using the lid and steel lock ring provided with the 30 L drum. To ensure a watertight seal, the neoprene gasket attached to the underside of the lid was inspected and cleaned before each test. Water was provided to the sample during testing through the permeameter lid via a bulkhead fitting (Figures 8 and 9). A wooden stand was built for the permeameter to allow for vertical loading of the waste sample and to provide stability.

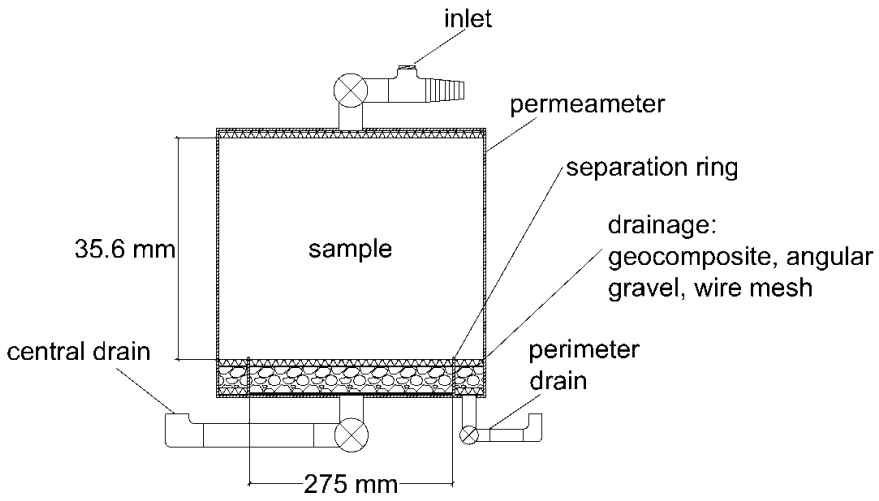

Figure 8. Schematic diagram of permeameter

Figure 9. Photograph of permeameter

The Mariotte bottle was built using a large diameter acrylic tube, a smaller acrylic pipe, two acrylic sheets cut to shape as end caps, a vacuum plug, various PVC piping parts, and a brass compression fitting. The main body of the Mariotte bottle consisted of a 200 mm outer diameter 1.80 meter long clear acrylic tube with a wall thickness of 10 mm. The end caps were fabricated from 18 mm thick acrylic plate and were attached using a combination of pure silicone caulk, rubber strips, and hose clamps. After the application of vacuum grease to the contact surfaces, the connections between the end plates and the body were wrapped tightly with soft rubber strips. The strips were then fixed in place against the surface of the end plates and body using large diameter hose clamps. The top plate of the Mariotte bottle was drilled to include a fill port (that would be sealed with a rubber vacuum plug when in use) and a pass-through compression fitting sized for a 25 mm outer diameter bubble tube. A 1.08 m long acrylic tube with 25 mm outer diameter and 3 mm nominal wall thickness was used as the bubble tube. The bottom of the Mariotte bottle was drilled and tapped to accept a threaded 25 mm outlet port. A wooden stand was built to allow the Mariotte bottle to remain stable during testing. A schematic diagram and a photograph of the Mariotte bottle are presented in Figures 10 and 11.

The MTS load frame was used to compact samples into the permeameter. The sample was loaded in lifts of decreasing thickness to aid in achieving a more consistent sample compaction. Approximately 15 to 20 lifts were used to load the entirety of each sample into the permeameter. The lifts decreased in thickness from 75 mm down to 25 mm as filling progressed. A layer of composite drainage was placed on top of the sample prior to placement of the drum lid. Once the permeameter had been sealed, the

outlet from the Mariotte bottle was attached and air was purged from the water supply line.

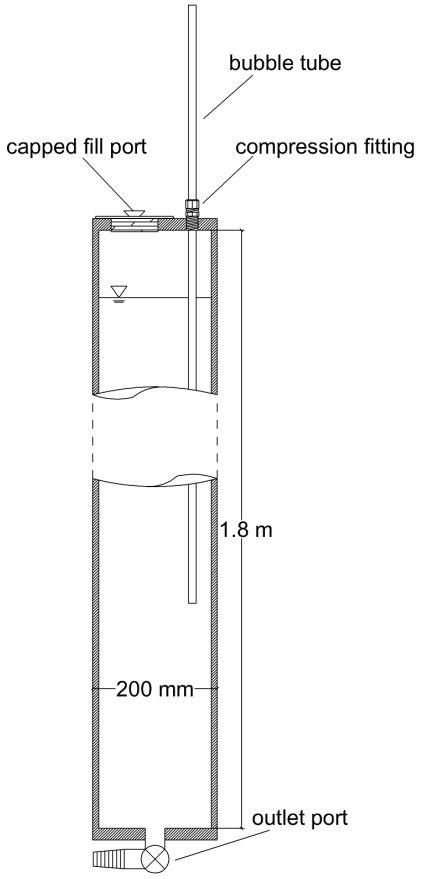

Figure 10. Schematic diagram of Mariotte bottle

All samples were tested under a constant head condition with a hydraulic gradient of 1 to minimize the migration of fine particles within the MMSW and the subsequent changes in flow behavior. To maintain a gradient of 1 for the sample, the bottom of the bubble tube in the Mariotte bottle was set at 35.56 cm above the height of the tops of the drain ports of the permeameter. The test apparatuses were not moved once each hydraulic conductivity test began. The sample cross sectional area was 613 cm^2, with a sample length of 35.56 cm for each test performed.

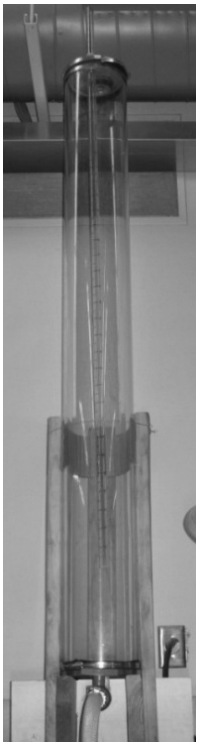

Figure 11. Photograph of Mariotte bottle

ASTM D-5084 for the measurement of hydraulic conductivity of a saturated porous material using a flexible wall permeameter provides two termination criteria for materials with a hydraulic conductivity greater than $1x10^{-10}$ cm/s under constant head conditions. The first criterion requires a range of the inflow of permeant to outflow of permeant and a steady hydraulic conductivity (as defined by 4 values within 25% of the mean). The second criterion requires a steady hydraulic conductivity (as defined by 2 consecutive values within 15% of the mean).

Falling head termination criteria as detailed in ASTM D-5084 were similar to constant head termination criteria. In one criterion, the ratio of inflow to outflow must be between 0.75 and 1.25 with a steady hydraulic conductivity (as defined by 4 values within 25% of the mean). The other criterion requires a steady hydraulic conductivity as defined by 2 consecutive values of hydraulic conductivity within 15% of the mean value.

Although the MMSW tests focused on determination of short term conductivity values, the termination criteria set forth in ASTM 5084 were used for most tests.

Due to a vacuum leak from the Mariotte bottle, constant head was not achieved during the initial trial. Although partial vacuum was achieved, full vacuum within the Mariotte bottle was not achieved, as evidenced by the partial (as opposed to full) drop in water level inside the bubble tube within the bottle. The top connection as well as all fittings were cleaned and resealed with high vacuum grease.

Testing after resealing the bottle allowed for creation of additional vacuum although sufficient vacuum was still not achieved and air bubbles were not seen exiting the bottom of the bubble tube. Numerous falling head tests were run on the trial 30% molding moisture content sample while attempts were made to trace and repair the vacuum leak. Constant head could not be maintained during the test and measurements were not taken to calculate hydraulic conductivity based on a falling head test.

Hydraulic conductivity testing of the test apparatus was conducted to verify that the permeameter was not the limiting factor in the MMSW hydraulic conductivity testing. When filling the central portion of the permeameter with water, it was observed that water began to pool and that the permeameter was not effectively draining. The limiting component was determined to be the lowest composite drainage layer. The height of the inner flange of the bulkhead fitting in combination with the compression of the drainage layer impeded flow out of the permeameter. The layer was replaced with three layers of steel mesh with an opening size of 13 mm by 13 mm. The angular gravel was washed and replaced and the permeameter reassembled. Flow rate improved

significantly once the composite drainage material had been replaced, and was deemed suitable for the purposes of the testing program.

Hydraulic conductivity tests were conducted on a total of 5 samples at 5 different moisture contents. The hydraulic conductivity of the first test on a trial 30% moisture content sample was not evaluated due to the possibility that drainage capacity may have been limited by the lowest drainage layer (as previously described).

Bottom up saturation of the sample was attempted using both the perimeter and central outlet ports. Neither was successful due to the pressure that built up within the permeameter. After several unsuccessful attempts to saturate the sample from the bottom up, it was decided that the sample would be saturated from the top down.

A minimum of 3 pore volumes of water were permeated through each sample under falling head conditions to ensure saturation of the sample. Once the three pore volumes of water flowed through the sample and no additional bubbles were visible in the drain ports, the Mariotte bottle was sealed to begin constant head testing.

Three short continuous constant head tests were performed on the 11% moisture content sample. The drain ports were monitored for air bubbles to visually verify saturation of the sample. The combined length of the three tests was 70 minutes. In that time, 41.5 kg of water flowed through the central portion of the permeameter.

Four short back-to-back constant head tests were performed on the 30% moisture content sample. The valves were opened and constant head conditions were used to indicate the start of the first of the tests on the 30% moisture content sample. The combined length of the four constant head tests was approximately 120 minutes.

Attempts were made to test the 56% moisture content sample at a constant head. Due to equipment limitations of the Mariotte bottle, a falling head test was conducted in lieu of a constant head test. The rate of the vacuum loss from the Mariotte bottle was higher than the rate of water passing through the sample, preventing attainment of a constant head state throughout the system. Three pore volumes of water flowed through the sample under falling head conditions. The falling head test was run for approximately 11 hours. Insufficient data was collected to verify satisfaction of ASTM termination criteria. The equation used for calculation of hydraulic conductivity under a falling head is presented in Equation 7.

$$k = \frac{-La}{At} \ln\left(\frac{h_t}{h_0}\right) \tag{7}$$

where:

L = length of the sample perpendicular to the direction of flow (length)

a = cross sectional area of the falling head water source (area)

A = cross sectional area of the sample being tested (area)

h_t = height of the sample above a reference datum at time t (length)

h_0 = height of the sample above a reference datum at time 0 (length)

The 85% moisture content sample was tested under a constant head condition. The 85% moisture content sample was tested for approximately 21.5 hours. The test was terminated when the hydraulic conductivity had decreased below the level necessary to sustain constant head conditions in the Mariotte bottle.

The 110% moisture content sample was tested under a constant head condition. Three pore volumes of water were flushed through the sample under a falling head and outflow was monitored for air bubbles. The 110% sample was tested for approximately 44 hours to verify that conditions for hydraulic conductivity test termination were met.

Flow, temperature, and height of the water level inside the Mariotte bottle were measured 11 times throughout the test. Comparisons between incremental flow in and flow out were made.

Subsequent tests using the permeameter outside the test program verified that fluid flow through the apparatus remained significantly greater than that of the MMSW assuring that flow through the permeameter was not a limiting factor during the MMSW tests.

3.7 Shear Strength Tests

Shear strength testing was performed using a Durham Geo-Slope Indicator interface shear device. Nominal dimensions of the top half of the shear box were 305 mm width by 305 mm length by 100 mm depth. The lower half of the shear box was 305 mm width by 380 mm length (in the direction of shearing) by 100 mm depth. A portion of the lower half of the shear box was closed off using plywood spacers to convert the sample area into a 305 mm by 305 mm by 200 mm depth area. Normal stress was applied to the sample via a pneumatic bladder connected to the laboratory pressurized air supply. A schematic diagram and photograph of the interface shear device can be seen in Figures 12 and 13.

Shear force was measured using a load cell with an operating range of 2.2 kN to 44.5 kN and a resolution of 0.01 kN. Displacement of the shear box was measured with a linear variable differential transducer (LVDT) with 100 mm stroke and 0.01 mm resolution. Normal stress applied to the sample was measured with a pressure transducer connected to the air bladder with a range of 103 kPa to 1,300 kPa and a resolution of 0.1 kPa (Durham Geo 2009).

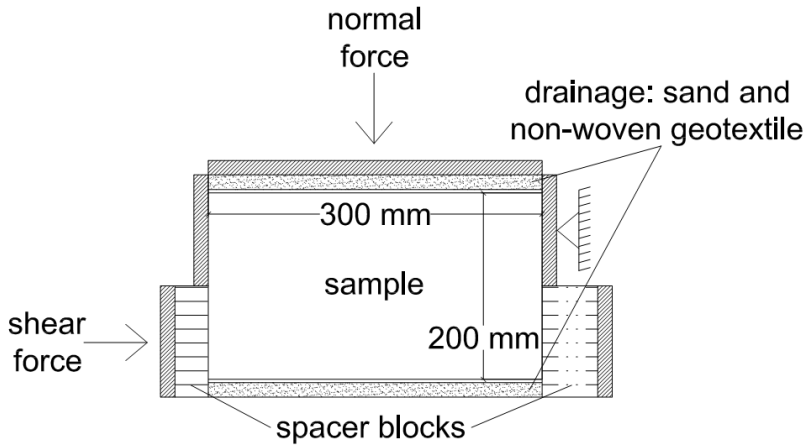

Figure 12. Schematic diagram of interface shear device

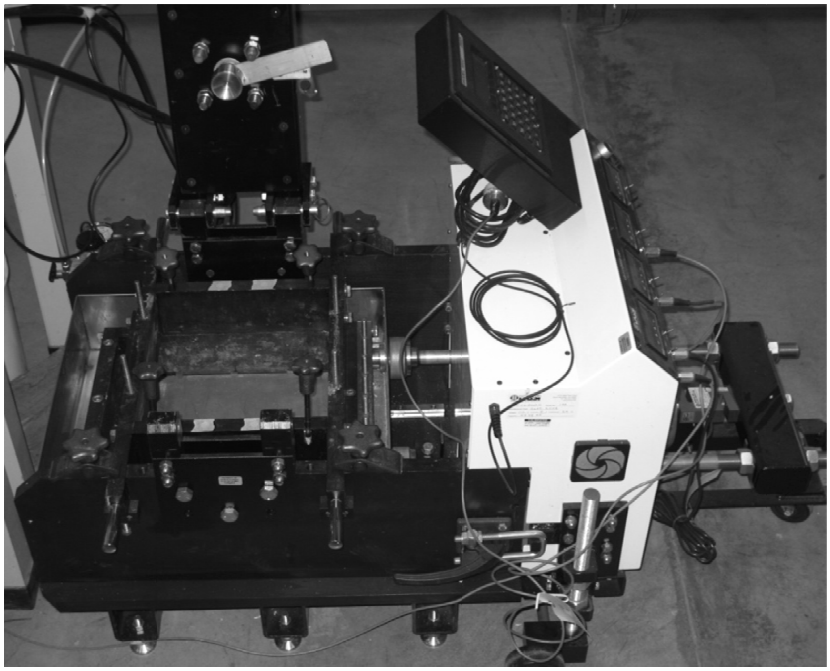

Figure 13. Photograph of interface shear device

The interface shear device was equipped with a high load normal force actuator capable of delivering up to 98 kN of vertical force to the sample. The actuator consisted of an air powered hydraulic pump that drove a single hydraulic piston into the shear box. To ensure that no moment was introduced to the sample, the force was transferred from

the hydraulic piston to the loading plate via a large diameter ball bearing. The high load actuator was used for sample loading and was not used during shear strength testing.

Bottom drainage for the samples was provided by means of a sand layer approximately 13 mm thick overlain by a non-woven geotextile. The geotextile was used to maintain separation between the drainage layer and the sample. A similar configuration consisting of non-woven geotextile and 13 mm of sand was used on top of the sample to provide drainage and to ensure that the pneumatic bladder providing normal stress to the sample was not punctured during testing by sharp waste components.

The walls of the top half of the shear box were lined with two layers of aluminum foil. A light coat of spray lithium grease was applied between the two layers of foil to minimize side wall friction and loss of normal force through the sample to the shear plane. The layer of aluminum foil mounted directly to the shear box was backed with duct tape for reinforcement. Careful attention was paid to ensure that no grease was mixed with the sample. During four of the five tests, the loading plate caught the surface of the aluminum foil, tearing it and pulling it down into the sample. To avoid introduction of any additional heterogeneities or preferential shear planes, the aluminum foil was removed entirely if it was damaged during the loading process.

Samples were placed in lifts of decreasing thickness with a maximum single lift thickness of approximately 50 mm (prior to compaction). Care was taken to ensure that there was no boundary between lifts at the plane of shearing. Lifts were compressed into place using the high load frame designed for the interface shear device. The surface of the sample was scored between lifts. Each sample was placed in 7 to 15 lifts of decreasing thickness.

The MMSW samples were tested to 15% strain over a minimum of 14 hours. The 11% moisture content sample was tested for 14 hours. The test procedure was revised for the remaining tests and the remaining four samples were tested for 15 hours. The resulting shearing strain rate was 2.78×10^{-6}/s.

Based on the shear box dimensions of 300 mm, total displacement during each test was 46 mm. To achieve 15% displacement over the 15 hour test, a displacement rate of 0.0508 mm per minute was used. The normal force applied to the sample was measured with a pressure transducer. All samples were tested at approximately 200 kPa of normal force. Data was acquired through the use of a computer connected via serial port to the interface shear device. Data including time, shear stress, shear box position, and normal force were recorded each minute over the duration of the tests.

Chapter 4: Experimental Results and Discussion

4.1 Introduction

Results from the experimental test program are presented in this chapter. The weight-volume relationships for the MMSW test material were established using published and experimentally determined values for specific gravity of individual waste components. Results of the baseline compaction tests are presented. Following, results from compressibility, hydraulic conductivity, and shear strength tests are provided. Test results are discussed within the framework of existing soil and waste mechanics analyses and theories. Finally, the engineering significance of this investigation is presented.

4.2 Waste Classification Results

Using the specific gravity data presented in Chapter 2, it was possible to develop the weight-volume phase relationships for various unit moisture content-dry unit weight combinations. An example phase diagram for 85% moisture content is presented in Figure 14. The composite initial specific gravity of solids was calculated by a volume weighted average to be 1.39. This compared reasonably well with previously reported values of 1.6 by Hettiarachchi (2005) for a manufactured waste. From the phase diagram, relevant parameters including initial void ratio and porosity could be determined. Initial void ratios ranged from 1.30 to 2.16 (for the 56% and 11% moisture content samples, respectively). Porosity ranged between 0.57 and 0.68 (for the 56% and 11% moisture content samples, respectively).

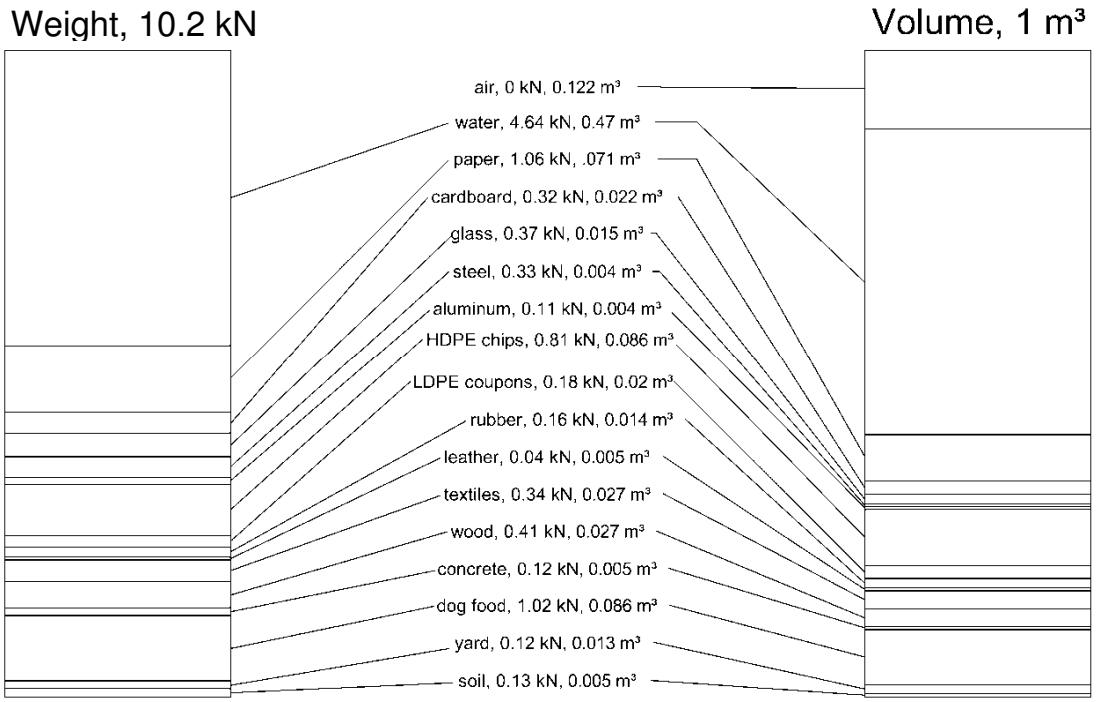

Figure 14. Example phase diagram for 85% moisture content sample

4.3 Compaction Test Results

The compaction test results illustrated the effects of compaction effort on the unit weight of the MMSW test material. For the modified compaction tests, a maximum dry unit weight of 5.1 kN/m^3 was determined at a moisture content of 66%. A maximum dry unit weight of 5.9 kN/m^3 and optimum moisture content of 56% was determined for the MMSW compacted at 4x modified effort. No significant differences in compaction characteristics were identified between samples that were hydrated in the conventional versus the non pre-wet manner and as a result, all data points (both conventional hydration and non pre-wet hydration) were used in generation of the curves. Conventional hydration versus non pre-wet hydration data is presented in Figure 15.

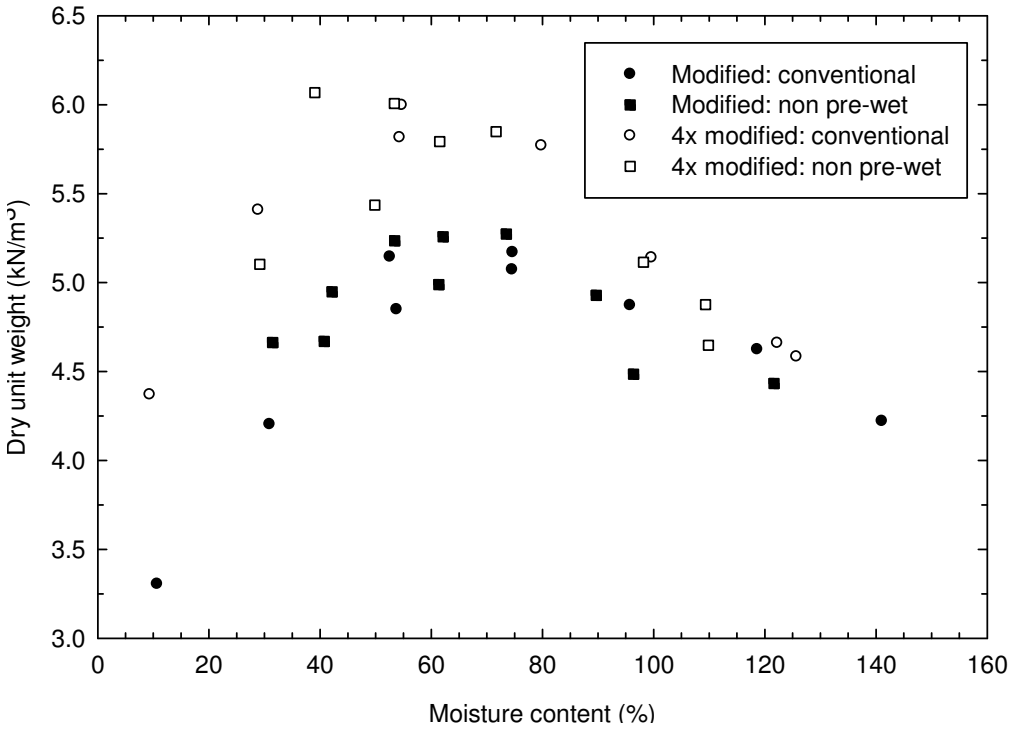

Figure 15. Compaction test results - conventional and non pre-wet hydration

A third-order polynomial trend line was fit to all the data points obtained at each energy level. Results of compaction testing are summarized in Figure 16. Curve fits to the modified compaction data fit slightly better than 4x modified data to a third order polynomial trend line as measured by the coefficient of determination (R^2). R^2 values of 0.897 and 0.892 were calculated for modified and 4x modified data, respectively).

The shapes of the Proctor compaction curves obtained from the data were in general agreement with the shapes of the curves for soils. The continued addition of water lubricated the waste particles during compaction until the optimum moisture content was reached, allowing for a tighter packing structure and increased dry unit weight. Wet of the optimum moisture content, water in the sample began to displace waste components and resulted in a lower dry unit weight.

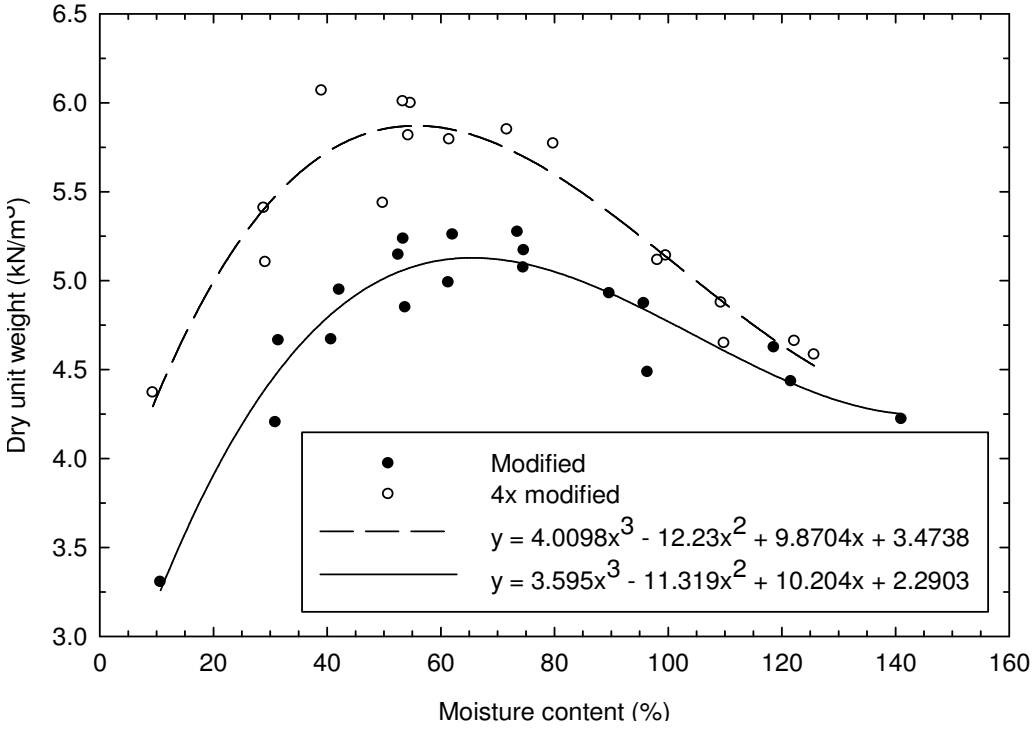

Figure 16. Compaction test results with third order polynomial trend lines

Variability in compaction data, as measured by R^2 was smaller for the samples subjected to conventional hydration (0.62 for conventional hydration versus 0.41 for non pre-wet hydration). This may indicate that the MMSW subjected to longer periods of hydration prior to compaction compacted more consistently than MMSW hydrated immediately prior to compaction. The longer period of hydration allowed for more even distribution of water throughout the sample and more consistent softening of materials prone to softening. Softening of the waste components led to increased deformation and densification of individual component solids during compaction.

The slopes of the compaction curves generated for the modified and 4x modified compaction curves were calculated by dividing the change in dry unit weight by the change in water content for both dry and wet of optimum. The slopes of the compaction curves of various soils were similarly calculated from numerous references. Results are presented in Table 5.

The slopes of the compactions curves generated for waste materials (MSW, MMSW) were significantly less steep than the slopes for soils both dry and wet of optimum moisture content. This was primarily due to the large range of water content for wastes. The soil with the most similar value of slope dry of optimum was the poorly graded sand (0.053 compared to 0.033 and 0.036 for modified and 4x modified, respectively). Wet of optimum, the soils that were the most similar to the slope of the MMSW were the sandy silt and silty clay.

Table 5. Slopes of Compaction Curves Dry and Wet of Optimum for Various Materials

Material	Compactive effort (kJ/m^3)	Optimum moisture content (%)	Dry of optimum slope	Wet of optimum slope	Source
Soil - sandy silt	600	12	0.222	-0.100	Estimated from Das (1997)
Soil - silty clay	600	14	0.119	-0.100	Estimated from Das (1997)
Soil - high plasticity clay	600	16	0.100	-0.175	Estimated from Das (1997)
Soil - poorly graded sand	600	17	0.053	-0.233	Estimated from Das (1997)
Soil - silty clay	2,635	15	0.275	-0.292	Estimated from Turnbull (1950) from Lambe and Whitman (1969)
MSW	600	31	0.081	-0.033	Gabr and Valero (1995)
MSW	600	70	0.051	-0.013	Reddy et al. (2008a)
MMSW	2,700	65	0.033	-0.010	This study
MMSW	10,800	56	0.036	-0.019	This study

The slopes of the compaction curves for materials containing non-compressible solids such as inorganic soils did not change at differing compactive efforts. Instead, the compaction curves were shifted upwards to higher dry unit weights at lower moisture contents.

The differences in slopes (0.033 to 0.036 and -0.010 to -0.019) from lower to higher compactive efforts in MMSW as presented in Table 5 may be indicative of a change in specific gravity of the test material. The differences in the value of the slopes of the compaction curves may be attributed, in part, to the difference between the specific gravity of the solids of the MMSW of the two test efforts. With additional compactive effort, individual compressible waste particles underwent volume reduction, leading to a change in specific gravity. An increased specific gravity of wastes was also observed by Hudson (2004) in large scale one-dimensional compression tests.

Compaction data based on the slope of the MMSW used in this test program agreed reasonably well with the landfill MSW compaction data reported by Gabr and Valero (1995) and Reddy et al. (2008a). As well, the slopes of the compaction curves of the MMSW and fresh wastes tested by Reddy et al. (2008a) were in general agreement.

Moist/total unit weight was also graphed against moisture content of the MMSW. Values of moist unit weight continued to increase even at moisture contents wet of optimum. As with the dry unit weight, data were more consistent with trend lines when the MMSW had been hydrated in a conventional manner. Moist unit weight data are presented in Figure 17.

The moist unit weight versus moisture content data generated at both compaction energies were asymmetric about the respective optimum moisture contents. This may be explained by the relatively small difference of composite specific gravity of

1.39 of the MMSW and that of water of 1.00. Due to the relatively small difference in specific gravities of the two materials, the decrease in moist unit weight wet of optimum was not as pronounced as it is for soil, where the difference in specific gravities between the soil solids and water is more prominent.

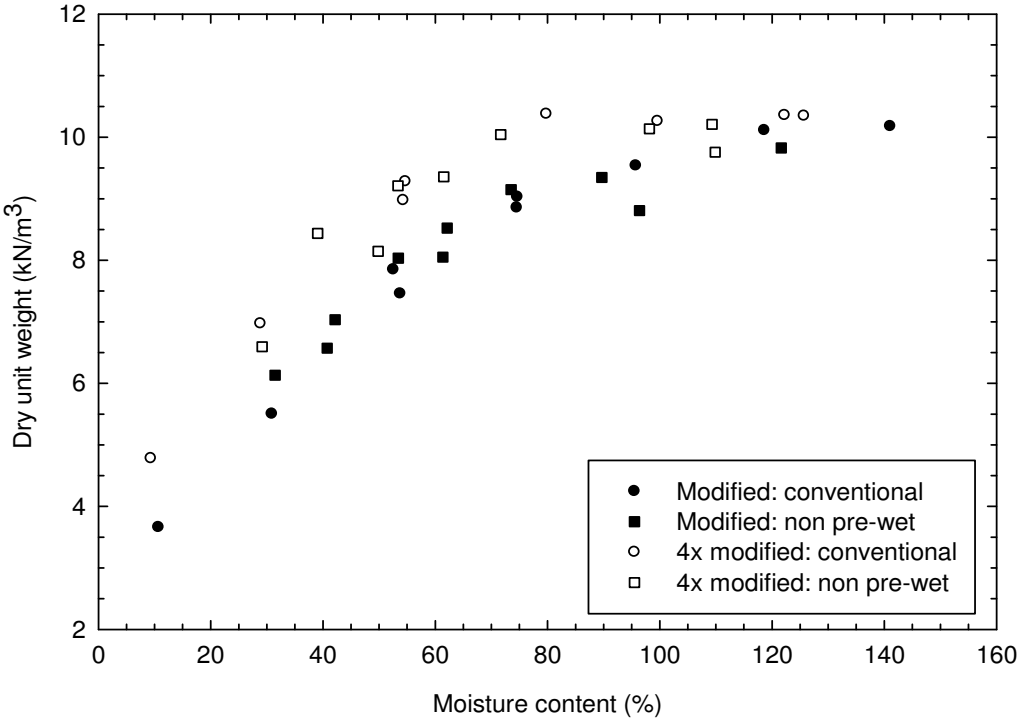

Figure 17. Compaction test data - total unit weight versus water content

For inorganic soils, the shape of the moist unit weight density curve is attributed to effects from both the soil and water. A portion of the combined increase in unit weight is due to the replacement of air in the soil voids with water, and the remainder of the increase in unit weight is due to the decrease of void ratio of the soil, as presented in Figure 18.

It is proposed that the increase in moist unit weight of the MMSW was the result of three, as opposed to two, distinct mechanisms: replacement of air with water, decrease of void ratio, and increase in specific gravity of waste components. The less pronounced decrease in moist unit weight of the MMSW at post-peak moisture contents (as compared to soils) is due to the relatively small difference between specific gravity of the waste and water. The difference in specific gravity of soil particles in comparison to water is generally greater than 1.5, whereas the difference in specific gravity of waste and water is approximately 0.4.

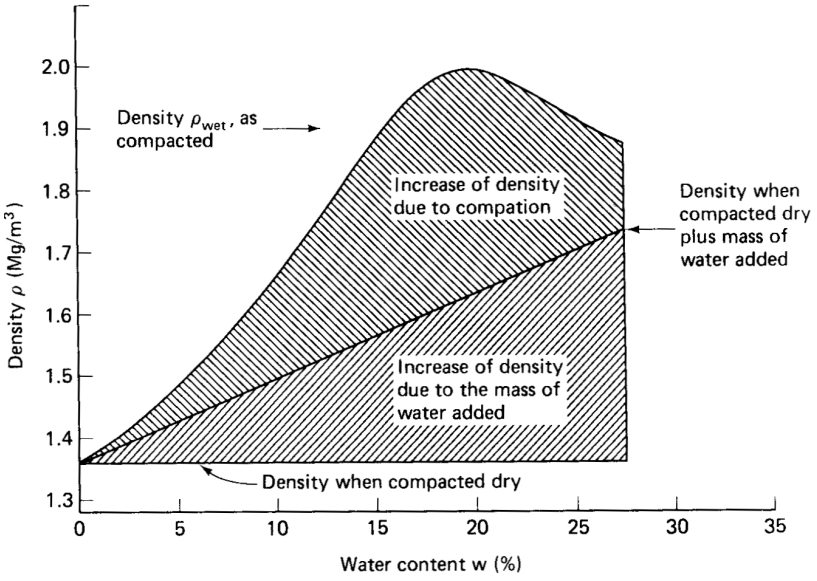

Figure 18. Contribution of water to change in moist unit weight (from Holtz and Kovacs 1981 after Johnson and Sallberg 1960)

The data collected from compaction tests was used to generate best fit compaction curves. Based on the equation of the polynomial trend line for the 4x modified compaction data, it was possible to determine corresponding combinations of moisture content and dry unit weight along the compaction curve. From the equation, an optimum moisture content of 56% and maximum dry unit weight of 5.9 kN/m^3 were determined. Due to the use of the third order polynomial trend line, there is a visible

secondary point of inflection wet of optimum on the modified effort compaction curve which is unlikely to be representative of actual conditions. Nevertheless, the third order polynomial equation for the 4x modified data was used to establish the values for subsequent tests because it provided the best overall fit to the data.

Remaining tests for compression, hydraulic conductivity, and shear strength were performed in sets of five: two below/dry of optimum moisture content, one at the optimum moisture content, and two above/wet of optimum moisture content. Target dry unit weights as calculated from the trend line for the tests are presented in Table 6.

Table 6. Target Values for Compression, Hydraulic Conductivity, and Direct Shear Tests

Moisture content (%)	Moist Unit Weight (kN/m^3)	Dry Unit Weight (kN/m^3)
11[a]	4.7	4.3
30	7.0	5.4
56[b]	9.2	5.9[c]
85	10.2	5.5
110	10.3	4.9

[a] natural moisture content
[b] optimum moisture content
[c] maximum dry unit weight

The compaction testing served as the baseline for the following tests. Moisture content-dry unit weight combinations were assumed to be feasible placement condition values at which subsequent, representative tests could be performed. Compressibility, hydraulic conductivity, and direct shear tests all followed the values established during compaction testing.

4.4 Compressibility Test Results

Constant rate of strain tests were performed on 5 samples at the established moisture content-dry unit weight combinations to determine variation in compressibility

as a function of placement conditions. In this section, analyses are performed based on the shape of the stress-strain curves and confined compression test theory. Next, stiffness trends are analyzed in relation to the soil stiffness curves. Next, apparent compression indices are calculated and compared to existing data. The section concludes with determination and discussion of the tangent and secant modulus at varying strains.

The development of excess pore pressures was not quantified during the testing program. Additionally, the examination of long term settlements was beyond the scope of the experimental procedure and as such, the effects of decomposition and physico-chemical changes within the waste mass were not accounted for.

Data recorded during each constant rate of strain compression test were used to determine the confined compression characteristics of the MMSW samples. The samples exhibited primarily strain hardening behavior within the range of strains tested, with some yielding demonstrated at low- and mid-level strains. The general shape of each strain curve as a function of the logarithm of stress was in accordance with the accepted bilinear compression curve that has been documented for soils. The stress versus strain and logarithm of stress versus strain plots for the 5 samples are presented in Figures 19, 20, and 21. The plots were generated based on individual data values and were not based on a data fit.

All five plots on Figure 19 have a similar slope once the preconsolidation stress (which varied between approximately 100 kPa and 300 kPa) had been surpassed, as evidenced by the nearly parallel plots to the right of the knee of Figures 19 and 21. Limited conclusions can be drawn from the value of the preconsolidation stress as the values are likely a function of the force used to load the sample into the test cell.

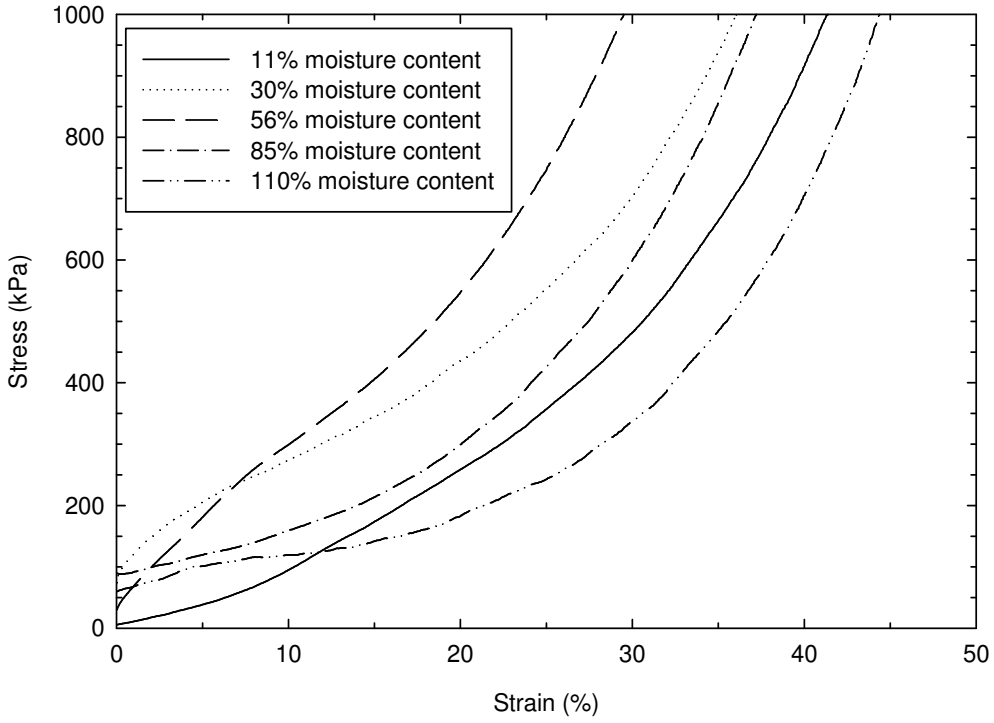

Figure 19. CRS compression test results–
stress as a function of strain

Several similarities between the MMSW stress-strain plots and trends reported by Lambe and Whitman (1969) for soils were observed. Specifically, a 3-stage confined compression trend was observed. Based on the stress-strain plots of the MMSW samples, the initial interlocking or raveling of particles (stage 1) was completed during loading of the samples for 3 of the 5 samples (30%, 56%, and 110%). The downward concavity of the initial portion of the 3 stress-strain plots Figure 20 suggests localized crushing of the particulate matter within the samples (stage 2). Continued strain of the MMSW resulted in additional raveling, or movement of newly formed fines into voids, demonstrated by further locking (stage 3). All samples with the exception of the 11% moisture content sample show a generally similar behavior. A schematic illustration of the 3 part process is presented in Figure 22.

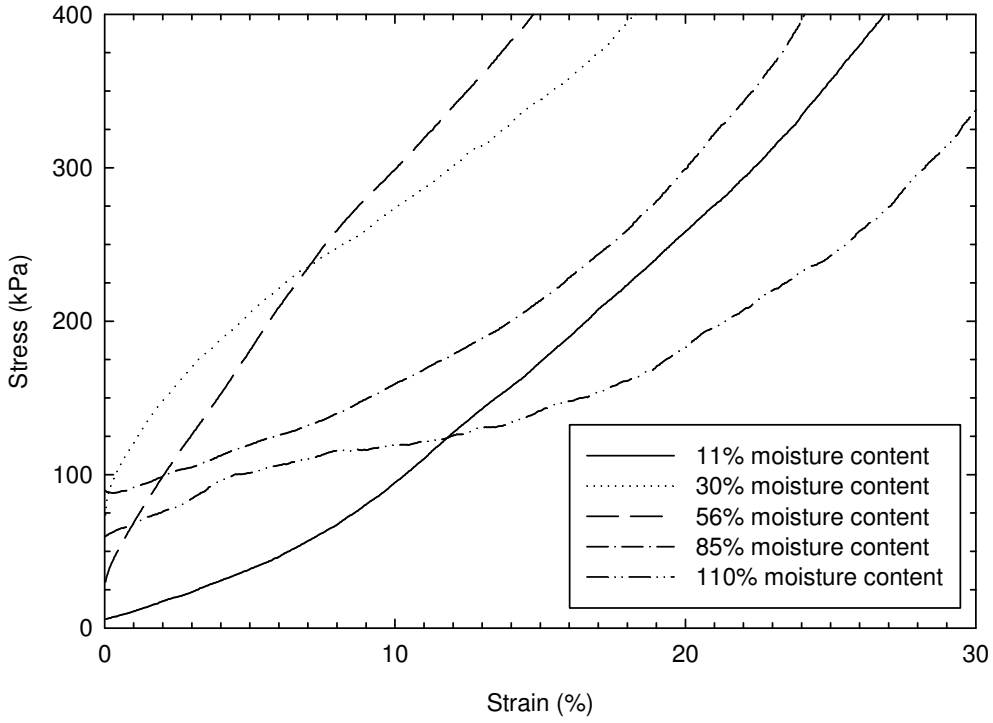

Figure 20. CRS compression test results – stress as a function of strain enlarged to show detail at low strains

Two points of inflection are visible on stress-strain plot of the 11% moisture content sample presented in Figures 19 and 20 at approximately 12% and 20% strain, suggesting that placement at natural water content did not allow for completion of particle raveling (stage 1) during loading. The lack of unbound water in the sample prevented lubrication of particle contacts, diminishing the ability of the 11% moisture content MMSW to completely seat during sample loading. The locking indicative of initial raveling of the waste components (stage 1) for the 11% moisture content sample is visible in Figures 19 and 20.

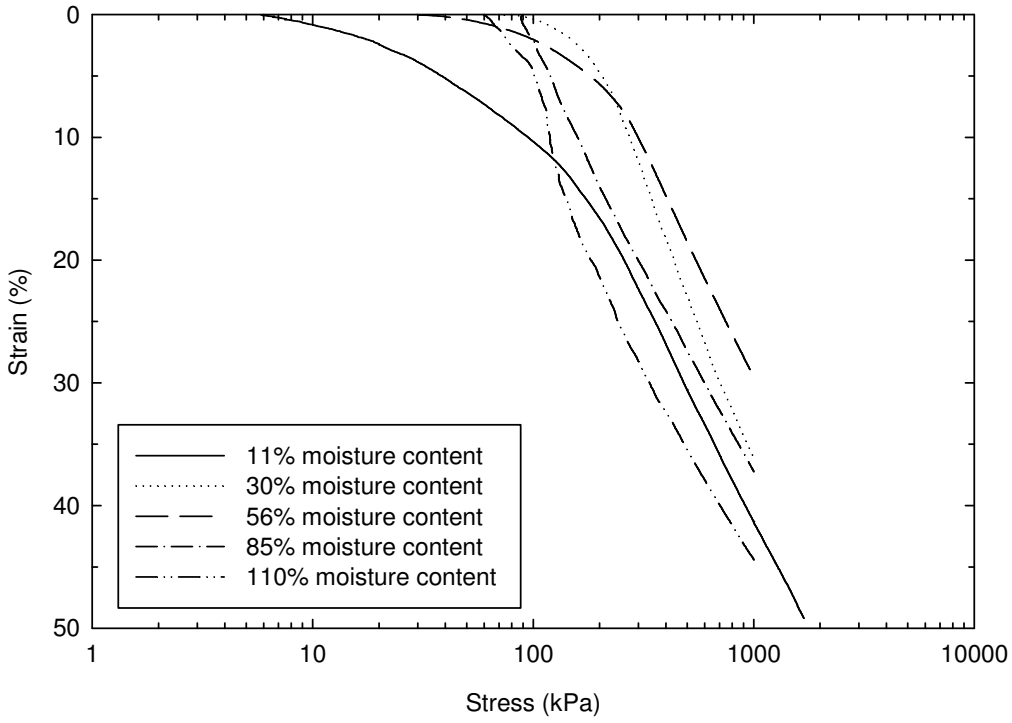

Figure 21. CRS compression test results – strain as a function of log stress

The deformability of the material increased with increasing moisture content. Samples at higher moisture contents showed noticeably more gradual yielding than the drier and denser samples which were concave downward over a smaller range of strain (Figures 19 and 20).

Once strains in Figures 19 and 21 exceeded approximately 12% (assumed to be the strain at which all samples were in stage 3), the stress-strain curves for each sample began to show locking as the components rearranged. If the behavior of the MMSW samples can be characterized by the region of strains in stage 3, the stress-strain properties of the MMSW were controlled by placement conditions. Increasing dry unit weight resulted in a stiffer material.

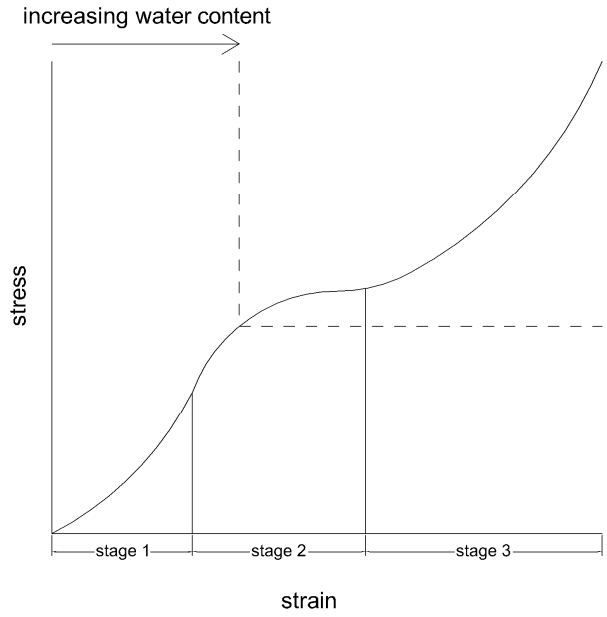

Figure 22. Shift in test initiation points from increasing molding water content

Similar to the silty clay samples tested by Seed and Chan (1959), the MMSW stress-strain curves for the two samples dry of optimum presented in Figures 19 and 20 had an initially steeper slope. The steeper slope was not visible on the stress-strain plot for the 11% moisture content sample, potentially due to the continued seating of the waste components that was not completed during loading. As strain continued to increase, the stress-strain curves for the 11% and 30% moisture content samples changed curvature as the waste microfabric and minifabric was broken down and particles were rearranged. The samples prepared wet of optimum did not change curvature throughout the tests as the waste structure had already softened and broken down during placement due to the additional water.

Based on the approximately linear portion of each strain versus log stress plot, an apparent compression ratio (apparent $c_{c\varepsilon}$) was calculated. From the apparent $c_{c\varepsilon}$ and initial void ratio, it was possible to calculate the apparent compression index

(apparent c_c). Although the values calculated are believed to represent compression characteristics of the MMSW, the development of excess pore pressures were not measured during the experiments. The apparent $c_{c\varepsilon}$ and apparent c_c values calculated herein are therefore based on total stress. The compression analyses conducted for this investigation are intended to provide index behavior of wastes as a function of molding water content. If excess pore pressure did develop, the stress-strain curves would become shallower and both apparent $c_{c\varepsilon}$ and apparent c_c would decrease. Therefore, apparent c_c represents a lower bound estimate for compression index although it is quite likely that c_c and apparent c_c were close in value except at high moisture contents. Calculated values for apparent $c_{c\varepsilon}$ and apparent c_c are presented in Table 7.

Table 7. Calculated Values for Constant Rate of Strain Compression Tests

Target w	11%	30%	56%	85%	110%
γ_m (kN/m^3)	4.9	7.0	9.2	10.2	10.3
γ_d (kN/m^3)	4.3	5.4	5.9	5.5	4.9
e_o	2.2	1.5	1.3	1.5	1.8
Apparent $c_{c\varepsilon}$	0.36	0.46	0.37	0.34	0.12
Apparent c_c	1.1	1.2	0.84	0.84	0.34

Although direct correlation would not be accurate due to the unknown factor of excess pore pressure, the apparent c_c calculated from the tests performed matched reasonably with several of the existing equations for calculation of compression index. Numerous researchers have developed predictive linear models to calculate compression index as a function of initial void ratio of MSW. The equations follow the general form presented in Equation 8.

$$c_c = x(e_0) + y \quad (8)$$

where:

c_c = compression index

e_o = initial void ratio

x, y = variables assigned to the investigations as a function of waste type and observed compression characteristics

The apparent c_c was plotted along with the predictive equations that have been generated by others and is presented as Figure 23. The correlations between the compression indices calculated in this investigation agreed well with parameters presented by Wardell (as referenced in Simpson 1997) and Sowers (1973). The Wardell and Sowers equations were based on tests performed on manufactured waste and paper sludge, respectively. Of the 5 compression tests performed, the 11%, 56%, and 85% moisture content samples showed compression indices within 10% of those calculated using Wardell's compression index equation modeled on shredded paper in which x = 0.31 and y = 0.44. The compression index-void ratio relationships proposed by Wardell and Sowers are shown on Figure 23. Initial void ratios outside the range of encountered within this test program are shaded in gray in Figure 23 for clarity.

The apparent c_c exhibited different behavior dry and wet of optimum. The apparent c_c was less sensitive to changes in initial void ratio at moisture contents dry of optimum and was in the upper half of the envelope of predicted values. At moisture contents wet of optimum, the apparent c_c decreased significantly from 85% to 110%, potentially due to the generation of excess pore pressure in the test cell, which decreased the apparent c_c to the lower portion of the envelope of predicted values.

An inverse relationship between moisture content and apparent c_c was observed based on MMSW testing and is presented in Figure 24. Changes in stress had

decreasing effects on changes in void ratio at higher water contents. This is due to an increase in the degree of saturation of the MMSW.

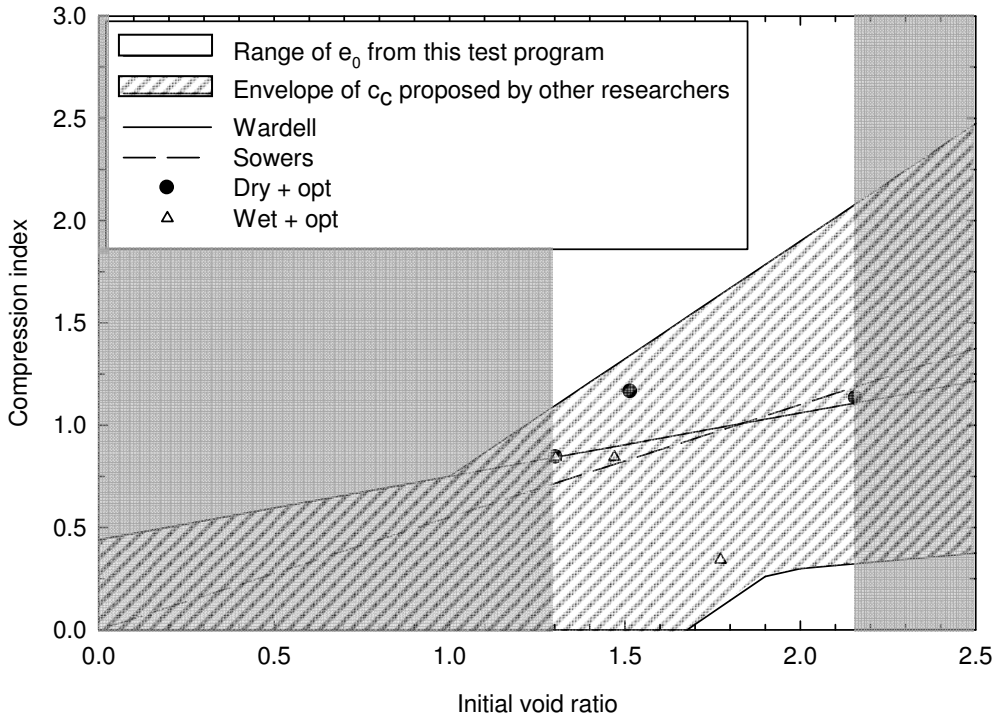

Figure 23. Envelope of published predictive equations for compression index including data from this test program

The apparent c_c was calculated as a change in void ratio to a change in stress and as such, it showed no direct correlation with increase in dry unit weight. The compression index decreased with increasing moist unit weight due to an increase in the degree of saturation although the correlation was not very strong.

Based on the apparent c_c values in tandem with the measured hydraulic conductivities at higher moisture contents, it is possible that excess pore pressure may have developed during loading of the high moisture content samples due to lower hydraulic conductivities and resulted in measurement of an undrained condition.

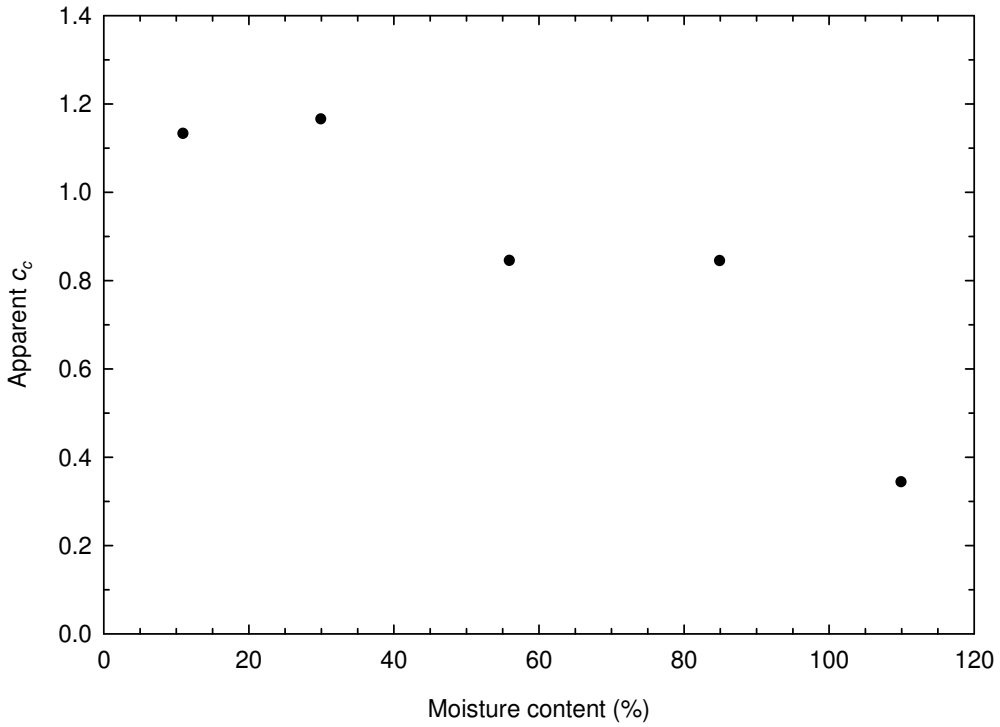

Figure 24. Apparent c_c as a function of moisture content

The general trends of secant and tangent moduli versus moisture content (Figures 25 and 26) were generally similar to that of the compaction curves, with a steep slope approaching a peak value from the dry side and then decreasing at a lower slope on the wet side of the peak value. Hand drawn envelopes bounding the calculated values were drawn to illustrate overall trends.

The addition of water to the samples controlled both the magnitude and variability of the moduli of elasticity over the range of moisture contents tested. The difference between the modulus (both secant and tangent) at 1% and 25% strain decreased as moisture content increased past 30% due to the water in the sample homogenizing the waste mixture. Figures 25 and 26 illustrate the softening behavior induced by the addition of water controlled the modulus for wet of optimum moisture contents.

As moisture content continued to increase, the secant modulus of elasticity first increased sharply to a peak values (for the 5%, 10%, 15%, and 25% strains) at the optimum moisture content sample, and then decreased and converged as water within the samples began to control the behavior. The effect of water was twofold: it resulted in convergence of the secant modulus due to homogenization of the sample; and it resulted in an apparent stiffening of the waste at higher moisture contents. The apparent stiffening for the 110% moisture content sample was attributed to development of excess pore pressure (i.e., drainage controlled behavior). This is illustrated in Figure 25. The secant modulus for 1% strain peaked dry of optimum. The 30% and 56% moisture content samples showed the most pronounced yielding, as illustrated by the wide range of secant moduli at varying strains.

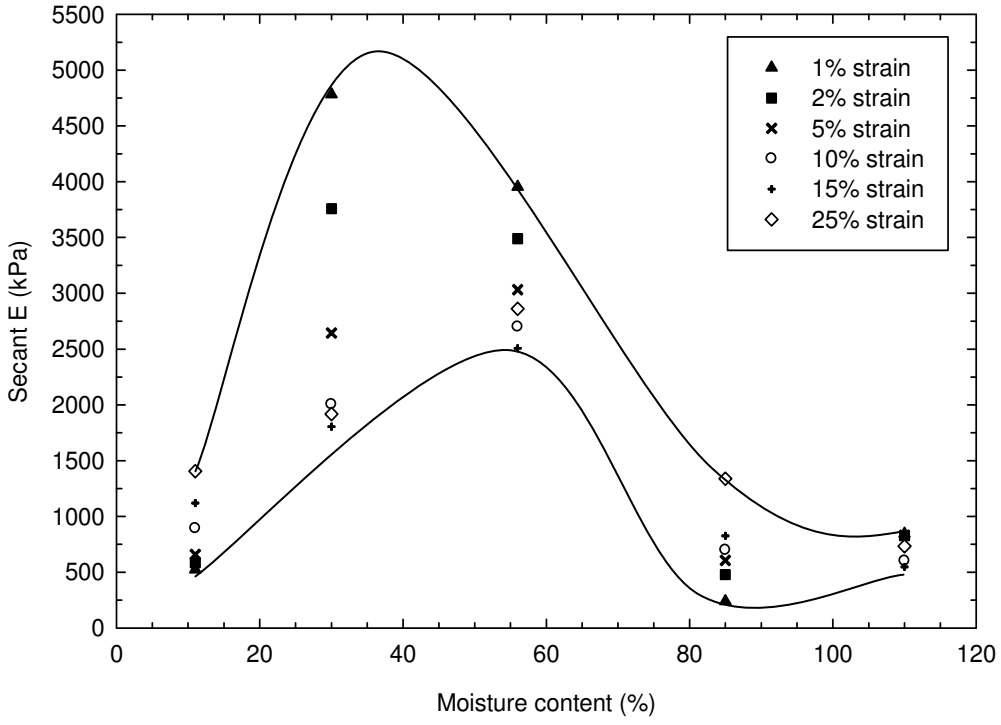

Figure 25. Secant modulus of elasticity as a function of moisture content

Comparison of the 30% and 85% moisture content samples illustrated the extent to which moisture content affected secant modulus. The samples had similar dry unit weight (5.4 kN/m^3 for the 30% sample and 5.5 kN/m^3 for the 85% sample) yet exhibited markedly different secant modulus values and data variability. The 85% moisture content sample, despite having a marginally higher dry unit weight, had a significantly lower average secant modulus (approximately 700 kPa versus 2,800 kPa) and more consistent behavior with increasing strain.

Similar results were found during analysis of the tangent modulus presented in Figure 26, although the highest average tangent modulus was calculated for a sample dry of optimum (in this case the 30% moisture content sample). The average tangent modulus at 85% moisture content was approximately one-third of the value of the 30% moisture content sample and had less variability amongst the modulus of elasticity values. This indicated moisture content controlled behavior in the MMSW.

As illustrated in Figure 27 the secant modulus of elasticity values were significantly higher at low strains in the 30% and 56% moisture content samples, likely due to a combination of relatively high dry unit weight and low moisture content. The 30% and 56% moisture content samples also exhibited the sharpest decrease in secant modulus of elasticity with increasing strain. The 85% and 110% moisture content samples had a much more consistent secant modulus of elasticity over the range of strains and a slightly strain hardening behavior.

The tangent modulus of elasticity increased with increasing strain across samples at all moisture contents as can be seen in Figure 28. The largest relative increases were visible in the 30% and 56% moisture content samples. Modulus of

elasticity values for both secant and tangent modulus of elasticity are plotted as a function of strain and presented in Figures 27 and 28.

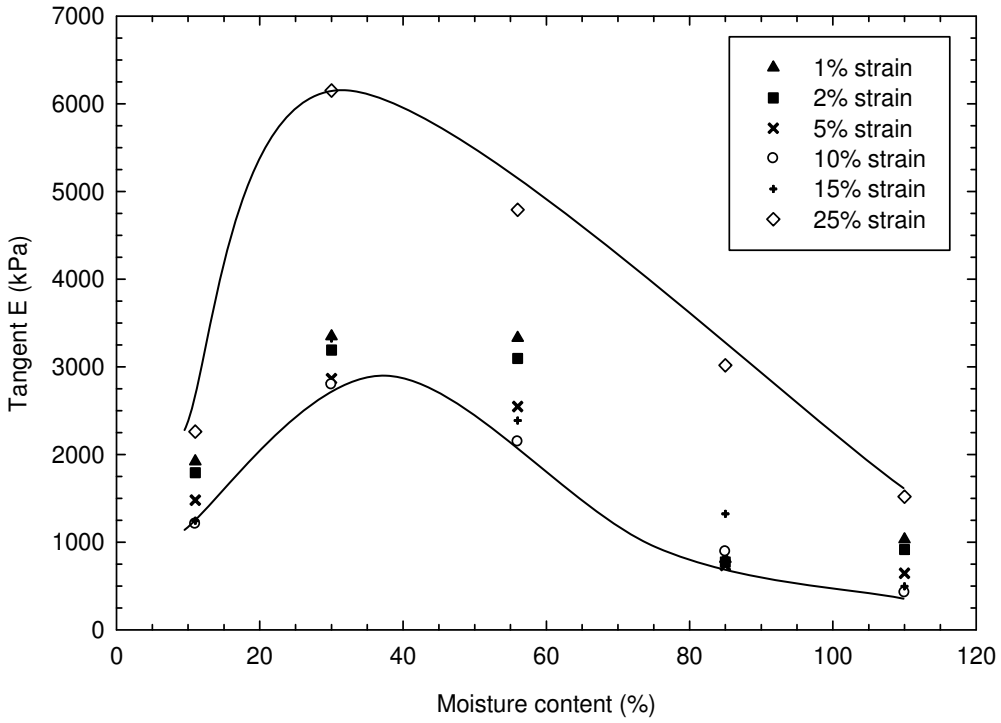

Figure 26. Tangent modulus of elasticity as a function of moisture content

The tangent modulus was determined at 100 kPa of stress to compare the behavior of the MMSW samples at similar levels of compressive stress. The tangent modulus of elasticity at 100 kPa ranged between 684 kPa (for the 110% moisture content sample) to 3,455 kPa (for the 30% moisture content sample). When plotted against moisture content, the data points showed a trend similar to that of the tangent moduli when plotted against moisture content with a mid-range value at natural moisture content, a peak value at 30% moisture content, and a sharp decrease at moisture contents wet of optimum.

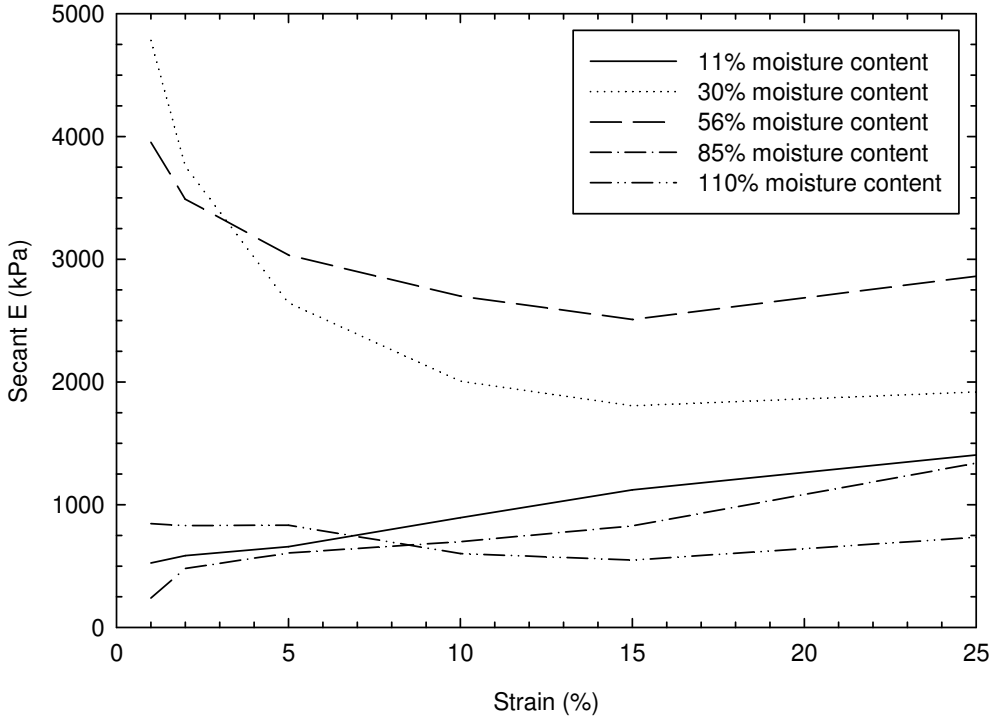

Figure 27. Secant modulus of elasticity as a function of strain

Lambe (1958b) published work that supported the notion that soils show significantly higher compressive stress-strain modulus at moisture contents dry of optimum. Although the sharp decrease in modulus of elasticity of MMSW was in accordance with the trends reported for CBR of soils (Turnbull and Foster 1956), the trends were not entirely comparable. Soil generally was strongest (as measured by CBR) at minimum water contents whereas the MMSW modulus increased to a maximum between 30% and 56% moisture content (depending on the modulus used). This implies that some amount of water addition was necessary for MSW to reach peak modulus of elasticity values. The wide variation in particle size and shape required water to facilitate rearrangement into a more stable, denser, and stiffer packing structure.

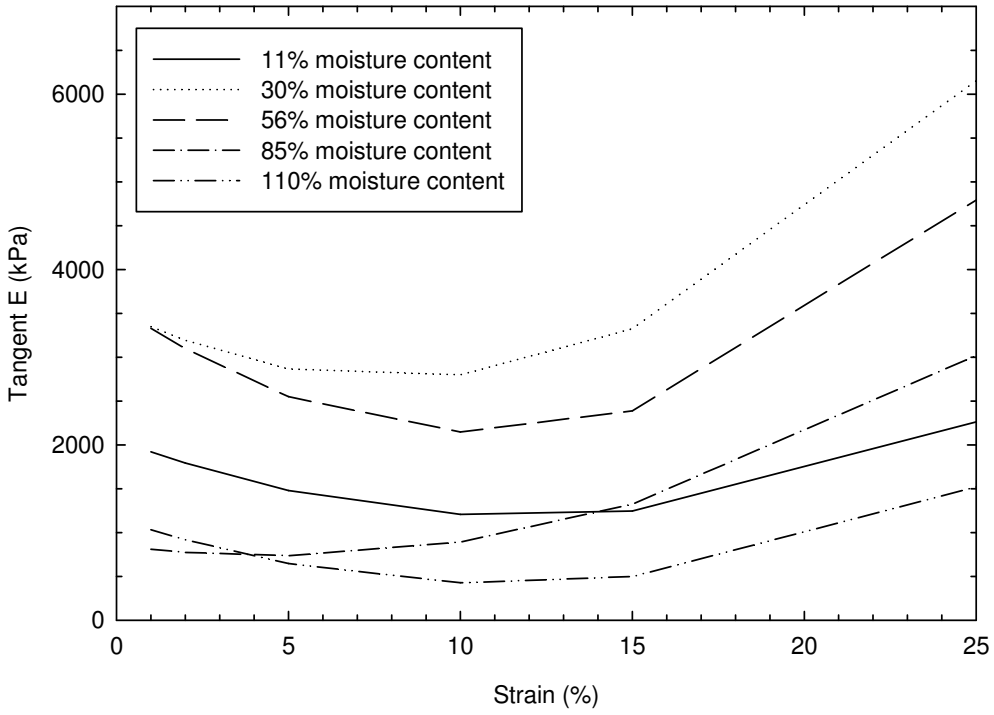

Figure 28. Tangent modulus of elasticity as a function of strain

4.5 Hydraulic Conductivity Test Results

A total of 5 hydraulic conductivity tests was conducted using the dual-ring permeameter and Mariotte bottle. Hydraulic conductivity varied from 7.99×10^{-5} cm/s to 1.28×10^{-2} cm/s. In this section, hydraulic conductivity is calculated in 3 ways to establish the framework to discuss the transient nature of hydraulic conductivity. Next, the relationship between waste dry unit weight and hydraulic conductivity is examined. Hydraulic conductivity trends in waste as a function of placement moisture content are compared to those of soils. Finally, attempts are made to categorize waste as a sand-like or clay-like soil using various void ratio formulae derived from the Kozeny-Carman equation.

As stated by Olivier and Gourc (2007) and Chen and Chynoweth (1995), multiple factors may change the hydraulic conductivity of MSW with time, including material softening, particle swelling, and particle migration. Once a steady state condition has been reached in soils, hydraulic conductivity will converge on a specific value. With a test material like MSW that changes physically (even before the start of decomposition effects) and chemically with time, a steady state condition may or may not be reached. Movement of water through the permeameter may cause the migration of small particles into voids (akin to raveling) and increase the rate of physical breakdown or decomposition of the putrescible components of the waste.

To evaluate changes in hydraulic conductivity throughout the test, hydraulic conductivity was calculated in three ways when data were available: $k_{incremental}$, $k_{running}$, and $k_{cumulative}$. Incremental *k* calculations were based on permeant flow between subsequent readings and the corresponding temperature. Incremental *k* was calculated to monitor variation for stabilization or until constant head conditions were no longer being achieved. The running *k* was calculated based on the summation of flow from the beginning of the test to each measurement interval (cumulative hydraulic conductivity up to that point). The cumulative *k* was calculated using the flow of liquid over the entire duration of the test and an average temperature for the temperature correction. All hydraulic conductivity calculations were corrected for temperature. Equations describing calculation of each hydraulic conductivity are presented in Equations 10 - 12.

$$k_{incremental} = \frac{\alpha\left[{(V_n - V_{n-1})}/{(t_n - t_{n-1})}\right]}{i(A)} \quad (10)$$

$$k_{running} = \frac{\alpha\left[{}^{(V_n - V_0)}/_{(t_n - t_0)}\right]}{i(A)} \quad (11)$$

$$k_{cumulative} = \frac{\alpha\left({}^{V_f}/_{t_f}\right)}{i(A)} \quad (12)$$

where:

k_x = hydraulic conductivity (cumulative, incremental, running) (length/time)

α = temperature correction based on the ratio of fluid viscosity at actual temperature to fluid viscosity at 20° C

V_x = volume at time f (final), n (reading number), 0 (initial) (volume)

i = hydraulic gradient

A = cross sectional area of the central portion of the permeameter (area)

Subscripts:

n = incremental reading number

0 = initial

f = final

Both $k_{incremental}$ and $k_{running}$ varied widely throughout the day during testing of the 110% moisture content sample. Values peaked during the day and were lowest during the night. Hydraulic conductivity appears to have varied somewhat with changes in temperature despite the application of a temperature correction. Ambient temperatures during this test were significantly lower than during the other tests. Temperature corrected $k_{cumulative}$ for all samples as measured throughout the test program are summarized in Table 8. Temperature corrected $k_{incremental}$ and $k_{running}$ values are presented in Table 9.

Table 8. Summary of $k_{cumulative}$ Values

Moisture content (%)	Total test time (s)	Flow (cm^3/s)	Test type	Average temperature (°C)	$k_{cumulative}$ (cm/s)
11%	5,161	8.05	constant	20.5	$1.28x10^{-2}$
30%	7,331	1.78	constant	18.8	$2.95x10^{-3}$
56%	35,700	0.054	falling	18.9	$7.99x10^{-5}$
85%	77,280	0.052	constant	18.4	$8.67x10^{-5}$
110%	157,620	0.053	constant	14.5	$8.27x10^{-5}$

Tests of greater duration were conducted for the lower hydraulic conductivity samples (i.e., 56%, 85%, and 110% moisture content samples). Both $k_{running}$ and $k_{incremental}$ varied throughout each test. The $k_{incremental}$ values from the 11% and 30% moisture content samples remained relatively stable over the short tests. The $k_{incremental}$ determined for the 85% moisture content sample decreased throughout the duration of the test. The 110% sample had a higher $k_{incremental}$ during the day than at night. Temperature corrected $k_{incremental}$ values were plotted as a function of the percentage of the test completion to evaluate for stabilization and time based trends. The results are presented in Figure 29.

The relative stability of the $k_{incremental}$ values at low moisture contents (11% and 30% moisture content) is attributed to the shorter duration of the tests. The shorter tests allowed for determination of hydraulic conductivity prior to the onset of time related transient hydraulic conductivity factors such as decomposition, and particle swelling. Data was not collected for determination of the $k_{incremental}$ of the 56% moisture content sample. The trend of decreasing $k_{incremental}$ visible for the 85% moisture content sample may be due to the initiation of particle swelling and migration of fines. The samples placed at higher moisture contents had greater changes in $k_{incremental}$ than those placed a low moisture contents.

As documented previously by Landva and Clark (1990), Al-Thani et al. (2003), Durmusoglu et al. (2006), and Reddy et al. (2008b), a correlation between hydraulic conductivity and waste density was observed. The hydraulic conductivity values demonstrated a decrease with increasing dry unit weight when dry of optimum and an effectively stable value with increasing dry unit weight wet of optimum. Results for $k_{cumulative}$ as a function of dry unit weight are presented in Figure 30. Similar results were obtained when comparing hydraulic conductivity to initial void ratio.

The observed decrease in hydraulic conductivity is a function of the waste unit weight, which may be correlated with depth (Chen and Chynoweth 1995, Al-Thani et al. 2003). As burial depth increases the compressive stress on the waste increases. This leads to a commensurate increase in unit weight of the waste which contributes to the decrease in hydraulic conductivity of the lower layers at landfills.

The lower bound of hydraulic conductivity of the MMSW was due to softening of the MMSW components with the addition of moisture during sample preparation and during placement. The overall trend was similar to the data reported for sandy clays and silty clays by Lambe (1958b) and Mitchell (2005), respectively. MMSW cumulative hydraulic conductivity reached a minimum value at the optimum moisture content and did not vary significantly wet of optimum. The addition of water to the sample allowed for softening and breakdown of the particles during static compaction into the permeameter and increased the likelihood of particle migration. As well, the softer MMSW was more easily rearranged into a structure with decreased interconnection between smaller voids.

Table 9. Summary of $k_{incremental}$ and $k_{running}$ Values

Moisture content (%)	Incremental time (s)	Running time (s)	Flow (cm^3/s)	Test type	Temperature (°C)	$k_{incremental}$ (cm/s)	$k_{running}$ (cm/s)
11%	1,595	1,595	8.57	constant	20.5	$1.36x10^{-2}$	$1.36x10^{-2}$
	1,946	3,541	8.18	constant	20.5	$1.30x10^{-2}$	$1.32x10^{-2}$
	1,620	5,161	7.39	constant	20.5	$1.17x10^{-2}$	$1.28x10^{-2}$
30%	1,800	1,800	1.62	constant	18.4	$2.72x10^{-3}$	$2.72x10^{-3}$
	1,816	3,616	1.95	constant	18.6	$3.26x10^{-3}$	$2.98x10^{-3}$
	1,805	5,421	1.88	constant	18.9	$3.11x10^{-3}$	$3.01x10^{-3}$
	1,910	7,331	1.67	constant	19.2	$2.74x10^{-3}$	$2.92x10^{-3}$
85%	5,280	5,280	0.280	constant	18.4	$4.70x10^{04}$	$4.70x10^{-4}$
	4,500	9,780	0.148	constant	18.4	$2.49x10^{-4}$	$3.68x10^{-4}$
	3,600	13,380	0.123	constant	18.4	$2.06x10^{-4}$	$3.25x10^{-4}$
	18,000	31,380	0.0554	constant	18.4	$9.28x10^{-5}$	$1.92x10^{-4}$
	45,900	77,280	0.00893	constant	18.4	$1.50x10^{-5}$	$8.67x10^{-5}$
110%	8,820	8,820	0.181	constant	15.2	$3.31x10^{-4}$	$3.31x10^{-4}$
	7,200	16,020	0.375	constant	15.3	$6.84x10^{-4}$	$4.89x10^{-4}$
	7,320	23,340	0.489	constant	15.2	$8.97x10^{-4}$	$6.18x10^{-4}$
	39,600	62,940	0.173	constant	14.2	$3.26x10^{-4}$	$4.41x10^{-4}$
	7,200	70,140	1.01	constant	14.1	$1.90x10^{-3}$	$5.92x10^{-4}$
	7,200	77,340	1.05	constant	14.4	$1.96x10^{-3}$	$7.15x10^{-4}$
	7,200	84,540	1.08	constant	14.8	$2.01x10^{-3}$	$8.17x10^{-4}$
	9,000	93,540	0.891	constant	15.4	$1.62x10^{-3}$	$8.82x10^{-4}$
	53,280	146,820	0.157	constant	13.2	$3.05x10^{-4}$	$7.09x10^{-4}$
	10,800	157,620	0.780	constant	13.2	$1.51x10^{-3}$	$7.64x10^{-4}$

This is in comparison to the sample loaded at natural moisture content, in which particles were dry, stronger and transferred the loading force into compressible components during loading. The structure formed when the MMSW was loaded in a drier condition maintained the large interparticle voids which would in turn allow for increased liquid flow.

The modified structure of the waste was the limiting factor in the measured hydraulic conductivity once a specific moisture content was reached, controlling the hydraulic conductivity even as dry unit weights decreased and void ratios increased wet of optimum. Results showing hydraulic conductivity as a function of placement moisture content with a hand drawn trend line are presented in Figure 31.

Numerous components of the waste mixture may have behaved similarly to clay clusters, or clods. Clods in soil are comprised of structured groups of clay particles and are important in controlling the hydraulic conductivity of the soil as the flow of permeant occurs through the intercluster particles (Benson and Daniel 1990, Mitchell and Soga 2005).

Similarly, waste components comprised of an initially structured arrangement of fine particles such as dog food, wood, and wood pulp based products could control the hydraulic conductivity of the waste mass. Mitchell (2005) stated that for soils of desired low permeability, low values of hydraulic conductivity are only obtained if the clods and intracluster voids are eliminated during compaction. The static compaction used to bring the waste sample to the correct unit weight would have the effect of breaking down the waste clods in the higher moisture content samples, lowering hydraulic conductivity.

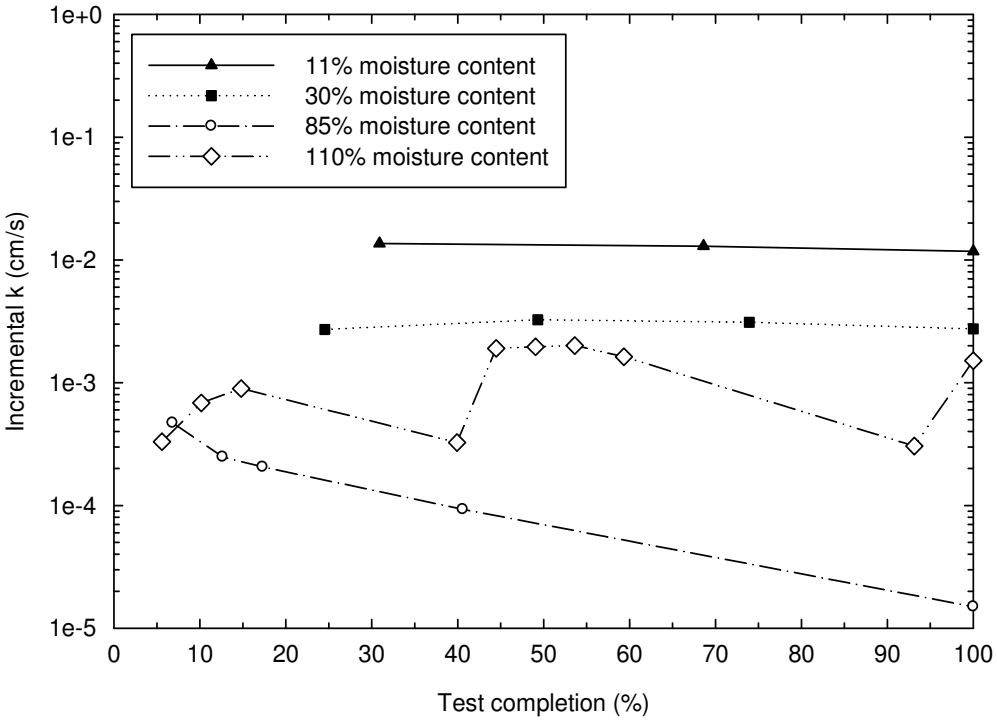

Figure 29. Incremental k as a function of percentage of test completion

In general, the hydraulic conductivity of the MMSW decreased throughout each individual test. This may have been due to migration of fines throughout the waste sample, blocking flow pathways despite the intentionally low hydraulic gradient of 1.0 used for testing. In addition, time-dependent swelling of the waste components may have contributed to the decreasing hydraulic conductivities. Furthermore, the initiation of biological activity may have begun to affect measurements of hydraulic conductivity as testing progressed, especially during tests of longer duration.

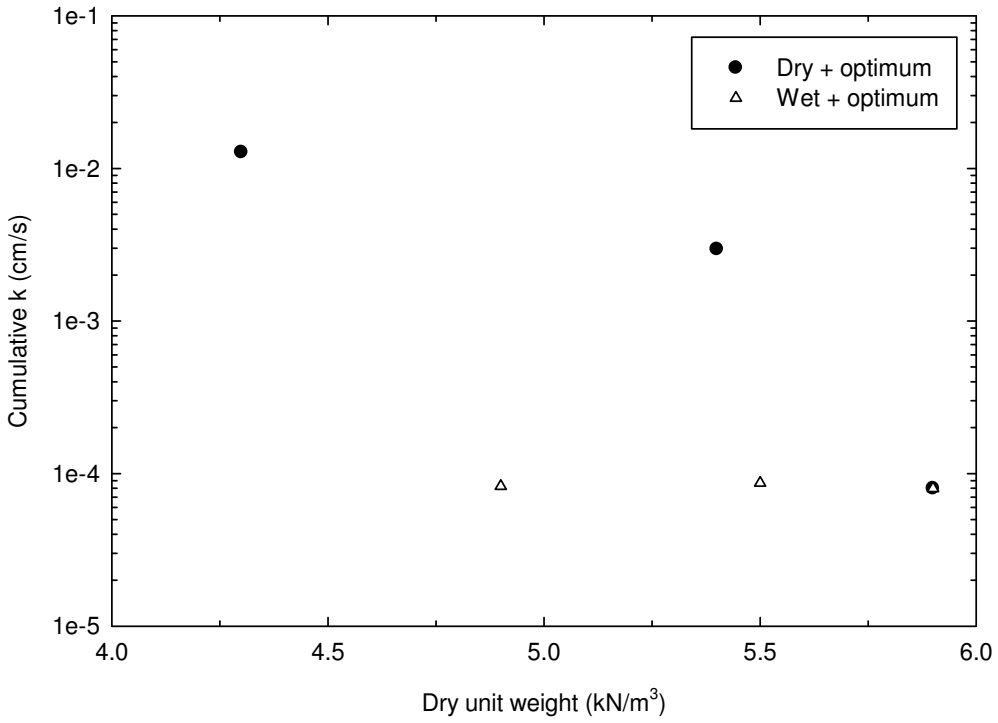

Figure 30. Cumulative hydraulic conductivity as a function of dry unit weight

The Kozeny-Carman equation was used to quantify the behavior of the MMSW as a sandy or clayey soil. Although the determination of the factors necessary to calculate hydraulic conductivity from the Kozeny-Carman equation was beyond the scope of work in this experimental program, several researchers have used the equation to propose a linear relationship between hydraulic conductivity and various void ratio functions for soils in which the Kozeny-Carman equation is applicable (uniformly graded sands and silts). Clay type soils, when analyzed by the same procedure will show a non-linear correlation.

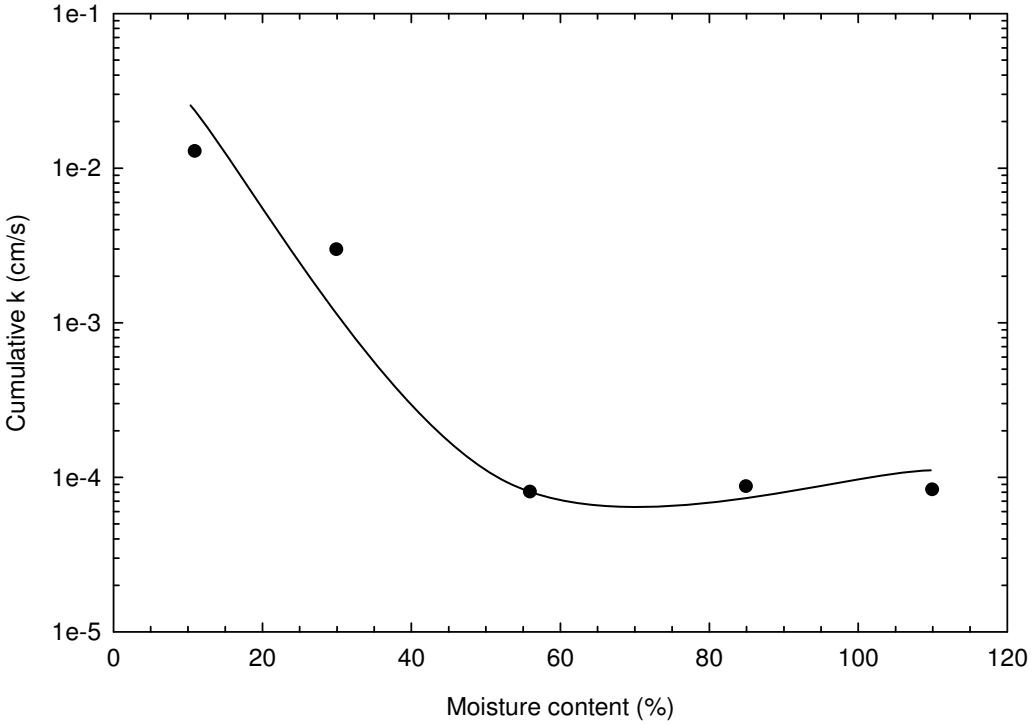

Figure 31. Cumulative hydraulic conductivity as a function of moisture content

Three void ratio functions were used for analysis of the MMSW. They are presented in in Equations 13 – 15.

$$k \propto e^2 \tag{13}$$

$$k \propto \frac{e^3}{1+e} \tag{14}$$

$$k \propto \frac{e^2}{1+e} \tag{15}$$

where:

k = hydraulic conductivity (length/time)

e = void ratio

The $k_{cumulative}$ values demonstrated a reasonable linear correlation with the void ratio formulae presented in Equations 13 – 15, with R^2 values of 0.76, 0.77, and 0.72, respectively. But, the non-linear correlation as defined by any number of non-linear data fits between hydraulic conductivity and the void ratio formulae was significantly stronger. For example, the R^2 values when fitted to a second order polynomial were 0.91 (Equation 13), 0.91 (Equation 14), and 0.89 (Equation 15), respectively. Based on the linear and non-linear data fits it is speculated that the hydraulic conductivity of MMSW is controlled by both sand-like and clay-like mechanisms, which is consistent with the make-up for MMSW having both discrete particle interactions and moldable particles that change in the presence of moisture.

Despite the generally non-cohesive (sand-like) appearance and relatively coarse component size distribution of the MMSW, the hydraulic conductivity of the material shares many similarities with clay-like soils. The variability in pore sizes within waste extend over a great range of compaction moisture contents, with relatively large voids between waste components and relatively small voids within individual waste components themselves, similar to the three previously described clay soil fabrics. As well, several of the components of the MMSW had a cohesive nature (e.g., dog food, paper, cardboard, and textiles), especially in the presence of moisture.

The void distribution of MSW, with large voids formed between relatively large, impermeable waste components, smaller voids between smaller components, and microscopic voids within the components themselves, can be described as having a combination of three fabrics. Although the constituents and aggregations comprising the minifabric of wastes may be much larger in scale than in clays, the three fabric system is aptly suited for description of the MMSW, which includes microfabric within waste components, minifabric between components, and macrofabric between large

components. It is also common for clay size fraction components to be present in wastes.

The microfabric consisted of interstitial voids within components such as the dog food, paper, and portions of cardboard, textile, wood chips, and concrete. Permeant fluid may have passed through at the microfabric level at different rates as a function of the gradient, geometry, pore size, tortuosity of the flow path, and time.

Particulate matter comprising the paper, dog food, and wood chips may also have swelled as time passed. Although quantification of the swelling phenomenon was not within the scope of this investigation, it was observed that several of the components had swelled during testing while removing samples from the permeameter between tests. The swelling particles resulted in decreases in hydraulic conductivity with time measured during the 11% and 85% moisture content sample tests.

4.6 Shear Strength Test Results

Shear strength data were analyzed to determine internal angle of friction from a single test assuming the waste did not have cohesive strength. This section includes analysis of internal angle of friction followed by an analysis of the shear stress-shear strain curves. A discussion of the sample dilation and contraction characteristics concludes the section.

Shear strength data from 5 tests were analyzed with the assumption that the MMSW was a cohesionless material within the range of strains to be tested (Singh and Murphy 1990, Edincliler et al. 1996). Based on that assumption, it was possible to approximate a linear failure envelope from a single direct shear test at each moisture content-dry unit weight combination.

Liquid was expelled during testing of the 85% and 110% moisture content samples and although captured, was not quantified. During sample unloading, it was noticed that the standing liquid that had drained from the shear box was tan/brown in color, turbid, malodorous, and developed a surficial film.

The friction angle was calculated using the peak value of shear stress and the corresponding normal stress recorded during the test. Shear stresses were corrected for the change in area that occurred during testing. Friction angles varied between 30.4° and 39.7°. The highest friction angle was measured from the 11% moisture content sample and decreased with increasing moisture content. The calculated internal angle of friction decreased despite increasing dry unit weight as optimum water content was approached from the dry side of optimum. A summary of the results is presented in Table 10 and Figure 32.

Table 10. Results of Direct Shear Testing

Water content (%)	γ_d (kN/m^3)	ϕ (degrees)	Maximum shear stress (kPa)	Corresponding ε (%)
11	4.3	39.7	165.8	14.6
30	5.4	35.9	145.6	14.6
56	5.9	33.9	134.5	14.7
85	5.5	32.5	127.7	14.8
110	4.9	30.4	118.7	14.8

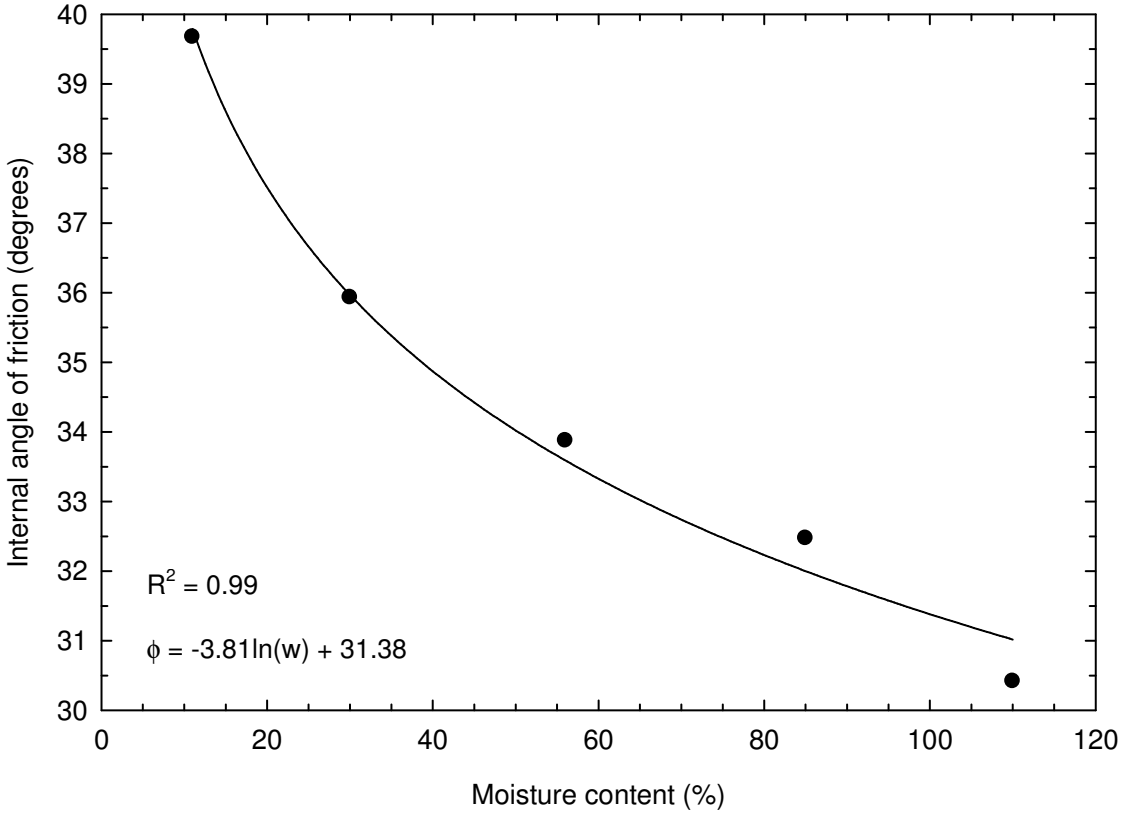

Figure 32. Internal angle of friction as a function of moisture content

The shear stress of each sample was plotted as a function of the shear strain (Figures 33 and 34). The plots were generated based on individual data values and were not based on a data fit. All shear stress-strain curves demonstrated a similar trend of yielding with increased shear stress. The sample at maximum dry unit weight (56% moisture content) developed the highest shear modulus at low shear strains, visible in Figure 34. At shear strains equal to or greater than 5%, the behavior of the 56% moisture content waste sample appeared to be controlled by the effects of the increased moisture content. The shear stress-strain curve of the 56% moisture content sample flattened out significantly at higher levels of shear strain, crossing through the 11% and 30% moisture content sample curves. This may be attributed to lubrication and

breakdown of the waste particles with increasing moisture content and shear strain, despite the increase in dry unit weight.

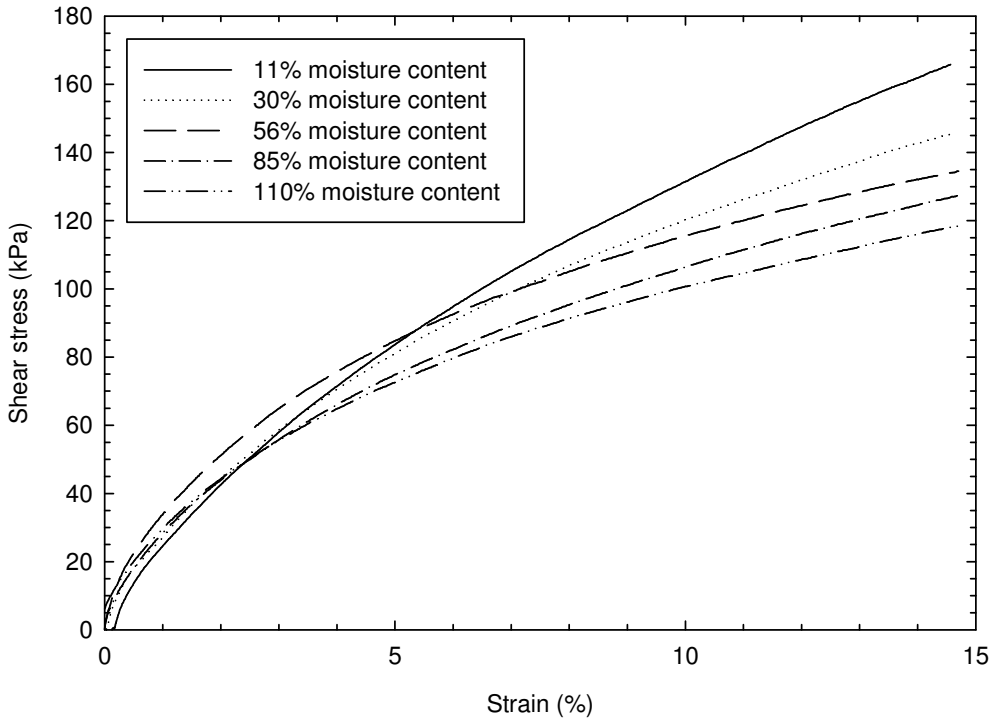

Figure 33. Shear strength as a function of strain

At 1% shear strain the shear modulus of elasticity varied between approximately 2,300 kPa (110% moisture content) and 3,100 kPa, with the peak value at 56% moisture content. At 14.5% strain the shear modulus of elasticity ranged from approximately 700 kPa (110%) to 1,100 kPa (11%), with the 56% moisture content sample in the middle of the range at 840 kPa. The shear modulus was not calculated at exactly 15% strain due to discrepancies in the starting strain reading that resulted in differences in termination strain magnitudes.

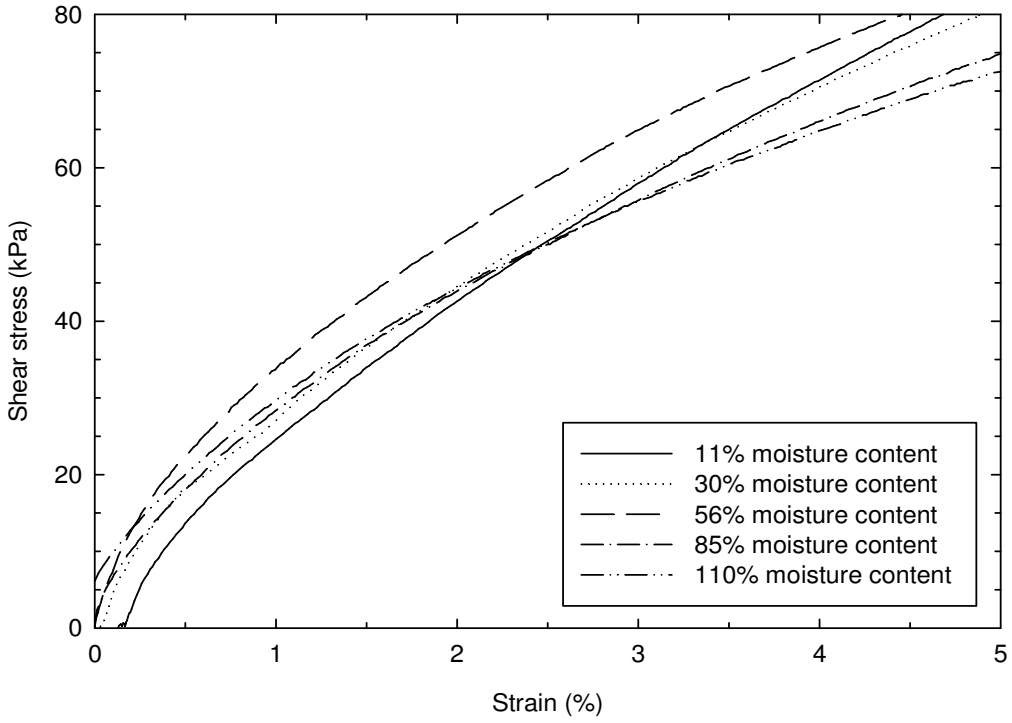

Figure 34. Shear strength as a function of strain
enlarged to show detail at low strains

A similar trend was visible for the shear stress curves of the 85% and 110% moisture content samples. The 85% and 110% moisture content curves crossed the 11% moisture content curve at approximately the same strain, indicating that at some minimum moisture content wet of optimum, shear strength is heavily controlled by moisture content. The relatively lower slopes of the 85% and 110% moisture content samples indicates that increases in moisture content wet of optimum resulted in moisture content controlled shear strength behavior at low strains. At high shear strains, the behavior of all the samples was controlled by the molding moisture content.

A similar behavior was reported in work on the effects of molding moisture content on the shear strength of clay performed by Cokca et al. (2004). The results of

the study indicated that the shear strength envelope for the clay changed with increasing moisture content. As the moisture content of the clay increased toward optimum, the frictional component of the shear strength decreased while the cohesion component increased. Toll (2000) suggested that for clay particles, the larger effective size of clods or clusters that were present dry of optimum may have resulted in more frictional behavior. The larger effective size of clods may have been responsible for the friction dominated behavior in a dry of optimum clay soil.

Similar to the data reported by Cokca et al. (2004), the increase in molding moisture content of the MMSW accounted for the softening and breakdown of susceptible components, as previously discussed in relation to compaction and hydraulic conductivity. The breakdown of components in turn decreased the frictional resistance to shearing and the presence of additional water lubricated particle contacts, resulting in a lower measured friction angle. This is illustrated in Figures 33 and 34 as the stiffness decreased both with increasing strain and with increasing moisture content. This is visible as a flattening of the shear stress-strain plot with increasing strain.

Examination of Figures 33 and 34 illustrates the continued increase in shear strength at 15% strain, albeit not as rapidly as during the first 2% of strain. All curves had a positive slope over the range of shear strains at which testing was conducted. The continued strength gain was attributed to the increased interlocking of fibrous materials resulting in the development of apparent cohesion within the MMSW test material with increasing strain. Fibrous materials that may have interlocked include paper, cardboard, plastic sheets, leather, and textiles.

Moisture content was an effective predictor of the internal angle of friction. Changes in moisture content were inversely related to changes in friction angle. A

logarithmic trend (presented in Figure 32) correlated well with internal angle of friction, with an R^2 of 0.99. The inverse relationship between moisture content and friction angle was attributed to breakdown of angular components of the MMSW and to lubrication of particle contacts due to water.

Some preferential orientation of particles and components occurs during both laboratory and field compaction processes. The breakdown of components into particles oriented with their long axes parallel to the direction of shearing would result in a decrease in frictional resistance along the shear plane imposed by the direct shear device. The addition of water would serve to further reduce the frictional force between particles not susceptible to softening and breakdown. Components in this category included plastic sheets, cardboard, leather, and grass clippings. Several of the components listed previously as having potential to interlock were also included as components that might reduce shear surface friction. It is hypothesized that such components may have acted in either manner, depending on the normal stress applied and the orientation and composition of neighboring components (e.g., a nail through a plastic sheet would interlock while a plastic sheet along a leather coupon would slide).

It was determined from the test program that dry unit weight alone was not an effective predictor of the internal angle of friction of the MSW. Plotting the friction angle as a function of dry unit weight resulted in a concave plot with slightly higher friction angles at the minimum and maximum dry unit weights as presented in Figure 35. Intermediate combinations of dry unit weight and compaction moisture content yielded varied results. This would lead to the conclusion that shear strength of wastes is a coupled phenomenon and that both dry unit weight and moisture content have important roles in the determination of shear strength.

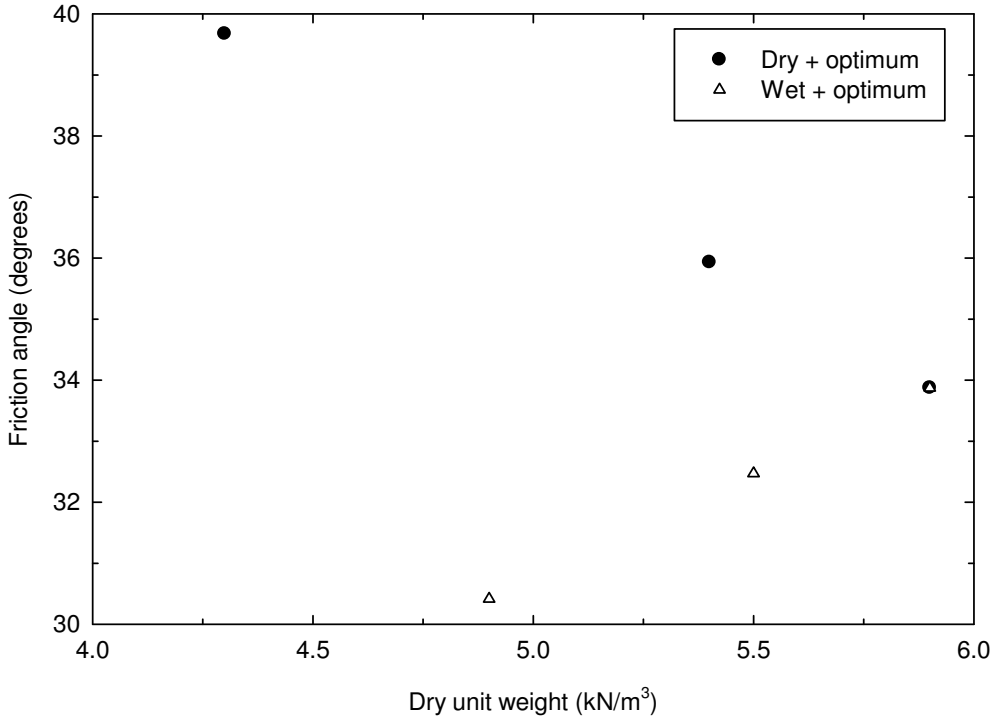

Figure 35. Plot of friction angle as a function of dry unit weight

To quantify the effects of moisture content on the friction angle, changes in friction angle as a function of moisture content were calculated. The sensitivity of the internal angle of friction to changes in moisture content was approximately 2 times higher when the samples were dry of optimum than wet of optimum. Internal angle of friction changed the least (per % moisture content difference) just wet of optimum (lowest slope between the 56% and 85% moisture content samples) and changed the most between natural moisture content and 30% moisture content. Over the range of moisture contents, the internal angle of friction decreased by approximately 0.1° for each percent change in molding moisture content. Changes in friction angle per change in moisture content are presented in Table 11.

Table 11. Change in ϕ Based on Moisture Content

Moisture content range	Change in ϕ for change in w (degrees/percent)	Notes
11% to 30%	-0.197	maximum change
30% to 56%	-0.079	
56% to 85%	-0.048	minimum change
85% to 110%	-0.082	
11% to 56%	-0.129	dry of optimum
56% to 110%	-0.064	wet of optimum
11% to 110%	-0.094	overall

If air pressure measured via the pressure transducer connected to the normal force bladder is taken as an indicator for volume change of the sample, several generalized trends may be determined from the air pressure data. The instantaneous air pressure was normalized over the average value for each test, yielding a value between 0.995 and 1.005. Pressure ratio values greater than 1 correlated with air pressures greater than the average value, which were interpreted as sample dilation. Pressure ratios less than 1 correlated with air pressures less than the average value, which were interpreted as sample compression. The normalized values of pressure ratio were plotted against strain in Figure 36. Moving averages with a 120 point period were used to smooth the data and show overall trends. Due to the use of a moving average, the first 120 data points (to approximately 1% strain) are not representative of actual sample behavior.

A pronounced period of sample dilation followed by compression was measured from the 11% water content sample. The sample at 30% moisture content generally shifted from the compression to dilation range. The 56% moisture content sample had the greatest relative dilation with a discernible change in slope at approximately 4% strain, which was consistent with the behavior that has been reported for dense soils (Holtz and Kovacs 1981). The samples at higher moisture contents had less range of

variation in sample height than drier samples which was attributed to softer waste particles that were able to break down instead of displace.

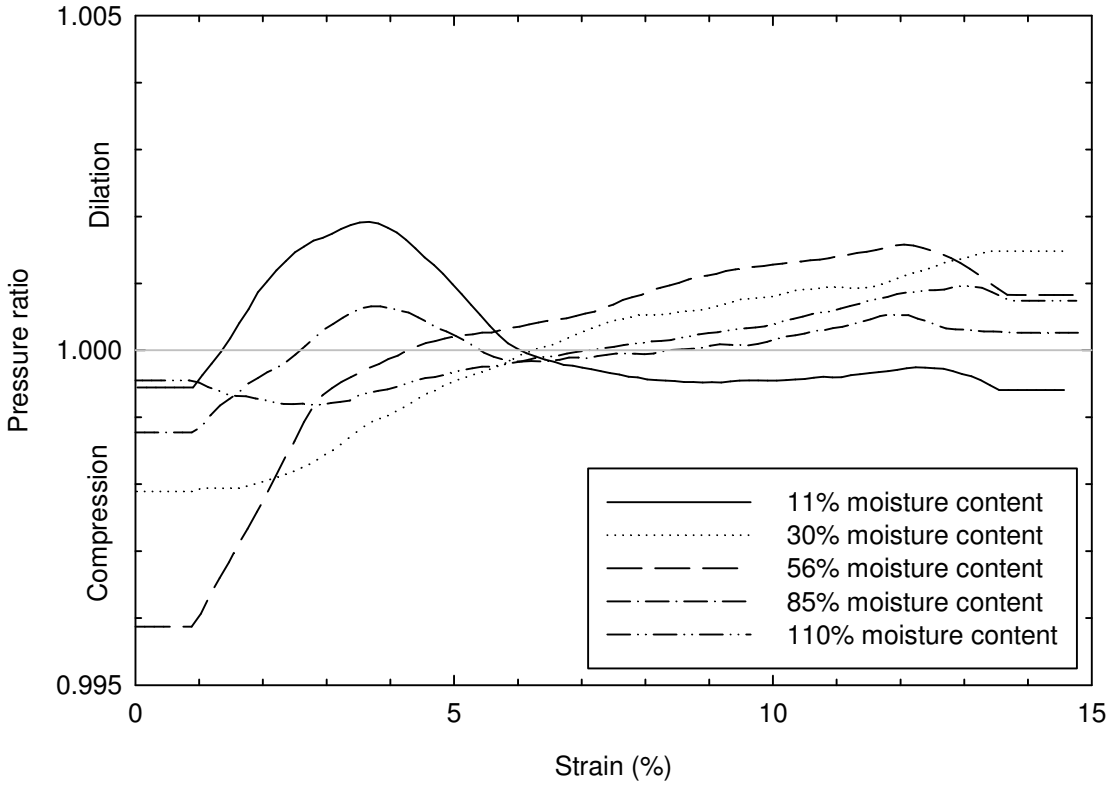

Figure 36. Running average normalized pressure ratio as a function of strain

Despite an initial period of dilation to approximately 5% strain, increasing shear strain on the 11% moisture content sample caused waste components to be broken down and the sample compressed as a result. At low shear strain (to approximately 5% strain), the particles of the 11% moisture content sample apparently rolled up and over each other, resulting in sample dilation. As shearing continued in the 5% to 7% shear strain range, the particles were crushed, leading to sample compression. Continued strain (from 7% to 15% strain) did not greatly alter the sample behavior, as the particles

had been crushed and rearranged into a different structure, resulting in an overall sample compression at high strains.

The mechanisms controlling the volume change behavior of the waste were different at higher dry unit weights. As with dense sands, the packing arrangement of the 56% moisture content sample forced waste components to roll up and over each other during shearing. Components were broken down in the 56% moisture content sample as strain increased (shown as a decrease in the slope at approximately 4% strain) but due to the high initial density of the sample, dilation continued despite component break down.

The samples up to optimum moisture content likely dilated due to the dry sample components rolling up and over other components. Both the 85% and 110% moisture content samples exhibited a lower range of volume change throughout the tests, likely due to softening of the samples wet of optimum. The softening allowed for waste components to shear during testing as opposed to rolling up and over each other (which would result in sample dilation) or densify (which would result in sample compression).

Chapter 5: Engineering Significance

Modification of moisture conditions during waste placement offer significant potential cost savings and environmental benefits. If such an operational strategy is implemented, engineering properties of waste would be affected. In this chapter, engineering properties of waste as a function of placement conditions are evaluated in a practical context of landfill design and operation. This section begins with discussion of the space savings possible with the use of MSW pre-wetting to increase dry unit weight. The effects of pre-wetting are then discussed in regards to changes in waste settlement. Next, the implications for leachate recirculation systems are discussed based on changes in hydraulic conductivity. Finally, a hypothetical slope is analyzed for slope stability based on the unit weight and shear strength properties as determined from this test program.

The results of the test program have implications for both geoenvironmental engineering practice and research. Refinement of the knowledge base of engineering parameters for municipal solid waste may assist in the safe, environmentally responsible design and operation of existing and future landfills. A summary of results for selected parameters as a function of compaction moisture content are presented in Figure 37.

5.1 Compaction Significance

MSW arrives at the landfill at approximately 30% - 50% moisture content (Von Stockhausen 2007). Due to the rapid change in MSW properties on the dry side of optimum as optimum is approached, the 30% moisture content MSW is already in a state of significantly decreased compressibility, hydraulic conductivity, and shear strength compared to drier conditions.

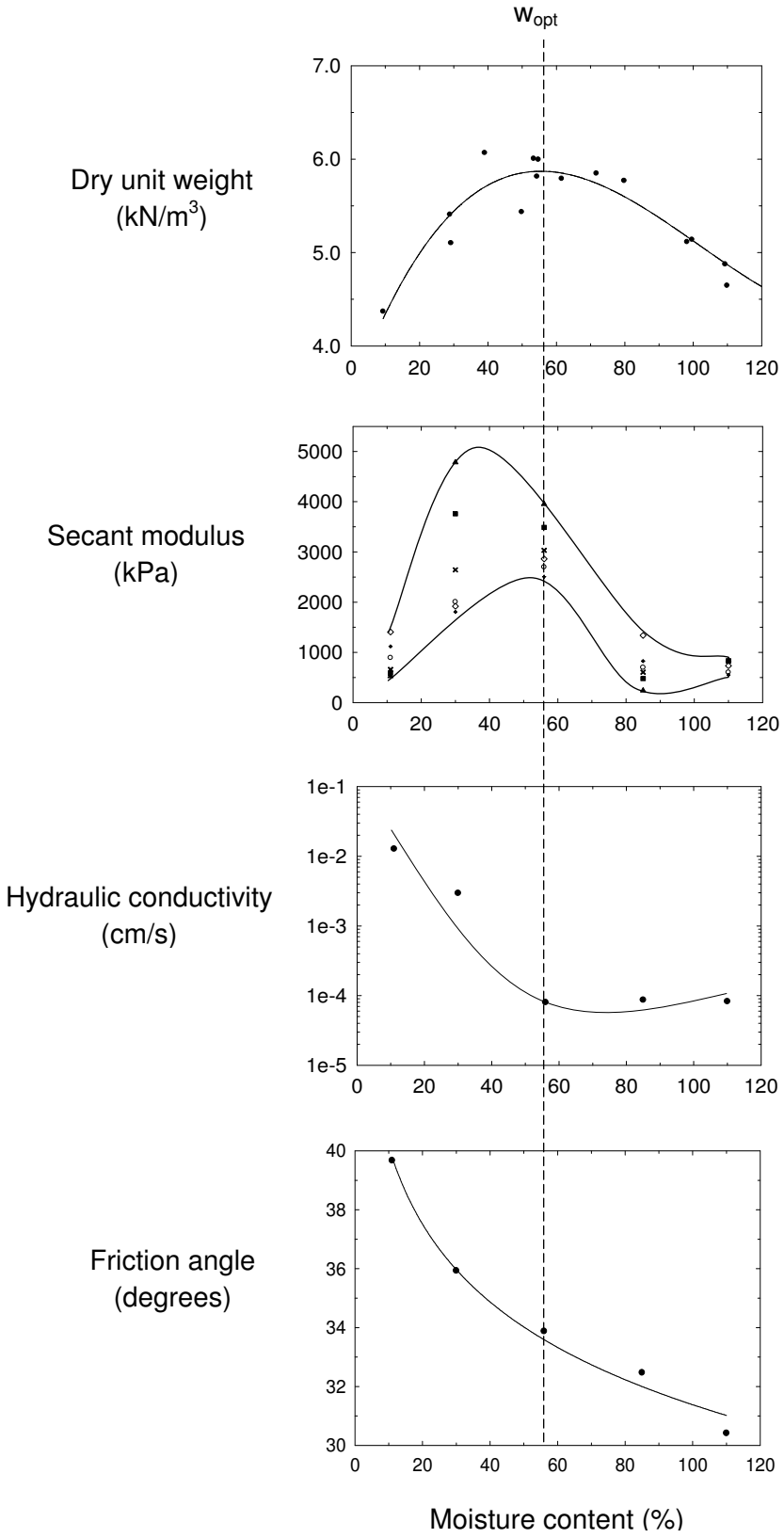

Figure 37. Dry unit weight, stiffness, hydraulic conductivity, and friction angle as a function of moisture content

The results of this study indicate that maximum density may be achieved if the moisture content of the waste is increased to optimum compaction conditions (on the order of 56% moisture content). The landfill operator must balance increases in moisture content (to allow a higher maximum dry unit weight) against reduced hydraulic conductivity (which may or may not be desirable) and shear strength to fit the maximum volume of waste within a given footprint of land while maintaining geotechnical stability for the final configuration.

Placement moisture content of wastes determines post placement geotechnical properties. To effectively use placement moisture content to control geotechnical properties, it would be necessary to conduct preliminary tests to establish the moisture content-dry unit weight relationship. Depending on the desired combination of properties, waste may be either dried or moistened.

Drying of waste to increase hydraulic conductivity and shear strength would not be practical from an operational point of view because it would be time consuming and energy intensive. To effectively decrease composite moisture content of incoming MSW, segregation of the high moisture content components (ie; yard wastes and foods) might be effective. The segregated food materials could be composted and the yard wastes could be chipped and distributed or sold as mulch, as is done at San Diego's Miramar Landfill (City of San Diego Environmental Services Department 2009). Alternatively, a water truck could be used to moisten the waste prior to compaction if the landfill operator were to decide to bring the waste to higher moisture content to increase maximum density (Von Stockhausen 2007).

Determination of the moisture-density relationship would allow for landfill operators to hydrate the waste to levels that would facilitate desired compacted unit weights. If the primary goal of the landfill operator was to maximize the weight of waste placed, maximum achievable density could be increased by wetting the waste to optimum moisture content. Based on the results of this investigation, the difference in dry unit weight between 30% (assumed typical as-delivered moisture content for MSW) and optimum would allow for an increase in dry unit weight of 0.5 kN/m^3.

For a waste disposal facility like Puente Hills Landfill located in Whittier, CA, with a daily disposal capacity of 120,000 kN (Sanitation Districts of Los Angeles County), the volume of waste per day would decrease by approximately 1,800 m^3 for the same weight of waste taken in, resulting in a daily volume savings of approximately 10%. Over the course of a year (assuming 260 days of operation per year) the increase in density/dry unit weight would amount to approximately 480,000 m^3 saved. Assuming a tipping fee of $3.80/kN (Sanitation Districts of Los Angeles County, 2009), the gross increase in annual collected tipping fees would be approximately $15 million. That value does not include the additional operational fees and fees for water that would be incurred with an MSW pre-wetting program. Such costs might include additional time required for placement, additional equipment, additional equipment operators, and the cost of water. These additional costs would act to offset the gross increase in collected tipping fees.

In summary, waste compaction at higher dry unit weights would have the practical effects of increasing the amount of waste that could be accepted daily as well as increasing the service life of landfills. Economic benefits would arise from the practical aspects and would result in an expected net increase in revenue.

5.2 Compressibility Significance

By controlling the variables associated with the compaction process, it is possible to control other properties of the waste as related to landfill performance. Variation in the compaction moisture content will change the compression characteristics of the waste. Knowledge of the compression characteristics will allow designers to more accurately predict the rates and magnitudes of settlement in waste. Understanding of the stress-strain behavior of waste materials will allow for increased accuracy in settlement prediction and reaction to loading.

Based on the theory of settlement and differing moist unit weight/apparent compression index values, it was possible to calculate settlement due to overburden stress associated with a waste column. Settlement was calculated for a 10 m thick waste fill. Calculations assumed that the waste began in a normally consolidated state and that 200 kPa of overburden stress was applied. The equation used to calculate settlement is presented in Equation 16.

$$s_c = c_c \left(\frac{H_0}{1+e_0}\right) \log\left(\frac{\sigma'_{0+\Delta\sigma}}{\sigma'_0}\right) \quad (16)$$

where:

s_c = settlement (length)

c_c = compression index (apparent c_c was substituted)

H_0 = initial height (length)

e_0 = initial void ratio

σ_0' = initial overburden stress (force/area)

$\Delta\sigma$ = change in overburden stress (force/area)

The magnitude of settlement of the initial 10 m waste fill ranged between 0.9 m and 3.8 m for the 110% and 30% moisture content samples, respectively. The 110%

moisture content fill was predicted to settle significantly less (half the next lowest value) than the other hypothetical waste fills despite having the largest change in overburden stress due to a lower apparent c_c, but as stated in Chapter 4, the development of excess pore pressure may have affected the calculated value of apparent c_c. Addition of moisture to the waste prior to compaction would lead to increased dry unit weight and decreased long-term settlement.

5.3 Hydraulic Conductivity Significance

Knowledge of the hydraulic behavior of a waste mass will assist in accurate determination of leachate collection and distribution rates and volumes, which affects the variation of effective stress within the waste mass. Based on the current trend toward bioreactor style landfills and accelerated settlements, an accurate determination of hydraulic conductivity has become increasingly important.

Advantages of placement of MSW at lower moisture content include significantly increased hydraulic conductivity, potentially making leachate recirculation more effective and expediting decomposition-induced settlement if increased recirculation rates can be assumed to evenly saturate the waste. As well, the increased rate of drainage of permeant through the waste mass would maintain lower pore pressures and higher effective stresses, aiding in slope stability.

The possibility also exists for drier placement conditions to allow for more heterogeneous waste structure, facilitating liquid flow through preferential paths of the macrofabric, resulting in uneven redistribution of leachate and spatial variability of engineering properties as specific regions undergo accelerated decomposition and physico-chemical breakdown. Channeled flow has been reported by numerous

researchers (Zeiss and Major 1992, Capelo and DeCastro 2006) when measuring leachate moisture flow through MSW.

If preferential flow does occur, then the addition of moisture prior to compaction would enable an increased dry unit weight and more even distribution of moisture (with decreased hydraulic conductivity) that might result in more even settlement. As a result, wetting during compaction may supersede the need for leachate recirculation.

If the waste were wetted to field capacity prior to compaction, compacting the waste into place would reduce field capacity. Leachate would be expelled from the current lift to lower lifts as a result of compaction (adding leachate to the surface of lower lifts, potentially mimicking a simple leachate reinjection).

Based on equations proposed in Maier (1998) and several simplifying assumptions, it was possible to calculate basic design parameters for leachate recirculation systems based on the cumulative hydraulic conductivities determined within this test program. By assuming the conditions listed in the following table; trench spacing, trench infiltration rate, and time for drainage could be calculated. Input values are presented in Table 12.

Table 12. Input Parameters for Leachate Trench Design Calculations

Head, h (m)	1
Minimum head, h_o (m)	0.03048
Waste suction, P_o (m)	0
Depth to wetting front, z_f (m)	6.1
Trench width, B (m)	0.9
Porosity of trench fill, n	0.3
Radius of well, r (m)	0.1524
Well filter hydraulic conductivity, k_w (cm/s)	0.01

Minimum head, waste suction, depth to wetting front, and trench width values were obtained as suggested values from Maier (1998). The ratio of horizontal to vertical hydraulic conductivity was assumed to be 13 to 1. Vertical hydraulic conductivity was varied to determine the effects of the variance on leachate system design values. The results of the calculations are presented in Table 13.

Table 13. Results of Leachate Trench Design Calculations

Sample	11%	30%	56%	85%	110%
Spacing (m)	7.2	7.2	7.2	7.2	7.2
Infiltration rate, bottom + sides (L/s)	0.2831	0.0652	0.0018	0.0019	0.0018
Infiltration rate, bottom + sides (L/h)	1,020	230	6.4	6.9	6.6
Infiltration rate, bottom (L/s)	$1.5x10^{-1}$	$3.4x10^{-2}$	$9.3x10^{-4}$	$1.0x10^{-3}$	$9.6x10^{-4}$
Infiltration rate, sides (L/s)	$7.4x10^{-2}$	$1.7x10^{-2}$	$4.6x10^{-4}$	$5.0x10^{-4}$	$4.8x10^{-4}$
Drain time (s)	1,403	6,362	234,883	216,461	226,931
Drain time (h)	0.4	1.8	65.2	60.1	63.0

Due to the formula used for calculation of leachate trench spacing, the spacing remained at 7.2 m despite changes in vertical hydraulic conductivity. Calculated infiltration rate ranged from approximately 6 to 1,000 L per hour, increasing with higher hydraulic conductivity. Drainage time, described as the time for a leachate infiltration trench to drain increased from less than 1 hour to more than 65 hours with decreasing hydraulic conductivity.

For a landfill operator interested in pumping a maximum volume of leachate through the waste mass using a leachate reinjection system, the same leachate trench would take greater than 30 times as long to drain if the waste were compacted at 56% moisture content as opposed to 30% moisture content. There is limited data available regarding the impact of the residence time of leachate. As such, the expedited drainage may or may not actually expedite settlement.

The long term and settlement induced effects of the increased infiltration rate are unknown; the result may be a more even wetting of the waste yielding more even and expedited settlements, or the establishment of preferential flow pathways, leading to uneven settlements. Wetting of the waste prior to compaction may serve to evenly wet the waste, resulting in more consistent, predictable settlement magnitudes and rates despite reduced hydraulic conductivity through the waste.

5.4 Shear Strength Significance

Evaluation of MSW shear strength properties may lead to a better understanding of the specific roles of moisture content and dry unit weight. Understanding the factors that affect MSW shear strength will allow more efficient engineering design of landfill slopes and post closure structures.

The work may have important implications for bioreactor style landfills in which leachate and air are continuously cycled to expedite the decomposition portion of waste settlement. Results of the research in this test program indicated that variation of placement moisture content would have commensurate effects on the shear strength of waste. Although each MSW composition would have a characteristic shear strength and governing waste mechanisms, the trends presented in this study indicated that increased moisture content within the waste decreased the frictional portion of waste shear strength. There are potentially serious implications for the operation of bioreactor landfills with regards to slope stability issues.

Variation of molding moisture content and unit weight would have implications for landfill slope stability. Based on a preliminary analysis using Winstabl slope stability software and a typical waste slope with 1:3 vertical to horizontal ratio, the change in factor of safety as a function of the varying moisture content-dry unit weight

combinations was analyzed. The factor of safety decreased by approximately 0.49 from a maximum value of 2.55 as the moist unit weight and friction angle were varied between the 11% and 56% moisture content soil values. Over the entire range of moisture contents measured in this study (11% to 110%), the factor of safety decreased by 0.75 as friction angle and moist unit weight varied. The critical failure surface consistently surfaced at the toe of the waste slope and appeared planar (as was expected based on the non-cohesive geotechnical material parameters used in the analysis). The trial slope and Winstabl generated critical failure surfaces for the 56% moisture content slope are presented in Figure 38. The failure surface with the lowest factor of safety is shown as a bold, dotted line.

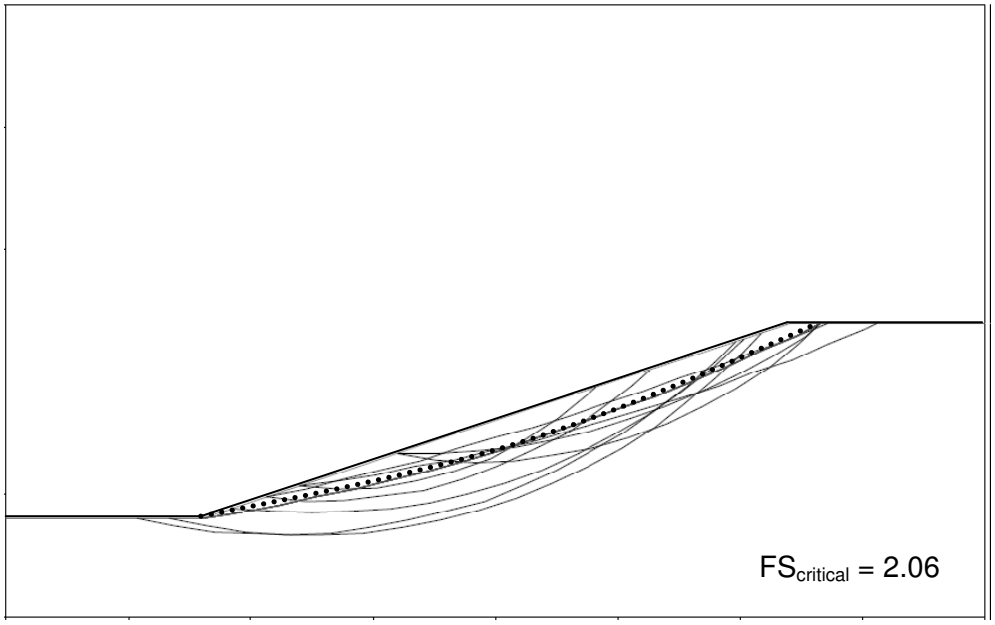

Figure 38. Trial waste slope at 56% moisture content
with critical failure surfaces

As land has become scarcer, it has become necessary to vertically expand landfills and re-use landfills after closure for other purposes. Understanding the trends in geotechnical properties of waste based on placement will lead to maximization of

reuse options and increased protection of human safety and the environment. Accurate control of waste placement conditions will allow landfill operators, engineers, and planners to effectively control geotechnical properties during operation and post closure. More specifically, understanding and control of placement moisture content in the compaction of wastes will have both immediate and long term effects on the dry unit weight, settlement, leachate recirculation properties, and slope stability.

Increasing the placement moisture content of waste to the optimum moisture content will increase dry unit weight, decrease settlement, decrease leachate infiltration rates, and slightly decrease the factor of safety of waste slopes. Depending on other factors such as landfill life span, waste slope steepness, and financial aspects, the addition of water to waste prior to compaction may be a viable alternative to the operation of conventional bioreactor style landfills.

Chapter 6: Summary, Conclusions, and Recommendations

6.1 Summary and Conclusions

The test program highlighted the importance of waste placement conditions on the geotechnical properties of waste. Controlling the placement moisture content of the waste had a significant influence on the dry unit weight, compressibility, hydraulic conductivity, and shear strength.

A representative, consistent, manufactured MSW was used for the test program. Tests were performed in large scale testing devices and included compaction, constant rate of strain compression, hydraulic conductivity, and shear strength.

Waste classification consisted of categorization by component, as used by the United States EPA. A representative material was selected initially and used throughout preparation of the remainder of the waste samples. This relatively heterogeneous mixture was reproducible, consistent, and allowed for meaningful analysis of the geotechnical properties and trends while varying initial placement conditions. Determination of the initial specific gravities of individual components allowed an analysis of the MMSW via a standard geotechnical engineering phase diagram.

Compaction testing data were used as the baseline for the testing program. Tests were performed at both modified and four times modified compactive efforts using conventional and non pre-wet hydration. No significant differences were observed between the two hydration methods. Based on the compaction test program, the following conclusions were drawn:

1. The MMSW compaction curve had a bell shaped curve with maximum dry unit weights of 5.1 kN/m^3 and 5.9 kN/m^3 correlating to optimum moisture contents of 66% and 56% for the modified and 4x modified compactive efforts, respectively.

2. Increased compactive effort resulted in a higher dry unit weight at decreased moisture content.
3. Compaction of wastes at increased compactive effort resulted in an increased composite specific gravity of the waste.
4. Compaction behavior of waste was similar to that of soils with waste specific mechanisms altering the shape of the compaction curve from the standard bell shaped curve established for soils.

Data obtained from the four times modified tests were used to establish 5 moisture content-dry unit weight pairs used in subsequent testing.

Constant rate of strain compression testing was performed in a large scale test cell on five samples. Each sample was loaded into the test cell at a pre-determined dry unit weight and moisture content. Samples were strained to 50% of their original height over the course of each 12 hour test or until a threshold value of force was reached. The development of excess pore pressure during loading was not accounted for during testing. Secant and tangent moduli and stiffness were determined at varying strains. Based on the compressibility test program, the following conclusions were drawn:

1. The MMSW required more force to reach a designated strain value when prepared dry of optimum than when prepared wet of optimum.
2. Stress required to reach designated strain and modulus values converged to similar values wet of optimum.
3. The MSW underwent a 3 part confined compression process including locking, yielding, and renewed locking.

4. Secant and tangent moduli demonstrated bell shaped curves with respect to moisture content. Peak values of moduli occurred at approximately the optimum moisture content and decreased wet of optimum.
5. The shape of the secant and tangent moduli curves appeared to be a result of the interaction of both placement moisture content and dry unit weight.
6. Apparent c_c followed a generally decreasing trend with increasing moisture content and fit within the envelope of compression indices reported by previous researchers for numerous soils and geomaterials.

Samples dry of optimum had higher secant and tangent moduli than samples placed wet of optimum. At strains greater than approximately 15%, the modulus for each sample became more similar as demonstrated by the nearly parallel stress-strain plots. The apparent c_c of the MMSW used in this program was less sensitive to changes in initial void ratio than many of the previously reported equations.

Hydraulic conductivity testing was performed in a large scale dual ring permeameter. Tests varied in duration between 1.5 hours and 44 hours. Based on the results of the hydraulic conductivity testing program, the following conclusions were drawn:

1. Cumulative hydraulic conductivity decreased asymptotically (from 7.99×10^{-5} cm/s to 1.28×10^{-2} cm/s) as moisture content increased to optimum with a slight rebound wet of optimum.
2. Incremental hydraulic conductivity values decreased with increased molding moisture contents.

3. Particle swelling and breakdown of material structure (structured components in waste compared to clusters in soil) resulted in a decrease in hydraulic conductivity.
4. Waste behaved similarly to both sand and clay soils based on the MMSW data fit to the void ratio term of the Kozeny-Carman equation.
5. Waste hydraulic conductivity was transient.

Large scale direct shear tests were performed in a 300 mm shear box. Tests ranged in duration from 14 to 15 hours. A single test was performed at each moisture content-dry unit weight combination. Tests were conducted at 200 kPa normal stress and sheared to 15% strain. The analysis of the strength data was based on an assumption of zero cohesion. Based on the data obtained from shear strength testing, the following conclusions were drawn:

1. Initial shear stress-strain behavior was controlled by dry unit weight.
2. Shear strength at high shear strains was controlled by placement moisture content.
3. Internal angles of friction varied between 30.4° and 39.7° from dry (11% moisture content) to wet (110% moisture content) and had the largest decrease in friction angle per % increase in moisture content between 11% and 30%.
4. The samples continued to gain strength with increased shearing due to increased component interlocking and had not reached peak values at test termination.
5. Internal angle of friction decreased monotonically with increasing moisture content.
6. Increasing moisture content (in combination with high shear strains) resulted in particle softening, breakdown of susceptible particles, and slippage between component contacts along the shear plane.

7. Waste samples exhibited volume change behavior similar to soils.

Overall, the results of the tests indicate that the MMSW test material used in this test program was strongly influenced by placement conditions. Molding moisture content had the effect of softening the waste material and lubricating particle contacts in tests where compression or shearing was involved (compaction, compressibility, direct shear). Numerous similarities were found between waste behavior and soil behavior when analyzed as a function of placement conditions including: a bell shaped compaction curve, bell shaped stiffness/moduli of elasticity curves with a peak near optimum moisture content, convergence of stiffness and modulus values wet of optimum, minimized hydraulic conductivity wet of optimum, and decreasing shear strength with increasing moisture content. As well, existing soil data and data gathered in this test program highlighted the importance of material fabric and structure on all geotechnical parameters, and the importance of moisture content in controlling geotechnical parameters.

The values for the varying geotechnical parameters were used to perform a basic study of effects on numerous landfill processes. Increased compaction moisture content would allow for a higher waste density and increased landfill capacity and financial profits while affecting other geotechnical engineering properties. Settlements varied by a factor of 4 based on the varying apparent compression indices, void ratios, and moist unit weights. Increasing placement moisture content would result in more even distribution of moisture throughout the waste as well as increased homogeneity of the waste packing structure despite decreasing hydraulic conductivity. Changes in vertical hydraulic conductivity did not change leachate trench spacing although the changes strongly affected leachate trench infiltration rates and drainage times. The factor of safety of a trial landfill slope decreased 0.49 when moist unit weight and internal angle of

friction were varied according to the values as determined in this test program (from 11% moisture content to 56% moisture content values).

6.2 Recommendations

In this section, recommendations for improvements to tests performed within the scope of this test program are made. Next, recommendations for general conceptual topics of additional related research are made.

Compaction testing may have benefitted from the use of a larger compaction mold. Although the apparent volume of each waste component was not a significant portion of the volume of the compaction mold, the compaction data may have been affected by scaling and edge effects. A thorough understanding of the potential issues with the automatic compactor should be gained prior to the use of either unit. Each of the compactors posed unique issues to obtaining representative data.

Future compressibility testing should include measurement of pore pressures within the sample. Alternatively, compressibility testing could mimic oedometer testing more closely, with the application of load in steps and prior calculation of drainage times to minimize development of pore pressures. In general, compressibility tests should be longer in duration to more accurately measure compression index (without the potential effect of pore pressure) and/or secondary compression index. The loading cap used in the test cell should be reinforced with bracing to ensure that flexure of the cap is not a concern during testing and loading. A connection between the test cell cap and loading rod should be made that allows for the application of tensile force (as the cap often became stuck within the test cell, requiring significant time and energy to remove).

Future hydraulic conductivity testing should be conducted for longer duration once the permeameter has been filled. Hydraulic conductivity testing should be

conducted prior to other tests (where possible) to calculation of drained loading rates. As well, the bottom of the permeameter should be reinforced to better resist the loading stress imposed during sample loading. A better connection for the perimeter drain should be devised to prevent leakage and allow bottom up saturation. Measurement of field capacity of waste should be made if time allows after each hydraulic conductivity test. Computer aided data collection would help greatly in allowing longer tests with consistent reading intervals.

Future shear strength testing should include more tests to determine the absence/presence of apparent cohesion within the MMSW. The additional tests would also serve the purpose of verifying the accuracy of the data collected during each individual test.

Heights of each lift prior to and post placement should be recorded for all tests. All leachate that is expelled from the test equipment should be quantified. A mechanical mixer would aid in thorough mixing and wetting of wastes.

Further research is needed to refine MSW trends as a function of moisture content and waste type, to separate out the effects of moisture content and dry unit weight on geotechnical properties, and to examine alteration of waste fabric due to compaction, compressibility, permeation, and shearing.

To expand the applicability of the index compressibility tests conducted herein to conventional consolidation parameters, larger constant rate of strain or step-stress tests should be conducted. The compressibility data would have uses in prediction of landfill settlement.

To improving the understanding of the effects of different components on waste behavior, it is necessary to vary waste mixture while holding other variables constant.

An increased understanding of waste trends based on moisture content and waste type would allow engineers to more accurately predict the range of parameters to use while designing landfills. Analysis of the effects of moisture content without varying dry unit weight is necessary to determine the specific effects of one placement condition on MSW geotechnical behavior. In this manner, it may be possible to determine the point at which molding moisture content begins to control the behavior of each geotechnical property.

Research is recommended to evaluate the distribution of moisture through wastes at varying moisture content-dry unit weight combinations (and hence hydraulic conductivities). If preferential flow pathways are found for wastes of relatively high hydraulic conductivity, it may have implications for the design and operation of bioreactor landfills.

Additional work should also include examination of the waste fabric at different points (prior to placement, post placement, post testing) of the testing process to verify the changes in fabric as a result of placement and testing. Work of this type would also enhance the understanding of waste mechanics although it would be critical to use representative components within any manufactured MSW.

Examination of the hydraulic conductivity as a function of the overburden stress would aid in the understanding of the variation of hydraulic conductivity based on coupled stress and moisture conditions. Data could be used for more efficient design of leachate recirculation or gas collection systems.

Continued research of the properties of waste will allow for a better understanding and more efficient engineering design of landfills. The production of municipal solid waste will continue indefinitely and only through further experimentation

and experience can landfill design be optimized, public safety be protected, and environment be preserved.

References

Alger, M. S. (1989). *Polymer Science Dictionary.* Elsevier Science Publishers Co Inc., New York, New York.

Al-Thani, A., Beaven, R., and White, J. (2003). "Modelling Flow to Leachate Wells in Landfills," *Waste Management* , 24, 3, 271-276.

ASTM. (2007a). "*D 698 - Standard Test Methods for Laboratory Compaction Characteristics of Soil Using Standard Effort,"* ASTM International, West Conshohocken, PA. DOI: 10.1520/D0698-07E01.

ASTM. (2007b). "*D 1557 - Standard Test Methods for Laboratory Compaction Characteristics of Soil Using Modified Effort,"* ASTM International, West Conshohocken, PA, DOI: 10.1520/D1557-07.

Beaven, R., and Powrie, W. (1996). "Determination of the Hydrogeological and Geotechnical Properties of Refuse in Relation to Sustainable Landfilling," *Proceedings of the Nineteenth International Madison Waste Conference: Municipal and Industrial Waste*, University of Wisconsin, Madison, Madison, WI, 435-453.

Benson, C., and Daniel, D. (1990). "Influence of Clods on Hydraulic Conductivity of Compacted Clay," *Journal of Geotechnical Engineering*, ASCE, 116, 8, 1231-1248.

Bjarngard, A., and Edgers, L. (1990). "Settlement of Municipal Solid Waste Landfills," *Proceedings of the Thirteenth Annual Madison Waste Conference* , University of Wisconsin, Madision, Madison, WI, 192-205.

Bleiker, D., Farquhar, G., and McBean, E. (1995). "Landfill Settlement and the Impact on Site Capacity and Refuse Hydraulic Conductivity," *Waste Management and Research*, 13, 6, 533-554.

Boutwell, G., and Fiore, V. (1995). "Settlement of Clay Cover on Saturated Garbage," *Proceedings of the Specialty Conference on Geotechnical Practice in Waste Disposal. Part 1 (of 2),* ASCE, New Orleans, LA, 964-979.

Bowles, J. E. (1997). *Foundation Analysis and Design - Third Edition,* Mcgraw-Hill Book Company, Singapore.

Brandrup, J., and Immergut, H. (1989). *Polymer Handbook - Third Edition.* Interscience, John-Wiley and Sons, New York, New York.

Bray, J.D., Zekkos, D., Kavazanjian, E., Athanasopoulos, G.A., Riemer, M.F. (2009). "Shear Strength of Municipal Solid Waste," *Journal of Geotechnical and Geoenvironmental Engineering*, 136, 6, 709-722.

Caicedo, B., Yamin, L., Giraldo, E., and Coronado, O. (2002). "Geomechanical Properties of Municipal Solid Waste in Dona Juana Sanitary Landfill," *Proceedings of the*

4th International Conference on Environmental Geotechnics: Environmental Geotechnics. De Mell and Almeida.

Capelo, J., and DeCastro, M. (2007). "Measuring Transient Water Flow in Unsaturated Municipal Solid Waste - A New Experimental Approach," *Waste Management* , 27, 6, 811-819.

Carman, P. (1956). *Flow of Gases through Porous Media,* Butterworths Scientific Publications, London, United Kingdom

Chen, T., and Chynoweth, D. (1995). "Hydraulic Conductivity of Compacted Municipal Solid Waste," *Bioresources Technology*, 51, 205-212.

City of San Diego Environmental Services Department. (2009). *Pricing and Pick Up Instructions*. Last accessed: 22 June 2009, from *http://www.sandiego.gov/environmental-services/miramar/cmw.shtml*

Coduto, D. (1999). *Geotechnical Engineering: Principles and Practices,* Prentice Hall Inc, Upper Saddle River, NJ.

Coduto, D., and Huitric, R. (1990). "Monitoring Landfill Movements Using Precise Instruments," *Geotechnics of Waste Fills - Theory and Practice, ASTM STP 1070* , 358-370.

Cokca, E., Erol, O., and Armangil, F. (2004). "Effects of Compaction Moisture Content on the Shear Strength of an Unsaturated Clay," *Geotechnical and Geological Engineering*, 22, 2, 285-297.

Cotton, Inc. (2008). *US Cotton Fiber Chart*. Last accessed: 4 December 2008, from Cotton, Inc. from, *http://www.cottoninc.com/CottonFiberChart/?Pg=8*

Cowland, J., Tang, K., and Gabay, J. (1993). "Density and Strength Properties of Hong Kong Refuse," *Proceedings Sardinia '93, 4th International Landfill Symposium*, Eds. T.H. Christensen, R. Cossu and R. Stegmann, CISA, S. Margherita di Pula, Cagliari, Italy, 1433-1446.

Das, B. (1997). *Principles of Geotechnical Engineering - 4th Edition,* PSW Publishing Co., Boston, MA.

Del Grecco, O., and Oggeri, C. (1993). "Geotechnical Parameters of Sanitary wastes," *Proceedings Sardinia '93, 4th International Landfill Symposium*, Eds. T.H. Christensen, R. Cossu and R. Stegmann, CISA, S. Margherita di Pula, Cagliari, Italy, 1421-1431.

Deutsch, W., Esterly, O., and Vitale, J. (1994). "Modeling Settlement of an Existing Municipal Solid Waste Landfill Sideslope Using and Earthen Surcharge Pile," *Vertical and Horizontal Deformations of Foundations and Embankments,* Eds. A. Yeung, and G. Felio, ASCE Geotechnical Special Publication, 1135-1148.

Dixon, N., and Jones, D. R. (2005). "Engineering Properties of Municipal Solid Waste," *Geotextiles and Geomembranes*, 23, 205-233.

Dixon, N., and Langer, U. (2006). "Development of a MSW Classification System for the Evaluation of Mechanical Properties," *Waste Management*, 26, 3, 220-232.

Durham Geo Slope Indicator. (2009). Direct Shear Machine LG-116 Operator's Manual, V1.0. Stone Mountain, GA.

Durmusoglu, E., Sanchez, I., and Corapcioglu, M. (2006). "Permeability and Compression Characteristics of Municipal Solid Waste Samples," *Environmental Geology*, 50, 773-786.

Edgers, L., Noble, J., and Williams, E. (1992). "A Biologic Model for Long Term Settlement in Landfills," *Proceedings of the Mediterranean Conference on Environmental Geotechnology,* Cesme, Turkey: A.A. Balkema, Rotterdam, Netherlands, 177-184.

Edil, T., Ranguette, V., and Wuellner, W. (1990). "Settlement of Municipal Refuse," *Geotechnics of Waste Fills - Theory and Practice,* Eds. A. Landva, and D. Knowles, American Society of Testing and Materials STP 1070, Philadelphia, PA, 225-239.

Edil, T., den Haan, Evert J. (1994). "Settlement of Peats and Organic Soils," *Proceedings of the Conference on Vertical and Horizontal Deformations of Foundations and Embankments,* ASCE, College Station, TX, Vol. 2, 1543-1572.

Edincliler, A., Benson, C., and Edil, T. (1996). "*Shear Strengh of Municipal Solid Waste,"* University of Wisconsin, Madison, Madison, WI.

El-Fadel, M., and Al-Rashed, H. (1998). "Settlement in Municipal Solid Waste Landfills, Field Scale Experiments," *The Journal of Solid Waste Technology and Management*, 25, 2, 89-98.

El-Fadel, M., and Khoury, R. (2000). *Modeling Settlement in MSW Landfills: A Critical Review,* CRC Press LLC, Boca-Raton, FL.

El-Fadel, M., Findikakis, A., and Leckie, J. (1989). "A Numerical Model for Methane Production in Managed Sanitary Waste Landfills," *Waste Management and Resource Recovery*, 7, 1, 31-42.

EPA. (2008). *Municipal Solid Waste Generation, Recycling, and Disposal in the United States: Facts and Figures for 2006*., Last accessed: 3 June 2008, from United States Environmental Protection Agency, http://www.epa.gov/osw/nonhaz/municipal/msw99.htm

Fassett, J., Leonardo, G., and Repetto, P. (1994). "Geotechnical Properties of Municipal Solid Waste and Their Use in Landfill Design," *Waste Technology '94, Landfill Technology Technical Proceedings.* Charleston, SC.

Gabr, M., and Valero, S. (1995). "Geotechnical Properties of Municipal Solid Waste," *Geotechnical Testing Journal*, ASTM, 18, 2, 241-251.

Gibson, R., and Lo, K. (1961). "A Theory of Consolidation of Soils Exhibiting Secondary Compression," *Norweigan Geotechnical Institute Publication*, 41, 1-16.

Grisolia, M., and Napoleoni, Q. (1995). "Deformability of Waste and Settlements of Sanitary Landfills," *Proceedings of World Congress on Waste Management,* Wien: ISWA'95.

Grisolia, M., Napoleoni, Q., and Tancredi, G. (1995). "Contribution to a Technical Classification of MSW," *Proceedings of the 5th International Landfill Symposium,* Eds. T.H. Christensen, R. Cossu and R. Stegmann, CISA, S. Margherita di Pula, Cagliari, Italy, 703-710.

Grisolia, M., Napoleoni, Q., and Tancredi, G. (1995). "The Use of Triaxial Tests for the Mechanical Characterization of MSW," *Proceedings of the 5th International Landfill Symposium*, Eds. T.H. Christensen, R. Cossu and R. Stegmann, CISA, S. Margherita di Pula, Cagliari, Italy, 703-710.

Hardcastle, J., and Mitchell, J. (1974). "Electrolyte Concentration - Permeability Relationships in Sodium-Illite-Silt Mixtures," *Clay and Clay Minerals*, 22, 143-154.

Hettiarachchi, C. (2005). *Mechanics of Biocell Landfill Settlements, PhD Dissertation., D*epartment of Civil and Environmental Engineering, New Jersey Institute of Technology, Newark, NJ.

Hettiarachchi, C., Meegoda, J., and Hettiarachchi, J. (2005). "Towards A Fundamental Model to Predict the Settlements in Bioreactor Landfills," *Waste Containment and Remediation*, 130, 1-15.

Hilf, J. (1991). *Chapter 8: Compacted Fill in Foundation Engineering Handbook, 2nd Ed,* Van Nostrand Reinhold, New York, NY.

Hillel, D. (1971). *Soil and Water, Physical Principles and Processes,* Academic Press, New York, NY.

Holtz, R., and Kovacs, W. (1981). *An Introduction to Geotechnical Engineering*, Prentice Hall, Englewood Cliffs, NJ.

Howland, J., and Landva, A. (1992). "Stability Analysis of a Municipal Solid Waste Landfill," *Stability and Performance of Slope and Embankments II, Geotechnical Special Publication No. 31,* ASCE, 1216-1231.

Hudson, A., White, A., Beaven, R., and Powrie, W. (2004). "Modeling the Compression Behavior of Landfilled Domestic Waste," *Waste Management*, 24, 259-269.

Itoh, T., Towhata, I., Kawano, Y., Kameda, M., Fukui, S., Koelsch, F., et al. (2005). "Mechanical Properties of Municipal Waste Deposits and Ground Improvement," *Proceedings of the Sixteenth International Conference on Soil Mechanics and Geotechnical Engineering, Volume 4*, Millpress Science Publishers, Rotterdam, the Netherlands, 2273-2276.

Jain, P., Powell, J., Townsend, T., and Reinhart, D. (2006). "Estimating the Hydraulic Conductivity of Landfilled Municipal Solid Waste Using the Borehole Permeameter Test," *Journal of Environmental Engineering*, 645-652.

Jang, Y. -S., Kim, Y. -W., and Lee, S. -I. (2002). "Hydraulic Properties and Leachate Level Analysis of Kimpo Metropolitan Landfill, Korea," *Waste Management*, 22, 3, 261-267.

Jansen, D. D. (2009, April 29). Associate Professor. (W. Wong, Interviewer).

Jessberger, H. (1994). "Geotechnical Aspects of Landfill Design and Construction, Part 2: Materials Parameters and Test Methods," *Institution of Civil Engineers Geotechnical Engineering Journal*, 105-113.

Jessberger, H., Syllwasschy, O., and Kockel, R. (1995). "Investigation of Waste Body Behaviour and Waste-Structure Interaction," *Proceedings of the 5th International Landfill Symposium,* Eds. T.H. Christensen, R. Cossu and R. Stegmann, CISA, S. Margherita di Pula, Cagliari, Italy, 731-743.

Johnson, A. W., and Sallberg, J. R. (1960). *Factors that Influence Field Compaction of Soils,* Bulletin 272, Highway Research Board.

Kavazanjian, E. (2001). "Mechanical Properties of Municipal Solid Waste," *Proceedings Sardinia 2001, Proceedings of the 8th International Waste Management and Landfill Symposium*, Eds. T.H. Christensen, R. Cossu and R. Stegmann, CISA, S. Margherita di Pula, Cagliari, Italy, 415-424.

Kavazanjian, E. (1999). "Seismic Design of Solid Waste Containment Facilities," *Proceedings of the 8th Canadian Conference on Earthquake Engineering,"* Vancouver, B.C.

Kavazanjian, E. (2006). "Waste Mechanics: Recent Findings and Unanswered Questions," G*eotechnical Special Publication, No. 148, Proceedings of the GeoShanghai Conference - Advances in Unsaturated Soil, Seepage, and Environmental Geotechnics,* ASCE, Shanghai, China, 34-54.

Kockel, R., and Jessberger, H. (1995). "Stability Evaluation of Municipal Solid Waste Slopes," *Proceedings, XI ECSMFE*, Balkema, Rotterdam, 267-272.

Kolsch, F. (1995). "Material Values for Some Mechanical Properties of Domestic Waste," *Proceedings Sardinia '95, Fifth International Landfill Symposium*, Sardinia, Italy, 20.

Kolsch, F. (1996). *The Influence of Fibrous Constituents on Shear Strength of Municipal Solid Waste. Ph.D. Thesis,* Technische Universitat Braunschweig Brauschweig, Germany Leichtweiss-Institut.

Konig, D., and Jessberger, H. (1997). "Waste Mechanics," *ISSMFE Technical Committee TC5 on Environmental Geotechnics*, 35-76.

Lambe, T. (1951). *Soil Testing for Engineers,* John Wiley and Sons, New York, NY.

Lambe, T. (1958a). "The Structure of Compacted Clay," *Journal of the Soil Mechanics and Foundations Division,* ASCE, 125, 1654-1 - 1654-34.

Lambe, T. (1958b). "The Engineering Behavior of Compacted Clay," *Journal of the Soil Mechanics and Foundations Division,* ASCE, 84, SM2, 1655-1 - 1655-35.

Lambe, T., and Whitman, R. (1969). *Soil Mechanics,* John Wiley and Sons, New York, NY.

Lamothe, D., and Edgers, L. (1994). "The Effects of Environmental Parameters on the Laboratory Compression of Refuse," *Proceedings of the 17th International Madison Waste Conference,* University of Wisconsin, Madison, Madison, WI, 592-604.

Landva, A., and Clark, J. (1986). "Geotechnical Testing of Waste Fill," *Proceedings of Canadian Geotechnical Conference*, Ottawa, Ontario, 371-385.

Landva, A., and Clark, J. (1990). "Geotechnics of Waste Fill," *Geotechnics of Waste Fills - Theory and Practice,* ASTM STP 1070 , 86-106.

Lee, S., and Park, H. (1999). "Discussion of Estimation of Municipal Solid Waste Landfill Settlement," by H.I. Ling et al., *Journal of Geotechnical and Geoenvironmental Engineering*, 125, 8, 722-724.

Lide, D. R. (2008). *Handbook of Chemistry and Physics, 89th Edition,* CRC Press, Boca Raton, FL.

Ling, I., Leshchinsky, D., Yoshiyuki, M., and Toshinori, K. (1998). "Estimation of Municipal Solid Waste Landfill Settlement," *Journal of Geotechnical and Geoenvironmental Engineering*, 124, 1, 21-28.

Liu, C.-N., Chen, R.-H., and Chen, K.-S. (2006). "Unsaturated Consolidation Theory for the Prediction of Long-Term Municipal Solid Waste Landfill Settlement," *Waste Management and Research*, 24, 80-91.

Maier, T. B. (1998). "Analysis Procedures for Design of Leachate Recirculation Systems," *SWANA's 3rd Annual Landfill Symposium*, Palm Beach Gardens, FL, 49-58.

Manassero, M., Van Impe, W., and Bouazza, A. (1996). "Waste Disposal and Containment," *Proceedings of the 2nd International Congress on Environmental Geotechnics, Preprint of Special Lectures,* A.A. Balkema, Osaka, Japan, 1425-1474.

Marques, A. C., Filz, G. M., and Vilar, O. M. (2003). "Composite Compressibility Model for Municipal Solid Waste," *Journal of Geotechnical and Geoenvironmental Engineering*, 129, 4, 372-378.

Merz, R., and Stone, R. (1962). "Landfill Settlement Rates," *Public Works* , 103-106, 210-212.

Mesri, G., and Ajlouni, M. (2007). "Engineering Properties of Fibrous Peats," *Journal of Geotechnical and Geoenvironmental Engineering*, 133, 7, 850-866.

Miller, P., Clesceri, N. (2002). *Waste Sites as Biological Reactors: Characterization and Modeling,* CRC Press, Boca Raton, FL.

Mitchell, J. (1956). "The Fabric of Natural Clays and its Relation to Engineering Properties," *Proceedings of the Highway Research Board*, 693-713.

Mitchell, J., and Soga, K. (2005). *Fundamentals of Soil Behavior, 3rd Edition,* John Wiley and Sons, Hoboken, NJ.

Moore, R., Dahl, K., and Yazdani, R. (1997). "Hydraulic Characteristics of Municipal Solid Waste: Findings of the Yolo County Bioreactor Landfill Project," *Proceedings of the International Conference on Solid Waste Technology and Management,* University of Pennsylvania, Philadelphia, PA, 8A-8A.

Morris, D., and Woods, C. (1990). "*Settlement and Engineering Considerations in Landfill and Final Cover Design,"* ASTM Special Technical Publication 1070, American Society of Testing and Materials, Philadelphia, PA.

Murphy, W., and Gilbert, P. (1985). *Settlement and Cover Subsidence of Hazardous Waste Landfills, EPA600/2-85-035,* Office of Research and Development, U.S. Environmental Protection Agency, Cincinnati, OH.

Olivier, F., and Gourc, J.-P. (2007). "Hydro-Mechanical Behavior of Municipal Solid Waste Subject to Leachate Recirculation in a Large-Scale Compression Reactor Cell," *Waste Management*, 27, 1, 44-58.

Olsen, H. (1962). "Hydraulic Flow through Saturated Clay," *Proceedings of the Ninth National Conference on Clays and Clay Minerals,* Pergamon Press, West Lafayette, IN, 131-161.

Oweis, I., and Khera, R. (1986). "Criteria for Geotechnical Construction on Sanitary Landfills," *Proceedings of the Conference on Environmental Geotechnology*, Allentown, PA, 205-223.

Park, H., and Lee, S. (2002). "Evaluation of Decomposition Effect on Long-Term Settlement Prediction for Fresh Municipal Solid Waste," *Journal of Geotechnical and Geoenvironmental Engineering,* 128, 2, 107-118.

Park, H., and Lee, S. (1997). "Long-Term Settlement Behavior of Landfills with Refuse Decomposition," *Journal of Solid Waste Technology and Management*, 20, 159-165.

Powrie, W., and Beaven, R. (1999). "Hydraulic Properties of Household Waste and Implications for Liquid Flow in Landfills," *Proceedings of the Institution of Civil Engineers, Geotechnical Engineering,* Thomas Telford Services Ltd, London, UK, 235-247.

Proctor, R. (1933). "Fundamental Principles of Soil Compaction," *Engineering News Record*, 111, 245-248.

Rao, S., Moulton, L., and Seals, R. (1977). "Settlement of Refuse Landfills," *Proceedings of the Conference on Geotechnical Practice for Disposal of Solid Waste Materials,* ASCE, 574-598.

Reddy, K., Hettiarachchi, H., Parakalla, N., and Gangathulasi, J. (2008a). "Geotechnical Properties of Fresh Municipal Solid waste at Orchard Hills Landfill, USA," *Waste Management*, 29, 2, 952-959.

Reddy, K., Gangathulasi, J., Hettiarachchi, H., and Bogner, J. (2008b). "Geotechnical Properties of a Municipal Solid Waste Subjected to Leachate Recirculation," *Geocongress 2008,* Eds. A.N. Alshawabkeh, K. R. Reddy, and M.V. Khire, ASCE, New Orleans, LA, 144-151.

Salgado, R. (2006). *The Engineering of Foundations,* McGraw Hill, New York, NY.

Sanitation Districts of Los Angeles County. (2009, June 22). *LACSD Website - Disposal Rates*, Last accessed: 22 June 2009, from http://www.lacsd.org/info/solid_waste/disposal_rates.asp

Sanitation Districts of Los Angeles County. (2009). *Puente Hills Landfill Brochure.* Last accessed: 22 June 2009, from Los Angeles County Sanitation District: http://www.lacsd.org/education/downloadable_brochures.asp

Seed, H., and Chan, C. (1959). "Structure and Strength Characteristics of Compacted Clays," *Journal of the Soil Mechanics an Foundations Division, ASCE*, 85, SM5, 87-128.

Siegel, R., Robertson, R., and Anderson, D. (1990). "Slope Stability Investigations at a Landfill in Southern California," In *Geotechnics of Waste Fills - Theory and Practice, ASTM Special Technical Publication 1070,* ASTM, Philadelphia, PA, 259-284.

Simpson, P. T., Zimmie, T. F., and Komisar, S. J. (1997). "Laboratory Analysis of Solid Waste Consolidation Due to Mechanical Compression and Biodegradation," *Proceedings of the 1997 13th International Conference on Solid Waste Technology and Management, Part 1 (of 2),* Widener University School of Engineering, Philadelphia, PA, 3D.

Singh, S., and Murphy, B. (1990). "Evaluation of the Stability of Sanitary Landfills. In *Geotechnics of Waste Fills - Theory and Practice," ASTM STP 1070,* American Society for Testing and Materials, Philadelphia, PA, 240-258.

Soler, N., Maher, A., and Chae, Y. (1995). "Time-Dependent Settlements in Landfills," In D. Vidic, and F. Pohland, *Innovative Technologies for Site Remediation and Hazardous Waste Management,* Proceedings of the National Conference, Pittsburgh, PA, 504-511.

Sowers, G. (1973). "Settlement of Waste Disposal Fills," *Proceedings of the International Conference on Soil Mechanics and Foundation Engineering,* International Society for Soil Mechanics and Foundation Engineering, Montreal, Quebec, Canada, 207-210.

Tchobanoglous, G., Theisen, H., and Vigil, S. (1993). *Integrated Solid Waste Management: Engineering Principles and Management Issues,* Irwin/McGraw-Hill, Boston, MA.

Terzaghi, K., and Peck, R. (1948). *Soil Mechanics in Engineering Practice,* John Wiley and Sons, New York, NY.

Thomas, S., Aboura, A., Gourc, J., Gotteland, P., Billard, H., Delineau, T., et al. (1999). "An In Situ Waste Mechanical Experimentation on a French Landfill," *Proceedings of the 7th International Landfill Symposium,* Eds. T.H. Christensen, R. Cossu and R. Stegmann, CISA, S. Margherita di Pula, Cagliari, Italy, 445-452.

Thurgood, M. (1999). "*Solid Waste Landfills: Decision-Makers Guide Summary,"* World Bank, World Health Organization, Swiss Agency for Development and Cooperations, and Swiss Center for Development Cooperation in Technology and Management.

Toll, D. (2000). "The Influence of Fabric on the Shear Behavior of Unsaturated Compacted Soils," In *Geotechnical Special Publication,* ASCE, 99, 222-234.

Turnbull, W., and Foster, C. (1956). "Stabilization of Materials by Compaction," *Journal of the Soil Mechanics and Foundations Division, ASCE*, 123, 934-1 - 934-23.

United States Environmental Protection Agency. (2008, November 13). *Municipal Solid Waste, Wastes, US EPA.* Last accessed: 29 June 2009, from United States Environmental Protection Agency: http://www.epa.gov/epawaste/nonhaz/municipal/pubs/06numbers.pdf

Vilar, O., and Carvalho, M. (2004). "Mechanical Properties of Municipal Solid Waste," *Journal of Testing and Evaluation*, 1-12.

Von Stockhausen, S. (2007). *Optimization of Waste Compaction Practices for Landfills, Master's Thesis,* California Polytechnic State University, San Luis Obispo, San Luis Obispo, CA.

Weyerhaeuser Company. 10 December, 2008. Email Communication.

Xie, M., Aldenkortt, D., Wagner, J., and Rettenberger, G. (2006). "Effect of Plastic Fragments on Hydraulic Characteristics of Pretreated Municipal Solid Waste," *Canadian Geotechnical Journal*, 43, 1333-1343.

Yen, B., and Scanlon, B. (1975). "Sanitary Landfill Settlement Rates," *Journal of Geotechnical Engineering, ASCE, 105*, 5, 475-487.

Zeiss, C., and Major, W. (1992). "Moisture Flow through Municipal Solid Waste; Patterns and Characteristics," *Journal of Environmental Systems*, 23, 3, 211-231.

Zimmerman, E. (1972). *A Mathematical Model for Solid Waste Settlement. Ph.D. Dissertation, Northwestern University,* Evanston, IL.

Zoino, W. (1973). "Stabilizing Landfills with Surcharge," *Utilization of Sanitary Landfill as a Foundation for Transportation Facilities,* Conference, Highway Research Board, Session No. 44, Washington, D.C.